THERMODYNAMICS OF MOLTEN IRON ALLOYS CONTAINING OXYGEN, ALUMINIUM, SILICON AND CHROMIUM

A study has been made of the aluminium-oxygen equilibrium in liquid iron by studying the reaction:

$$Al_2O_{3(s)} + 3\ H_{2(g)} = 2\ \underline{Al} + 3\ H_2O_{(g)}$$

Electrolytic iron in pure alumina crucibles was maintained at a constant temperature under a controlled water-vapour/hydrogen gas mixture until equilibrium was established between solid, liquid and gas phases. The melts were then quenched in a stream of hydrogen and subsequently analysed for aluminium and oxygen.

The value of this type of work is largely dependent upon accurate analytical techniques and in the present case analytical uncertainties have been reduced by carrying out experiments at 1723°C and 1823°C at which temperatures the equilibrium aluminium and oxygen concentrations are high enough for accurate analyses. Extrapolation of the data to 1600°C yields values which are probably more reliable than direct experimental determinations would be at that temperature, using the same technique.

Interaction parameters have been used to represent the effect of one solute on the chemical behaviour of another and equilibrium constants have been determined for the following reactions:-

$$Al_2O_{3(s)} = 2\ \underline{Al} + 3\ \underline{O}$$

$$Al_2O_{3(s)} + 3\ H_{2(g)} = 2\ \underline{Al} + 3\ H_2O_{(g)}$$

$$H_{2(g)} + \underline{O} = H_2O_{(g)}$$

where the underlined symbols represent substances dissolved in liquid ir

ProQuest LLC.
789 East Eisenhower Parkway
P.O. Box 1346
Ann Arbor, MI 48106 – 1346

The reactions have also been studied at 1723°C using iron-chromium alloys (0-10 per cent Cr) and iron-silicon alloys (0-4 per cent Si) to investigate the effect of these elements in combination with aluminium. Chromium was found to increase the activity coefficient of aluminium and to decrease the activity coefficient of oxygen in liquid iron.

In view of the results obtained during this investigation some of the published data on Fe-Si-O equilibria have been re-examined and a hypothesis has been put forward based on the formation of silicon monoxide in an attempt to explain the discrepancy which exists in the published data for the activity of silicon in liquid iron.

Wherever possible the results derived from the present work have been compared with other experimental data as well as with values derived from available thermodynamic data.

THERMODYNAMICS OF MOLTEN IRON ALLOYS CONTAINING OXYGEN, ALUMINIUM, SILICON AND CHROMIUM

THESIS

presented to the

UNIVERSITY OF GLASGOW

for the

DEGREE OF DOCTOR OF PHILOSOPHY

by

ALEXANDER McLEAN, B.Sc., A.R.C.S.T.

January, 1963

C O N T E N T S

CHAPTER I

INTRODUCTION

INTRODUCTION

Most of the reactions involved in steelmaking are associated with the removal of impurities from the iron. In this respect the most active refining agent is oxygen dissolved in the melt. The oxygen required for this purpose may be supplied to the bath in several ways. (a) by the addition of iron oxides, (b) by absorption from the furnace atmosphere via the slag, and (c) by blowing oxygen or air into the bath.

From the time the bath is molten, the concentration of impurities decreases and the oxygen content increases. Consequently, towards the end of a heat, it is usually found that for most purposes the oxygen content of the steel is excessive. If defective ingots and inferior steels are to be avoided, the oxygen content must be reduced.

Although oxygen is always present in steel to some extent, it can be controlled by the addition of elements whose oxides have a greater negative free energy of formation than that of iron. Many elements could be used, for example, chromium, vanadium, titanium and calcium, but the most common are manganese, silicon and aluminium. The choice of deoxidiser will depend on the degree of deoxidation required and also the secondary effects of the deoxidising element on the properties

of the finished steel. Depending on the type of steel being made, the amount of oxygen removed may be relatively large as in the case of fully killed steels, or relatively small as in rimming steels.

The effect of an element on the oxygen content of liquid steel will depend upon (a) its own activity, (b) the activity of oxygen and (c) the nature of the deoxidation product. The interaction effects which occur between liquid iron, dissolved oxygen and the deoxidiser make deoxidation a complex process even in the simplest system. In normal practice it is made even more complex by the fact that single deoxidisers are seldom used, and in cases where they are, other solutes are always present. It is evident, therefore, that any investigation of the reactions involved in deoxidation must take into account not only the chemical behaviour of oxygen and the deoxidiser when dissolved separately in iron, but also their behaviour when in solution together. In addition it must be recognised that the presence of other alloying elements may have a profound effect on the reactions under consideration.

When a deoxidiser is added to molten iron containing oxygen, the final oxygen content of the metal will be determined by the equilibrium in a reaction of the type.+

+ In the chemical equations, underlined symbols represent substances dissolved in liquid iron.

$$MO = \underline{M} + \underline{O} \qquad K = a_M \cdot a_O / a_{MO}$$

If the deoxidation product is precipitated as a pure solid, a_{MO} can be taken as unity and the equilibrium content for the reaction is given by:

$$K = a_M \cdot a_O$$

A convenient method for investigating the above reaction is the use of a controlled water-vapour/hydrogen gas mixture in a reaction of the type:

$$MO + H_{2(g)} = \underline{M} + H_2O_{(g)}$$

The advantage of this approach is that the oxygen activity in the melt can be controlled by adjusting the oxygen potential of the gas phase. This technique is used in the present work to study the aluminium-oxygen equilibrium in liquid iron contained in alumina crucibles. A study has also been made of the effects of chromium (up to 10 per cent) and silicon (up to 4 per cent) on the activity coefficients of the aluminium and oxygen dissolved in the liquid iron. Extensive use has been made of the interaction parameters introduced by Wagner[1,2] as a convenient means of representing the effect of one solute on the chemical behaviour of another. The different parameters and the relationships existing between them are discussed in detail in Chapter II.

C H A P T E R II

Some Thermodynamic Aspects of Liquid Metallic Solutions

1. Activity Coefficients in a Multi-Component System.

2. Interaction Parameter Relationships.

3. Interaction Parameters and the Chemical Potential of Electrons.

SOME THERMODYNAMIC ASPECTS OF LIQUID METALLIC SOLUTIONS

1. Activity Coefficients in a Multi-Component System

In a study of the chemical equilibria existing in a multi-component metallic solution it is possible to express the various thermodynamic properties of that solution in terms of the activity coefficients and concentrations of its components. However, an adequate representation of the equilibria involved will only be possible provided the interaction effects between the various components are taken into account.

Chipman et alia[3] have shown that when a solvent metal, 1, contains a number of solute metals, 2, 3, 4 etc., the activity coefficient of any one of these, for example γ_2, may be expressed as a product of factors which represent the effects of each of the other components. Thus for a solution containing mole fractions N_2, N_3, N_4, etc. of the various solutes:-

$$\gamma_2 = \gamma_2' \times \gamma_2^{(3)} \times \gamma_2^{(4)} \times \cdots\cdots > \quad \ldots\ldots\ldots\ldots [1]$$

where γ_2' is the activity coefficient of 2 in the binary solution 1 - 2 of mole fraction N_2, and $\gamma_2^{(3)}$, $\gamma_2^{(4)}\cdots$ represent the effect of 3, 4, etc. on the activity coefficient of 2. The reference state for the activity coefficients is based on Henry's Law, i.e. they are measured on such a scale that they become equal to unity in the infinitely dilute solution

i.e. $\gamma = \frac{a}{N}$, where $\gamma \to 1$, as $N \to 0$.

Wagner[1] has derived an equivalent expression for activity coefficients which are based on Raoult's Law, i.e. where the standard state is taken as that of the pure substance so that the activity coefficient, γ i, approaches unity as the mole fraction Ni approaches unity.

Thus the activity coefficient of component 2 is given by:-

$$\ln \gamma_2 (N_2, N_3 \ldots) = \ln \gamma_2^0 + \left[N_2 \frac{\partial \ln \gamma_2}{\partial N_2} + N_3 \frac{\partial \ln \gamma_2}{\partial N_3} + \ldots\right] + \left[\frac{1}{2} N_2^2 \frac{\partial^2 \ln \gamma_2}{\partial N_2^2} + N_2 N_3 \frac{\partial^2 \ln \gamma_2}{\partial N_2 \partial N_3} + \ldots\right] + \ldots$$

where the derivitives are to be taken for the limiting case of zero concentration of all solutes.

If terms involving second and higher order derivitives are disregarded, the logarithm of the activity coefficient becomes a linear function of the mole fractions of the various solutes.

$$\ln \gamma_2 (N_2, N_3, \ldots) = \ln \gamma_2^0 + N_2 \epsilon_2^{(2)} + N_3 \epsilon_2^{(3)} + \ldots\ldots [2]$$

where the coefficients $\epsilon_2^{(2)}$, $\epsilon_2^{(3)}$ etc. are defined as:

$$\epsilon_2^{(2)} = \partial \ln \gamma_2 / \partial N_2$$

$$\epsilon_2^{(3)} = \partial \ln \gamma_2 / \partial N_3 \text{ etc.} \qquad \ldots\ldots [3]$$

If the reference state is taken as that of the infinitely dilute solution, γ_2^0 becomes equal to unity and equation [2] simplifies to:-

$$\ln \gamma_2 (N_2, N_3 \ldots) = N_2 \epsilon_2^{(2)} + N_3 \epsilon_2^{(3)} + \ldots\ldots [4]$$

For practical applications, it is convenient to express the concentrations in terms of weight per cent rather than mole fractions and to replace the natural logarithms with common logarithms. Equation [4] can then be rewritten in the form:-

$$\log f_2(\%2, \%3, \ldots\ldots) = e_2^{(2)}[\%2] + e_2^{(3)}[\%3] + \ldots\ldots$$

where the coefficients $e_2^{(2)}$, $e_2^{(3)}$, etc. are defined as,

$$e_2^{(2)} = \partial \log f_2 / \partial[\%2],$$

$$e_2^{(3)} = \partial \log f_2 / \partial[\%3], \text{ etc.} \quad \ldots\ldots\ldots [5]$$

The coefficients or interaction parameters $\epsilon_j^{(i)}$ and $e_j^{(i)}$ may be regarded as a convenient means of representing the effect of one solute on the thermodynamic behaviour of another. A parameter is expected to vary with temperature, but for a given temperature its value determined at infinite dilution may remain constant over a range of concentration. Thus the magnitude of the parameter $\epsilon_j^{(i)}$ may be deduced from a graph of $\log \gamma_j$, v Ni. Similarly, a graph of $\log f_j$ v [% i] will yield information on the parameter $e_j^{(i)}$.

2. Interaction Parameter Relationships

(a) Wagner has shown[1] that for the limiting case of a solution which is infinitely dilute with respect to solutes 2 and 3 in solvent 1, the effect of 2 on the activity coefficient of 3 is related to the effect of 3 on the activity coefficient of 2, by the following equation:-

$\partial \ln \gamma_3 / \partial N_2 = \partial \ln \gamma_2 / \partial N_3$, for $N_2 = 0$, $N_3 = 0$.

i.e. $\epsilon_3^{(2)} = \epsilon_2^{(3)}$ .....[6]

(b) The parameters $e_j^{(i)}$ and $\epsilon_j^{(i)}$ are related in the manner that weight per cent is related to mole fraction and common logarithm to natural logarithm. Where the solvent metal is iron, then

$$e_j^{(i)} = \frac{55{\cdot}85}{100 \times 2{\cdot}303\ M_i} \epsilon_j^{(i)}$$, where Mi is the atomic weight of solute i

$$= \frac{0{\cdot}2425}{M_i} \epsilon_j^{(i)} \quad \ldots\ldots\ [7]$$

This equation is strictly valid only at infinite dilution, and thus the values obtained directly for $\epsilon_j^{(i)}$ from an experimental plot of log γ_j v N_i over a wide concentration range, may differ slightly from the values derived indirectly from a plot of the same data against weight per cent. The difference is significant only for elements whose atomic weight is considerably different from that of iron.

(c) Combining equations [6] and [7], yields the following expression:-

$M_3\ e_2^{(3)} = M_2\ e_3^{(2)}$, where M_2 and M_3 are the atomic weights of solutes 2 and 3 respectively.

i.e $$e_2^{(3)} = \frac{M_2}{M_3} e_3^{(2)} \quad \ldots\ldots\ [8]$$

The restrictions placed on the use of equations [6] and [7] also apply to equation [8]. As mentioned previously, the equations are strictly valid only at infinite dilution, however, experimental studies of a number of metallic binary and ternary solutions[4] have shown them to be true for finite concentrations,

with deviations occurring only in rather concentrated solutions.

3. Interaction Parameters and the Chemical Potential of Electrons.

In addition to the interaction effects between solute ions discussed in the previous sections, Wagner[2] has shown that consideration must also be given to the effect of metal solute atoms on the chemical potential of the electrons in an alloy, i.e. on the number of valence electrons per atom.

The chemical potential of a solute i is given by:-

$$\mu_i = \mu_i^\circ + RT \ln N_i + RT \ln \gamma_i \quad \ldots[9]$$

where μ_i° is the chemical potential of the substance i in its pure state. μ_i can also be expressed as the sum of two components:-

$$\mu_i = \mu_i(\text{ion}) + z_i \mu_{(e)} \quad \ldots..[10]$$

where $\mu_i(\text{ion})$ represents the chemical potential of i ions of valence Zi and $\mu_{(e)}$ represents the chemical potential of the electrons. It is evident from this equation that a change in $\mu_{(e)}$ will affect the chemical potential of the neutral solute μ_i in two ways:-

(1) directly, in view of the second term on the right-hand side of equation [10],

and (2) indirectly, since a change in $\mu_{(e)}$ will result in a change in $\mu_i(\text{ion})$, due to a stronger or weaker interaction between positively charged metal ions and electrons.

Wagner[2] has pointed out that these effects will predominate provided (a) only positively charged metal ions are present, and (b) direct interaction between metal ions can be disregarded.

Consequently it may be assumed that in equation [9]. the term RT $\ln \gamma_i$, which accounts for deviations from ideal behaviour, is mainly a function of $\mu_{(e)}$, and will be affected by changes in the alloy composition only in so far as $\mu_{(e)}$ varies.

$$\text{i.e.} \quad d(RT \ln \gamma_i) \cong 0 \text{ , if } d(\mu_{(e)}) = 0 \ldots\ldots \quad [11]$$

Combining equations [6] and [11] with the general equation for Gibbs free energy G for a system consisting of n_1, n_2 and n_3 moles of components 1, 2 and 3 respectively,

$$\text{i.e. } G = n_1 \mu_1 + n_2 \mu_2 + n_3 \mu_3$$

Wagner[2] has shown that:-

$$\frac{\partial \ln \gamma_2}{\partial N_3} = \frac{\partial \ln \gamma_3}{\partial N_2} \cong \pm \left[\frac{\partial \ln \gamma_2}{\partial N_2} \cdot \frac{\partial \ln \gamma_3}{\partial N_3} \right]^{\frac{1}{2}}, \text{ for } N_2 \to 0, N_3 \to 0.$$

$$\text{i.e. } \epsilon_2^{(3)} = \epsilon_3^{(2)} \cong \pm \left[\epsilon_2^{(2)} \cdot \epsilon_3^{(3)} \right]^{\frac{1}{2}} \ldots\ldots\ldots \quad [12]$$

Thus the mutual effects of solute metals 2 and 3 on their activity coefficient are related to their deviations from ideality in the binary systems 1 - 2, and 1 - 3. From this point of view, equation [12] will only be significant when the deviations from ideality in the binary systems are of the same sign, otherwise the square root will be imaginary. It can be shown that if the original assumption is valid, i.e. that interaction between metal ions can be disregarded, then the sign of $\partial \ln \gamma_i / \partial Ni$ for any solute i in solvent 1 will in fact be the same. The fact that this sign is not always the same exphasises the limitations of the assumption.

Since the sign of the square root may be positive or negative, the sign of the parameters $\epsilon_2^{(3)}$ and $\epsilon_3^{(2)}$ is not predicted

by equation [12]. However, it can be deduced from consideration of the effect of solutes 2 and 3 on the electron-atom ratio. Wagner[2] has pointed out that the parameters will have a positive sign, when solutes 2 and 3 change the electron-atom ratio in the same direction. Conversely, they will have a negative sign when solutes 2 and 3 change the electron-atom ratio in different directions.

In general, direct interaction between metal ions is significant and the change in the chemical potential of the electrons can be expected to be the predominant factor only when deviations from ideality are relatively large.

C H A P T E R III

LITERATURE REVIEW

1. The Activity of Oxygen in Liquid Iron

2. The Activity of Aluminium in Liquid Iron-Aluminium Alloys

3. Aluminium-Oxygen Equilibrium in Liquid Iron

4. The Activity of Chromium in Liquid-Iron-Chromium Alloys

5. Chromium-Oxygen Equilibrium in Liquid Iron

6. The Activity of Silicon in Liquid Iron-Silicon Alloys

7. Silicon-Oxygen Equilibrium in Liquid Iron

8. The Effect of Silicon on the Activity Coefficient of Aluminium in Liquid Iron-Silicon-Aluminium Alloys

LITERATURE REVIEW

1. The Activity of Oxygen in Liquid Iron

In the application of thermodynamics to the study of steelmaking reactions, particularly reactions associated with the deoxidation of steel, a knowledge of the thermodynamic properties of oxygen dissolved in liquid iron is of paramount importance.

Part of the iron-oxygen equilibrium diagram[5] is shown in Fig. 1, from which it can be seen that the solubility of oxygen in liquid iron is limited by the formation of a liquid iron oxide phase. Under equilibrium conditions, an iron-oxygen alloy containing, for example, 0·1% oxygen, would undergo a monotectic reaction at 1528°C when cooling down from some temperature in the liquid region. The oxygen content of the melt at the monotectic point would correspond to 0·16%. Due to the monotectic reaction, this oxygen would separate out from the iron in the form of a liquid iron oxide phase of oxygen content 22·6%. If on the other hand, the cooling rate was sufficiently fast the oxygen content of the iron in the solid state would be the same as that in the liquid state.

Chipman[6] has shown that oxygen dissolves in liquid iron according to the equation:-

$$O_2 = \underline{2O}$$

Based on this equation is one of the most important considerations

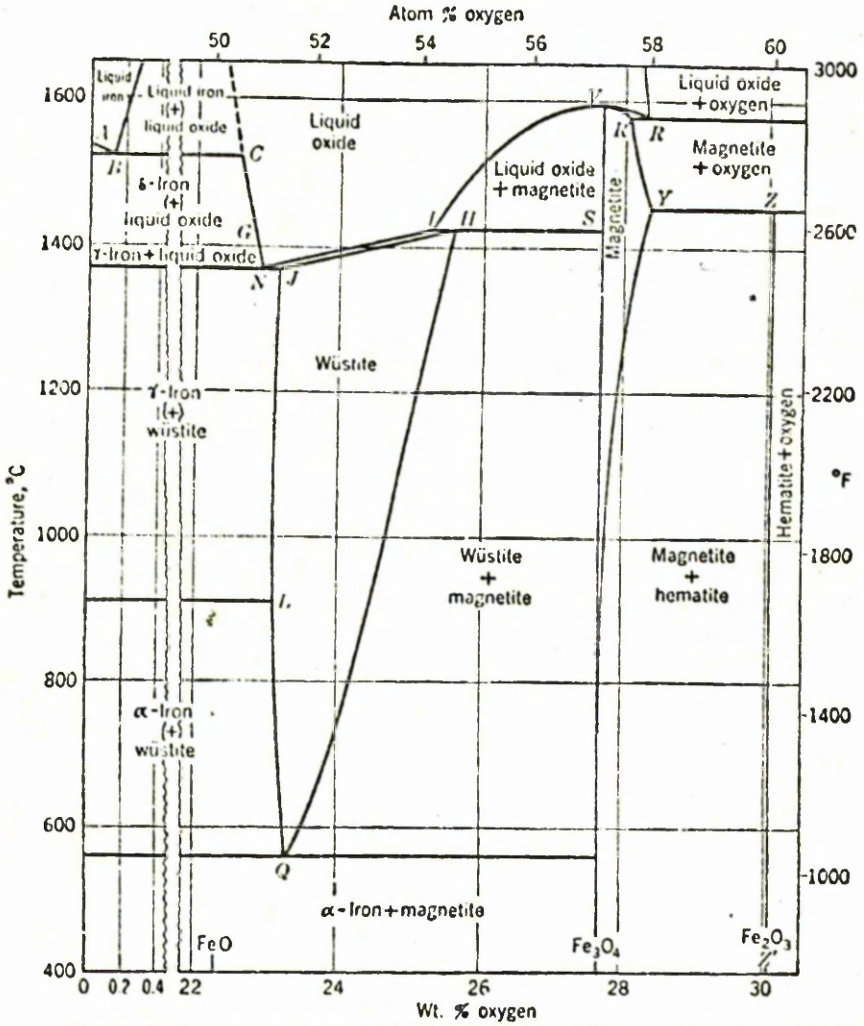

Point	°C	% O	p_{CO_2}/p_{CO}	Point	°C	% O	p_{CO_2}/p_{CO}	p_{O_2} (atm)
A	1539			*Q*	560	23.26	1.05	
B	1528	0.16	0.209	*R*	1583	28.30		1
C	1528	22.60	0.209	*R'*	1583	28.07		1
G	1400*	22.84	0.263	*S*	1424	27.64	16.2	
H	1424	25.60	16.2	*V*	1597	27.64		0.0575
I	1424	25.31	16.2	*Y*	1457	28.36		1
J	1371	23.16	0.282	*Z*	1457	30.04		1
L	911*	23.10	0.447	*Z'*		30.06		
N	1371	22.91	0.282					

* Values for pure iron.

FIG 1

concerning the behaviour of oxygen in liquid iron, namely, the free energy of dissolved oxygen relative to that of pure oxygen gas. Unfortunately, the oxygen pressure in equilibrium with iron and its lowest oxide wüstite is about 10^{-8} atmospheres at 1600°C which is far too low for direct experimental determinations[7]. Thus indirect methods are required which involve the use of gas mixtures having a controlled oxygen potential. (H_2O - H_2) and (CO_2 - CO) gas mixtures are frequently used for this purpose.

One of the most convenient methods for studying the activity and free energy of oxygen dissolved in liquid iron is based on the reaction:-

$$H_2(g) + \underline{O} = H_2O(g)$$

$$K_1' = p_{H_2O}/(p_{H_2} \times \% O)$$

In one of the earliest studies of this reaction by Chipman[6] a small charge of electrolytic iron was held in the molten condition in a high frequency furnace under a controlled water-vapour/hydrogen gas atmosphere, at constant temperature for periods up to two hours. At the end of a heat the melts were allowed to solidify and the oxygen content of the metal determined by vacuum fusion analysis.

The results obtained from this study were in the main confined to low oxygen concentrations (below 0·07 per cent), and in order to extend the data up to the limiting solubility of oxygen

in liquid iron, a further investigation was undertaken by Fontana and Chipman[8]. Their experimental technique differed in two respects from that mentioned above: (i) an attempt was made to minimise errors arising from thermal diffusion, by preheating the incoming gases, and (ii) some of the melts were quenched in liquid tin, others in water, in an effort to retain the equilibrium oxygen concentration in the metal at room temperature. The effect of temperature on the reaction was studied by Chipman and Samarin[9] using the same technique.

In a later study of the reaction by Dastur and Chipman[10] it was stated that errors due to thermal diffusion had been eliminated by the addition of argon to the steam-hydrogen mixture in the ratio of 4 : 1 argon-hydrogen and then preheating the inlet gases to the temperature of the melt.

Floridis and Chipman[11] compared data obtained by two experimental methods:

(a) A technique similar to that of Dastur and Chipman but with an argon : hydrogen ratio of 6 : 1.

(b) Several heats were made in a resistance furnace and thermal diffusion eliminated by bubbling the gas mixture through the melt, a technique previously used with some success by Gokcen[12]. The data obtained by these two methods were in reasonably good agreement.

The reaction has also been studied by Matoba[13] and Averin et alia[14] using a similar approach to that of Dastur and Chipman. The results of the different investigations are collected in Fig. 2 where a graph is presented of Log K_1' v [wt. % O].

From the various data it is evident that all the investigations except those of Fontana and Chipman, and Dastur and Chipman, indicate that the equilibrium ratio K_1' is not a true constant but in fact decreases with increasing oxygen concentration, implying that the iron-oxygen alloys studied do not obey Henry's Law. On the other hand, the data of Fontana and Chipman and Dastur and Chipman indicated that the equilibrium constant is independent of the oxygen concentration up to about 0·21 per cent.

It is possible to account for this discrepancy in the following way:

(a) Fontana and Chipman[8]. The conclusion that the iron-oxygen system obeyed Henry's Law for oxygen concentrations up to 0·21 per cent was based on the results of a small number of experiments in the range 0·16 to 0·22 per cent oxygen, for which the values of K_1' were in approximate agreement with those for melts containing less than 0·07 per cent oxygen. During their investigation it was assumed from the work of Tritton and Hanson[15], Herty and Gaines[16], and Körber and Oelsen[17], that the monotectic composition in the iron-oxygen system was about 0·21 - 0·22 per cent oxygen, from which it was concluded that little or no separation of primary liquid wüstite had occurred during the freezing of their melts.

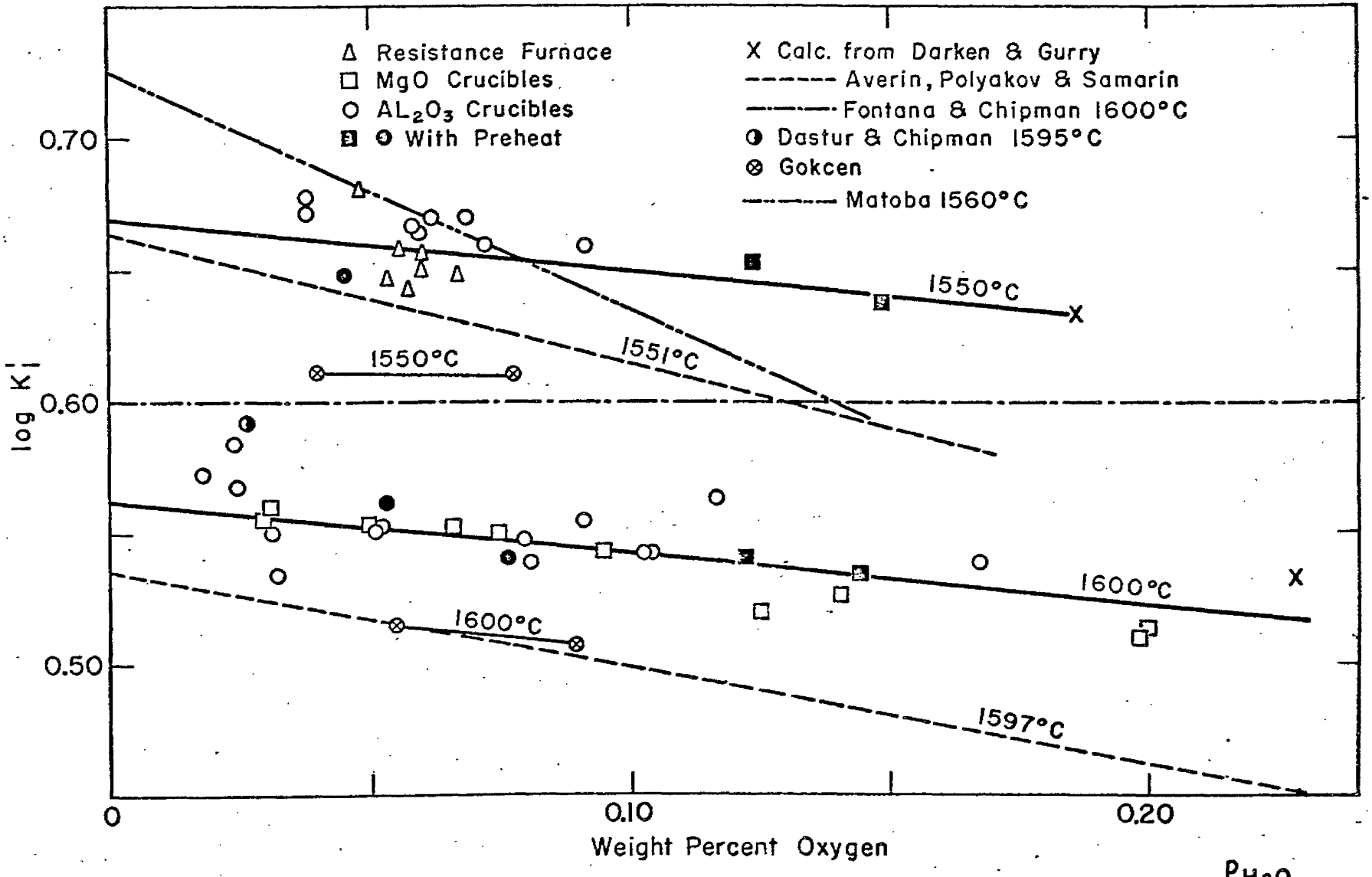

FIG 2. EFFECT OF OXYGEN CONCENTRATION ON EQUILIBRIUM RATIO, $K_1' = \frac{P_{H_2O}}{P_{H_2}[\%O]}$

Subsequent work by Chipman and Fetters[18], Taylor and Chipman[19], Sloman[20], Fischer and vom Ende[21], and Gokcen[12] has shown that the maximum solubility of oxygen in iron at its melting point is about 0·16 per cent. This discrepancy in the monotectic point composition was probably due mainly to errors in temperature measurement, since the earlier workers used optical pyrometers which under the experimental conditions would give low readings. Körber and Oelsen attempted to correct their values by the use of emission coefficients, but it would appear that their measurements were still slightly low. In the more recent work of Chipman and co-workers immersion thermocouples were employed.

Thus in the light of present knowledge on the monotectic composition, it is very probable that the values for K_1' in the range 0·16 - 0·22 per cent oxygen were high, due to the loss of appreciable amounts of iron oxide during freezing, despite the fact that some of the heats were quenched in liquid tin or water, since this method of quenching induces freezing from the bottom of the melt upwards which would tend to encourage the separation of primary liquid iron oxide. Unfortunately, no heats were made in the range 0·07 - 0·16 per cent oxygen, so that the apparent agreement between the data for heats containing more than 0·16 per cent oxygen and those containing less than 0·07 per cent oxygen may have been largely fortuitous.

(b) Dastur and Chipman[10]. A number of heats were made in the range 1563° to 1760°C, but the oxygen concentrations in the melts never exceeded 0·06 per cent, which is well below the saturation value in the liquid and so there was little likelihood of loss during cooling. On the basis of the results obtained by Fontana and Chipman[8], it was simply assumed that the activity of oxygen dissolved in liquid iron was directly proportional to its concentration.

In the study by Floridis and Chipman[11], the oxygen concentrations ranged up to 0·2 per cent and at the end of a heat, the melt was lowered into the cooler part of the furnace tube and quenched in a stream of cold helium, a technique introduced by Gokcen and Chipman[22]. The advantage of this technique is that freezing begins at the top surface and thus assists in the "freezing-in" of oxide. In the original paper their results at 1550° and 1600°C were compared with two values derived from the data of Darken and Gurry[23] who studied the equilibrium involved between CO - CO_2 gas mixtures, liquid iron and liquid oxide. Combining the results of this study with the solubility data for oxygen in liquid iron values were obtained for the equilibrium ratio of the following reaction.

$$CO_{(g)} + \underline{O} = CO_2(g)$$

$$K_2' = P_{CO_2}/(P_{CO} \times \% O)$$

By means of the known free energies of the gases involved, values

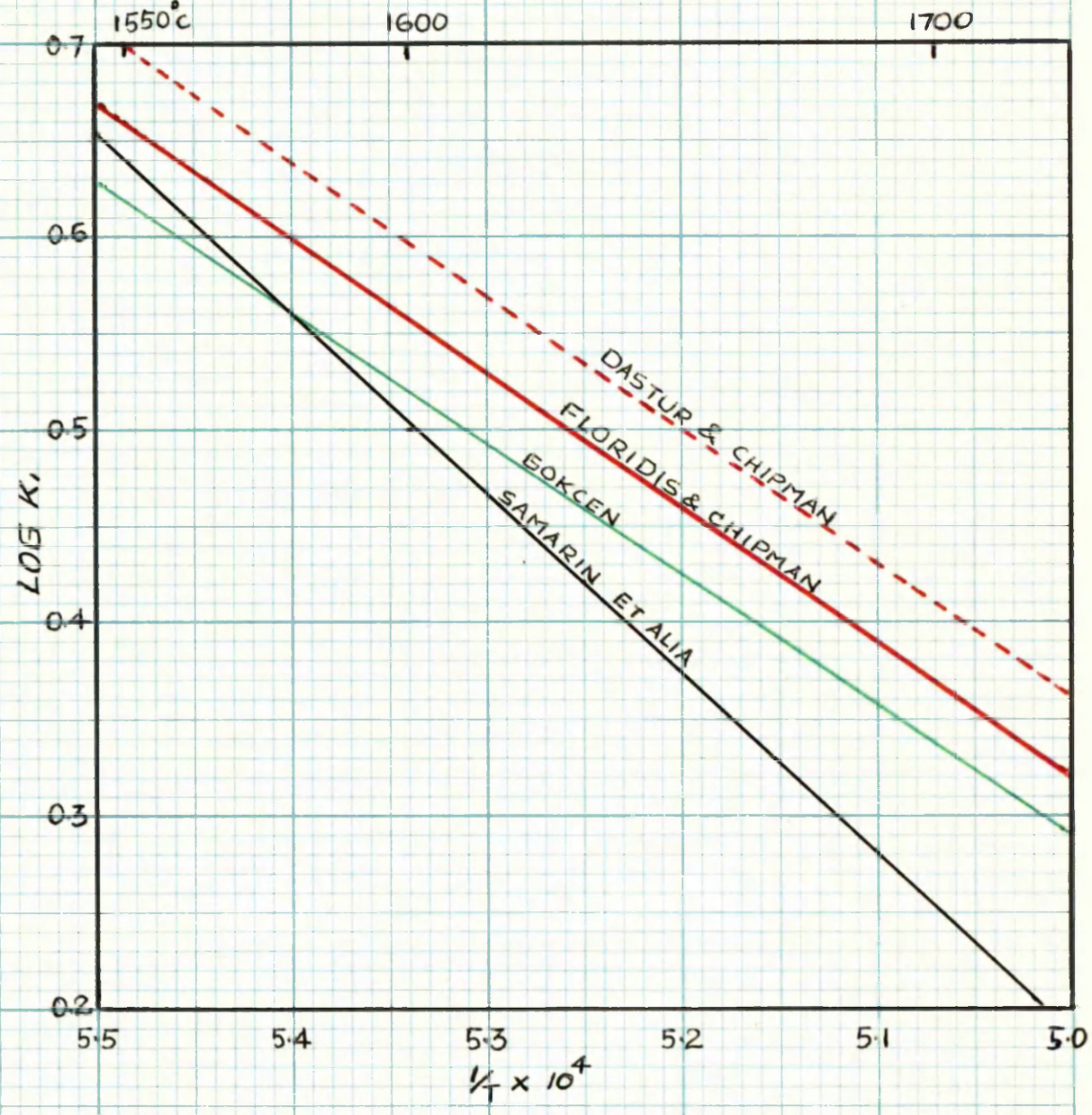

FIG 3 EFFECT OF TEMPERATURE ON THE EQUILIBRIUM CONSTANT $K_1 = P_{H_2O}/P_{H_2}[a_o]$

for K_1' were deduced from the values of K_2' and as shown in Fig. 2 these are in good agreement with the values for K_1' determined experimentally. The slope of the lines at 1550° and 1600°C indicates that the activity coefficient of oxygen f_o, decreases with the increasing concentration according to the equation.

$$\log f_o = -0.20[\% O]$$

In Fig. 2 the intercept at zero per cent oxygen represents the equilibrium constant $\log K_1$. The effect of temperature on this constant, as reported by several workers, is shown in Fig. 3. Since their data covered only a narrow range, Floridis and Chipman have represented the temperature effect by a line drawn through their data parallel to that of Dastur and Chipman. This line corresponds to the equations.-

$$\log K_1 = 7050/T - 3.20$$

and $$\Delta G^\circ = -32,200 + 14.63\ T \text{ CAL}$$

According to the data of Averin et alia the effect of temperature on $\log K_1$ is given by.

$$\log K_1 = 9440/T - 4.536$$

This agrees reasonably well with the data of Floridis and Chipman at 1600°C, but at higher temperatures the two sets of data gradually diverge.

2. The Activity of Aluminium in Liquid Iron-Aluminium Alloys

In the application of thermodynamics to the study of reactions occurring in liquid steel, the greatest uncertainty is usually associated with the determination of the activity of a minor constituent. Such is the case in the calculation of the aluminium deoxidation constant.

The most convenient method of determining the activity of aluminium in iron is by measuring its partition between liquid iron and silver which are almost immiscible. Taking the pure solute as the reference state, then at equilibrium the activity of aluminium in the silver layer is equal to that in the iron layer.

$$\text{i.e. } [N_{Al} \times \gamma_{Al}]_{silver} = [N_{Al} \times \gamma_{Al}]_{iron}$$

The atom fractions of aluminium, N_{Al}, in the iron and silver are determined from partition experiments and provided the activity coefficient of aluminium in silver is known, then that in iron can be calculated.

The earliest work done in this field was by Chipman[24] who calculated from distribution data a value for γ_{Al} in iron on the assumption that aluminium in silver formed an ideal solution and therefore that γ_{Al} in silver was unity. This assumption was based on the fact that aluminium and silver have similar atomic dimensions and internal pressures and have a high degree

of mutual solubility. Subsequent investigations have shown that this assumption was unjustified.

An important contribution was made by Chou[25] who determined the activity of aluminium in silver by the following method.

(a) The activity of silver in lead-silver alloys was calculated from the phase diagram and the known heat of fusion of silver by means of the equation.

$$\ln a_{Ag} = \frac{-\Delta H_f (T_m - T)}{R \cdot T_m \cdot T}$$, where ΔH_f and T_m are the heat of fusion and the melting point of silver respectively.

(b) From the distribution of silver between lead and aluminium, and values for the activity of silver in lead from (a), the activity of silver in aluminium was found over a wide range of concentrations.

(c) The activity of aluminium in silver was then calculated by means of a Gibbs-Duhem integration.

$$\ln a_{Al} = -\frac{N_{Ag}}{N_{Al}} \int d \ln a_{Ag}$$

In this way new values were calculated for the activity coefficient of aluminium in iron.

These calculations were repeated in greater detail by Elliott[26] who showed that for the infinitely dilute solution of aluminium in iron, γ°_{Al} had the value 0·043 at 1600°C.

Chipman and Floridis[27] estimated the activity of aluminium in liquid silver by a more direct method based on the data of Hillert et alia[28]. These workers had determined the activity of aluminium

in solid aluminium-silver alloys at temperatures up to 820°K by e.m.f. measurements of the cell.

$$\underset{\text{(Anode)}}{Al_{(s)}} \;\Big|\; Al\,Cl_3 \text{ in } Na\,Cl_{(liq)} \;\Big|\; \underset{\text{(Cathode)}}{Al - Ag_{(s)}}$$

The alloys studied were all in the terminal solid solution field. From e.m.f. measurements at 820°K and the temperature coefficient $d\mathcal{E}/dT$ in the range 642 - 820°K, values were calculated for the activity of aluminium at the solidus by means of the equation.

$RT \ln a_s = -Z\,Fe$, where a_s represents the activity of aluminium relative to the pure solid, Z is the number of electrons involved, F is the Faraday constant and e is the e.m.f.

The activity of aluminium relative to solid aluminium in the equilibrium liquid phase has the same value, $a_{(s)}$, but that relative to liquid aluminium, $a_{(\ell)}$ can be calculated using the heat of fusion of aluminium, by the following equation.

$$\ln a_{(\ell)} = \ln a_{(s)} - \frac{\Delta H_f (T_m - T)}{R\,T_m\,T}$$

For an accurate determination of the activity of aluminium at higher temperatures, data is required on the heat of mixing of aluminium and silver. Although this was available from the work of Kawakami[89] it was disregarded by Chipman and Floridis who believed it to be too high due to the reaction of aluminium with oxygen dissolved in the silver. For this reason it was assumed that aluminium in silver formed a regular solution and therefore that.

$$T_1 \log \gamma_1 = T_2 \log \gamma_2$$

In these calculations it was also assumed that the liquidus on the equilibrium diagram was a straight line, although Hansen's[30] diagram showed a curve. A revised diagram by Phillips[31] shows that this assumption was almost correct.

The data deduced from Hillert et alia, were combined with the results of partition experiments and it was found that at 1600°C the activity coefficient of aluminium in iron was given by:-

$$\log \gamma_{Al} = 2{\cdot}60\, N_{Al} - 1{\cdot}51, \text{ valid for } N_{Al} = 0{\cdot}0 \text{ to } N_{Al} = 0{\cdot}2$$

$$\text{At } N_{Al} = 0, \quad \log \gamma_{Al} = \log \gamma^{\circ}_{Al} = -1{\cdot}51$$

$$\text{i.e. } \gamma^{\circ}_{Al} = 0{\cdot}031$$

$$\text{Also, } \frac{\partial \log \gamma_{Al}}{\partial N_{Al}} = 2{\cdot}60$$

$$\therefore \epsilon^{(Al)}_{Al} = \frac{\partial \ln \gamma_{Al}}{\partial N_{Al}} = +6{\cdot}0$$

The positive sign implies that the activity coefficient of aluminium in liquid iron increases with increasing aluminium content. This can be interpreted in terms of a competition for iron atoms in the nearest neighbour shells. As the aluminium concentration increases this competition effect will also increase with the result that the activity coefficient of the aluminium, and incidentally that of the iron, will be increased.

Wilder and Elliott[32] have recently determined the activity of aluminium in liquid silver by measuring the e.m.f. of the cell

$$Al_{(liq)} \;\big|\; Al^{+++}\text{(in molten KCl)} + NaCl \;\big|\; Al\text{-}Ag_{(liq)}$$

in the temperature range 700 - 980°C.

Their results when extrapolated to 1600°C and combined with the distribution data of Chipman and Floridis[27] yielded values of + 5·3 for the parameter $\epsilon^{(Al)}_{Al}$ and 0·063 for γ°_{Al}.

These values are probably more accurate than those of Chipman and Floridis since in this case the extrapolation to 1600°C does not require the assumption of regular behaviour in the aluminium-silver system.

3. Aluminium - Oxygen Equilibrium in Liquid Iron

3. Aluminium - Oxygen Equilibrium in Liquid Iron

One method of deoxidation in steel making is to reduce the oxygen content of liquid iron, by adding an element which has a greater affinity for oxygen, than iron. The elements commonly used are manganese, silicon and aluminium, the most effective of which is aluminium. When aluminium is added to liquid iron containing dissolved oxygen, the equilibrium involved is:-

$$Al_2O_3 = 2\,\underline{Al} + 3\,\underline{O}$$

for which the equilibrium constant K_1 is given by:

$$K_1 = \frac{[a_{Al}]^2[a_O]^3}{a_{Al_2O_3}}$$

Provided the melt is in equilibrium with pure alumina or alumina saturated slags, $a_{Al_2O_3}$ in the above expression may be taken as unity, and therefore:

$$K_1 = [a_{Al}]^2[a_O]^3$$

or, using weight percentages

$$K_1' = [\%Al]^2[\%O]^3$$

In one of the earliest determinations, Wentrup and Hieber[33], using alumina crucibles and an induction furnace with an atmosphere consisting mainly of air at 10 - 20 m.m. mercury pressure, added aluminium to liquid iron of a high oxygen content, and after a period of about 10 minutes, poured part of the melt into a copper mould to freeze the equilibrium. Heats were made in the temperature range 1600° to 1720°C. Analyses of the samples for oxygen and aluminium yielded the following data for log K_1'.

$$\log K_1' = -71,200/T + 27.98$$

Geller and Dicke[34] measured the equilibrium between dissolved carbon (0.4 to 1.1 per cent) and aluminium in liquid iron contained in alumina crucibles. The metal samples were analysed for carbon and aluminium and the oxygen contents deduced from established data on the $\underline{C} - \underline{O} - CO$ equilibrium. This procedure yielded values for log K_1' given by.

$$\log K_1' = (-58,600/T + 18.90) \pm 1.5$$

The solubility of oxygen in liquid iron containing aluminium in the temperature range 1550°C to 1650°C has been studied by Hilty and Crafts[35] using a rotating crucible furnace. The rotating action of the furnace was intended to make the liquid iron, contained in an alumina crucible, form a "cup" which in turn would act as a container for slags consisting mainly of Al_2O_3, Fe_2O_3 and FeO. The furnace was continuously flushed out with argon and during the course of each heat additions were made of aluminium and ferric oxide. Hilty and Crafts have stated that"Throughout the range of aluminium

concentrations investigated, the experimental melts could not be brought into equilibrium with the pure alumina crucible....." This was attributed to the formation of a surface layer on the crucible walls consisting of some substance other than pure alumina and containing both iron oxide and alumina. Their results were expressed approximately by the equation.

$$\log K_1' = -58,600/T + 22{\cdot}75$$

It was claimed that this particular equation represented only a deoxidation constant and was of no other significance. The data from this study are compared with those of Wentrup and Hieber, and Geller and Dicke in Tables 1 and 2.

TABLE 1 Experimental Values of $K_1' = [\%Al]^2 \cdot [\%O]^3$

Temp. °C	Geller and Dicke (34)	Wentrup and Hieber (33)	Hilty and Crafts (35)
1600	4×10^{-13}	1×10^{-10}	$2{\cdot}8 \times 10^{-9}$
1700	$1{\cdot}6 \times 10^{-11}$	$7{\cdot}9 \times 10^{-9}$	1×10^{-7}

TABLE 2 Oxygen Concentrations of Liquid Iron Containing Aluminium at 1600°C

Al. wt. per cent	Geller and Dicke	Wentrup and Hieber	Hilty and Crafts
0·1	0·0004	0·0020	0·0066
0·01	0·0016	0·0093	0·0302
0·001	0·0074	0·0437	0·1413

From the results presented in this form it is evident that the data of Hilty and Crafts yield values for the oxygen concentration of liquid iron at 1600°C for a given aluminium concentration, which are about three times greater than those of Wentrup and Hieber and twenty times greater than those of Geller and Dicke.

The above studies of the aluminium deoxidation constant are all subject to relatively large analytical errors due to the small quantities of aluminium and oxygen involved. In an attempt to minimise the effect of errors from this source, Gokcen and Chipman[36] carried out work at temperatures of 1695°, 1760° and 1866°C, where both the aluminium and oxygen concentrations at equilibrium are greater.

Their experimental technique consisted of melting electrolytic iron, usually with some aluminium present, in alumina crucibles under a controlled water-vapour/hydrogen atmosphere and holding at constant temperature until equilibrium was established between the solid, liquid and gas phases. The melts were quenched in a stream of hydrogen to retain the equilibrium aluminium and oxygen concentrations at room temperature, and subsequently analysed for these constituents. The results obtained from these experiments allowed a study to be made of the following equilibria:-

$$Al_2O_3(s) = 2\,\underline{Al} + 3\,\underline{O}$$

$$K_1 = [a_{Al}]^2\,[a_O]^3 \quad : \quad K_1' = [\%Al]^2\,[\%O]^3$$

$$Al_2O_3(s) + 3H_2(g) = 2\,\underline{Al} + 3H_2O(g)$$

$$K_2 = [a_{Al}]^2\left(\frac{p_{H_2O}}{p_{H_2}}\right)^3 \quad : \quad K_2' = [\%Al]^2\left(\frac{p_{H_2O}}{p_{H_2}}\right)^3$$

$$H_2(g) + \underline{O} = H_2O(g)$$

$$K_3 = \frac{p_{H_2O}}{p_{H_2}}\,\frac{1}{[a_O]} \quad : \quad K_3' = \frac{p_{H_2O}}{p_{H_2}}\,\frac{1}{[\%\,O]}$$

It was found that the value of K_3' decreased with increasing aluminium concentration, implying that the activity coefficient of oxygen is reduced by the presence of aluminium. From the various data values were derived for the parameters $e_O^{(Al)}$ and $e_{Al}^{(O)}$ representing the effect of aluminium on the activity coefficient of oxygen and oxygen on the activity coefficient of aluminium, respectively. These interaction effects diminished with increasing temperature.

Although the values for the deoxidation product K_1' were much smaller than those found in previous investigations, they were shown to be of the same order of magnitude as values calculated from thermodynamic data[37], and corresponding to the equation:-

$$\log K_1 = -64{,}000/T + 20{\cdot}48$$

Values for the deoxidation constant K_1 at 1600°C and

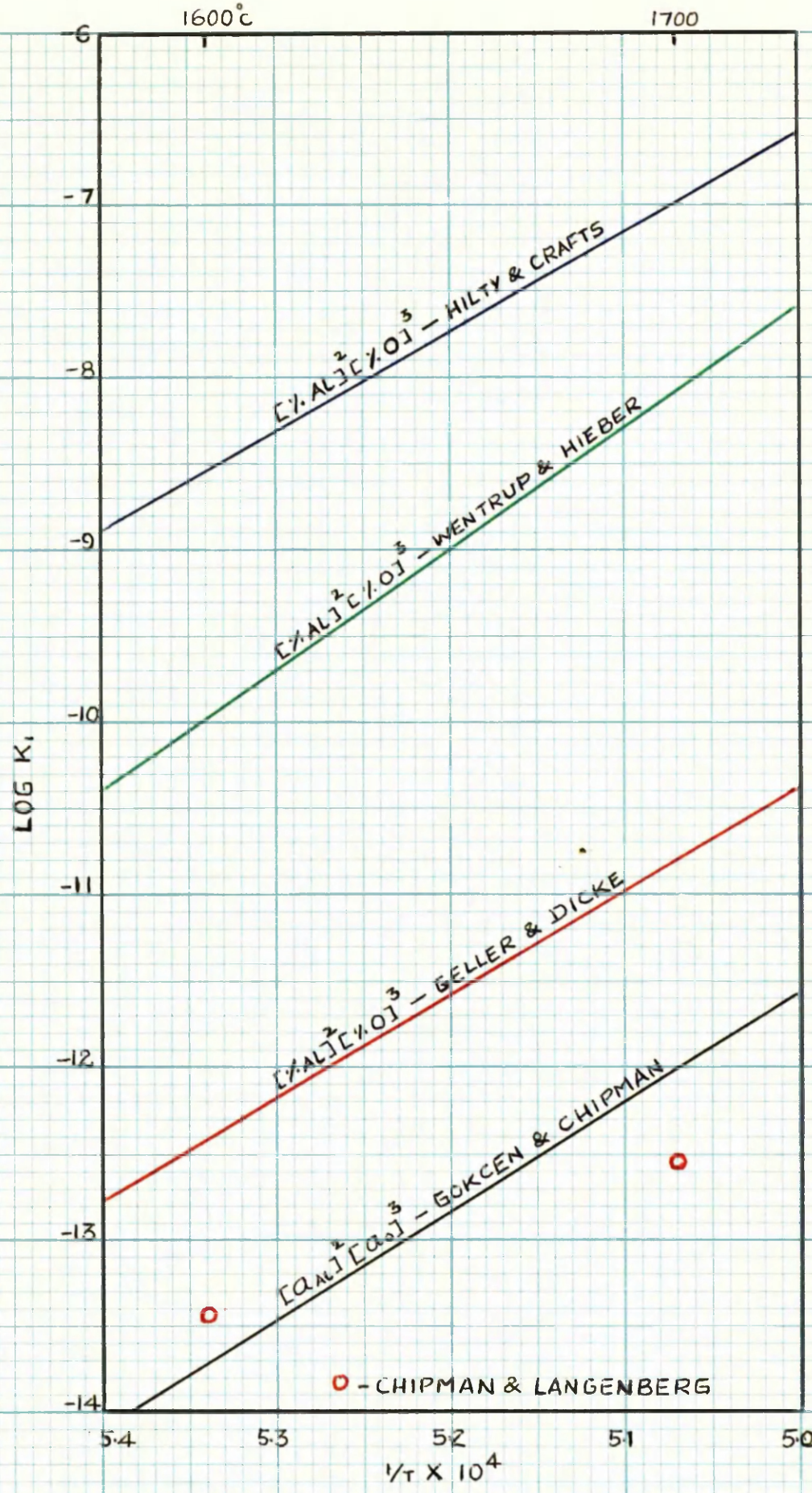

FIG 4 COMPARISON OF ALUMINIUM DEOXIDATION DATA

1700°C have been derived indirectly by Chipman and Langenberg[38] from a study of the aluminium-oxygen content of carbon saturated iron in equilibrium with pure alumina. Heats were made in graphite crucibles under a carbon monoxide atmosphere. The activity of oxygen in the melts was calculated using the data of Dastur and Chipman[10] for the free energy of solution of oxygen in liquid iron. The activity of aluminium was calculated from its concentration and its activity coefficient as determined by Chipman and Floridis[27].

This procedure yielded values for K_1 of 3.6×10^{-14} and 2.8×10^{-13} at 1600° and 1700°C respectively.

A comparison of the various data for the deoxidation constant of aluminium is shown in Fig. 4. The significance of the various results together with those of the present study will be discussed in the light of available thermodynamic data in Chapter VI.

4. The Activity of Chromium in Liquid Iron-Chromium Alloys

The phase diagram for iron-chromium alloys, first determined experimentally by Adcock[39], has been reviewed recently by Hellawell[40] (Fig. 5). Above 800°C, iron and chromium are miscible in all proportions in both the solid and liquid states. The atomic size and chemical properties of chromium are similar to those of iron. From consideration of these facts and other evidence[41], the liquid iron-chromium system has been regarded in the past as an

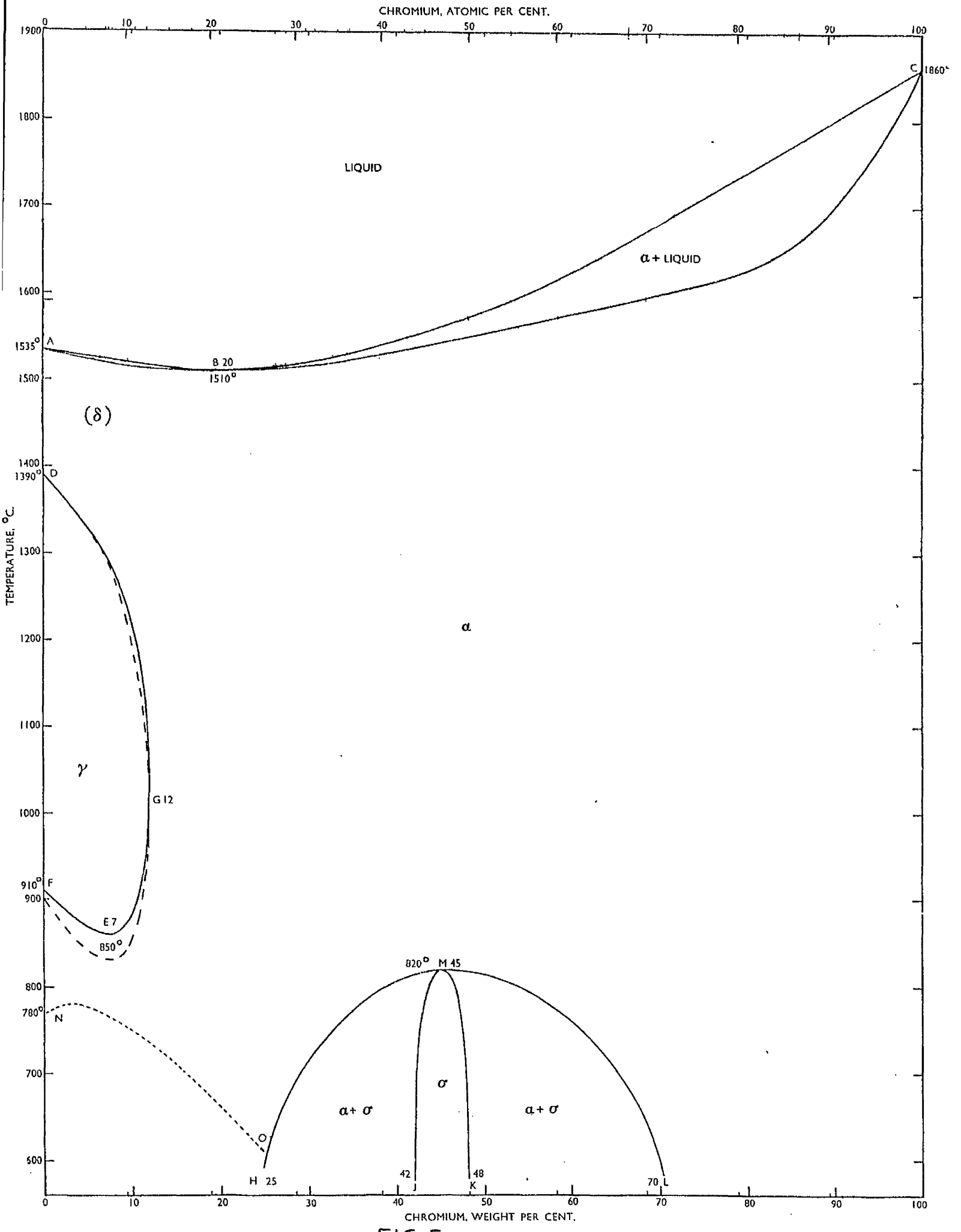
CHROMIUM, ATOMIC PER CENT.
0
10
20
30
40
50
60
70
80
90
100
1900
1800
1700
1600
1535°
A
1500
1400
1390°
D
1300
1200
1100
1000
910°
F
900
800
780°
N
700
600
TEMPERATURE, °C.
LIQUID
α + LIQUID
C
1860°
B 20
1510°
(δ)
α
γ
G 12
E 7
850°
820°
M 45
σ
α + σ
α + σ
O
H 25
42
J
48
K
70
L
CHROMIUM, WEIGHT PER CENT.

FIG 5

ideal solution.

Recently Lyubimov and Granovskaya[42] measured the partial pressure of chromium above liquid iron-chromium alloys using a radioactive technique. Their results indicated a positive deviation from Raoult's Law.

Using a similar technique, a more detailed study of the system has been made by Wada, Kawai and Saito[43]. Iron-chromium alloys, containing the isotope Cr^{51} were held at 1630°C in alumina crucibles. After degassing to a pressure of 5×10^{-4} m.m. Hg, a target was placed in the stream of vapourising atoms and a condensate collected over a period of 16 minutes. The ratio of the amount of chromium condensed to the total amount evaporated was considered to be a constant since the conditions were the same throughout the experiments. The amount of Cr^{51} condensed on the target was measured by a scintillation counter. Due to the high temperatures required, the investigation was confined to alloys containing up to 40 at. per cent chromium.

For the concentration range studied, the results indicated that the iron-chromium system could be regarded as a regular solution, showing a negative deviation from Raoult's Law. This deviation from ideality can be represented by the parameter

$$\epsilon_{C_R}^{(C_R)} = \partial \ln \gamma_{C_R} / \partial N_{C_R} \simeq +6.0 \quad \text{for } N_{C_R} = 0.0 \text{ to } N_{C_R} = 0.1$$

where the reference state for the activity coefficient is taken as the infinitely dilute solution of chromium in iron.

Charlton[44], who studied the reaction between chromium and oxygen in liquid iron at 1600°C using a water-vapour/hydrogen atmosphere to control the oxygen potential of the gas phase, has confirmed this negative deviation from ideality.

5. Chromium-Oxygen Equilibrium in Liquid Iron

In steelmaking processes one of the most important properties of any metal is the extent to which it reacts with oxygen in solution in the bath. This affinity of metals for oxygen dissolved in liquid iron varies over a wide range. Aluminium, for example, is a powerful deoxidising agent, whereas nickel, in this respect, is practically inert. Between these two extremes, there are a number of elements which have a moderate affinity for oxygen at steelmaking temperatures. An important alloying element in this category is chromium.

Although the oxide is not stable enough to make chromium a good deoxidiser, it is sufficiently stable for chromic oxide and chromite ($FeO \cdot Cr_2O_3$) inclusions to occur in steels containing significant amounts of the element. One of the practical problems of steelmaking is therefore to minimise the oxidation of chromium and its subsequent pick-up by the slag. From this point of view, a controlling factor which has a profound influence on the chromium -oxygen relationship, is temperature. This is evident from the following equation:

$$2Cr + 3/2O_2 = Cr_2O_3 \; , \; \Delta G = -267,750 + 62{\cdot}1\,T \text{ CAL}$$

The first detailed experimental investigation of the chromium-oxygen equilibrium in liquid iron was made by Chen and Chipman[41]. Iron-chromium alloys were melted in chromic oxide and chromite crucibles under a controlled water-vapour/hydrogen atmosphere and maintained at constant temperature until equilibrium was established between the crucible material, the melt and the gas phase. At the end of a heat the melt was quenched in a strong current of argon and subsequently analysed for chromium and oxygen.

Although the water-vapour/hydrogen gas mixture entering the furnace was preheated by suspended platinum wires at 1100°C, in an attempt to minimise thermal diffusion, it is quite possible in view of subsequent investigations[10,11,22] that this precaution was insufficient. Another source of error may be attributed to the fact that difficulty was experienced in determining the oxygen content of melts made in chromic oxide crucibles due to the entrapment of oxide particles. To overcome this effect a series of heats were made in alundum crucibles, the quantity of chromium charged being restricted and the gas atmosphere kept less strongly oxidising so that no chromite or chromic oxide was formed.

In the light of other investigations Chipman[45] has reassessed the experimental data of this study and has concluded that for the range 0 to 10 per cent chromium, the effect of chromium on the activity coefficient of oxygen at 1600°C may be represented by the parameter $\epsilon_O^{(Cr)} = 0.041$.

Similar investigations involving the equilibration of Fe-Cr-O melts with water-vapour/hydrogen atmospheres have since been carried out by Linczinskii and Samarin[46] and by Turkdogan[47]. Alumina crucibles were used in each case so that equilibrium was approached by oxidising chromium out of the metal. In the former study equilibrium was considered to have been attained as soon as an oxide phase appeared on the melt surface. This is obviously incorrect as it may have been necessary to oxidise considerable amounts of chromium out of the melt, for a particular gas composition. From this point of view it may well be that their results are subject to errors due to high chromium concentrations. As no further experimental details were given it is not known if adequate precautions were taken to prevent thermal diffusion. In addition no mention was made of the oxygen content of the melts studied.

In the study by Turkdogan, the gas was preheated and argon was added in the ratio 4 : 1. To ensure the attainment of equilibrium, heats were continued for two hours after the first appearance of slag on the melt surface. The composition range studied was from 4 to 12 per cent chromium and experiments were carried out at 1565°, 1600° and 1660°C. From the results obtained the activity coefficient of oxygen appeared to be independent of temperature.

In all three investigations mentioned above, it was assumed that chromium in iron behaved ideally.

Recently Charlton[44] has studied the solubility of oxygen in iron-chromium alloys in equilibrium with a water-vapour/hydrogen atmosphere

and either chromite or chromic oxide crucibles. The experiments were carried out in a molybdenum-wound resistance furnace and the gas mixture was bubbled through the melt. This procedure not only hastened the approach to equilibrium, but eliminated the possibility of thermal diffusion.

From the results of this particular study at 1600°C it was evident that iron-chromium alloys cannot be regarded as ideal solutions. Up to 10 per cent chromium a negative deviation from Raoult's Law was reported which substantiates the trend observed by Wada et alia[48].

The results of the different investigations are collected together in Table 3, where they are summarised in the form of interaction parameters.

Table 3 Chromium-Oxygen Parameters at 1600°C

Parameter	Chen and Chipman (41)(45)	Turkdogan (47)	Charlton (44)
$e_o^{(Cr)} = \partial \log f_o / \partial [\%Cr]$	- 0·041	- 0·064	-0·058
$\epsilon_o^{(Cr)} = \partial \ln f_o / \partial N_{Cr}$	- 8·8	-13·7	-12·4

6. The Activity of Silicon in Liquid Iron-Silicon Alloys

Silicon is widely used as an alloying element in steel and also as a deoxidiser in steelmaking. A knowledge of its behaviour in liquid iron is therefore of some importance. The fact that intermetallic compounds occur in iron-silicon alloys, implies that there is a chemical attraction between the two elements.

While it is probable that such compounds lose their identity in liquid metallic solutions, the attractive forces will still persist. This effect gives rise to a negative deviation from Raoult's Law and corresponds to a positive deviation from Henry's Law.

Chou[25] has determined the activity of silicon in liquid iron at 1550° and 1650°C by means of its partition between liquid iron and liquid silver. This work was later repeated and extended by Chipman, Fulton, Gokcen and Caskey[48] to cover the range $N_{Si}^{(Fe)}$ = 0·15 to 0·55. At concentrations greater than 0·55 $N_{Si}^{(Fe)}$ partial miscibility of the iron and silver layers occurred to an extent, which it was thought, might affect the activities in the two phases.

In order to determine the activity of silicon in liquid iron relative to that of pure silicon some further information is required in addition to that obtained from the partition experiments. As a check this information was derived from two independent sources. (1) the Fe-Si phase diagram and (2) the Ag-Si phase diagram. While calculations from data from these two sources were in reasonable agreement, it was felt that the data derived from the Fe-Si phase diagram were more dependable.

The distribution data were extrapolated to infinite dilution of silicon in iron with the aid of data derived from (a) the work of Gokcen and Chipman[22] on silicon-oxygen equilibrium in liquid iron, (b) the free energy of solution of oxygen in liquid iron[10,23] and (c) the free energy of formation of silica[49].

The distribution experiments were made at 1420°C and and the data for γ_{Si} in iron extrapolated to higher temperatures using the relationship $\partial \ln\gamma_{Si}/\partial(1/T) = \bar{L}_{Si}/R$. Since the temperature dependance of the heat of mixing was unknown, $\bar{L}_{Si}$ was treated only as a function of composition.

By this procedure a value of about 4 was obtained for the parameter $\epsilon_{Si}^{(Si)} = \partial \ln\gamma_{Si}/\partial N_{Si}$ at 1600°C. Chipman[50] has stated, however, that a more probable value from this data would be about 11. Very recently the results of two independent studies[51,52] of the distribution of silicon between liquid iron and silver have yielded a value of about 13 for this parameter at 1600°C.

7. Silicon-Oxygen Equilibrium in Liquid Iron

In steelmaking processes one of the most commonly used deoxidisers is silicon. Its behaviour in liquid iron containing oxygen can be represented by the following reaction.

$$SiO_2 = \underline{Si} + 2\,\underline{O}$$

$$K_1 = \frac{[a_{Si}][a_O]^2}{(a_{SiO_2})}$$

When considering the deoxidising power of silicon, an important factor is the nature of the slag. Thus in the case of basic slags the silica produced during deoxidation readily combines with the basic oxides CaO, MgO or MnO, its activity is reduced to

a low value and there is a consequent decrease in the product $[a_{Si}][a_o]^2$. If reoxidation of the melt by the slag can be prevented, this results in a more complete deoxidation than if slags saturated with silica were used, a condition closely approached in acid slag practice.

If the metal is in equilibrium with pure silica, or silica saturated slags, the equilibrium constant for the above reaction becomes.

$$K_1 = [a_{Si}][a_o]^2$$

or, as it is usually expressed.

$$K_1' = [\%Si][\%O]^2$$

The deoxidation product K_1', was first determined experimentally by Körber and Oelsen[53], who measured the equilibrium between molten iron containing manganese and $FeO-MnO-SiO_2$ slags contained in silica crucibles. Their value for K_1' at 1600°C was 3.6×10^{-5}.

Zapffe and Sims[54] studied the silicon-oxygen equilibrium in molten iron using silica crucibles and controlling the oxygen potential with a water-vapour/hydrogen gas mixture. Only a few melts were analysed for oxygen, the activity of oxygen in the remainder being calculated from the water-vapour/hydrogen equilibrium. Their results indicated that K_1' increased with the silicon content of the melts and this they explained by assuming that part of the

silicon existed as silicon monoxide dissolved in the metal. However, subsequent work by Gokcen and Chipman[22] on the rate of approach to equilibrium in Fe-Si-O melts, has shown that in the investigation by Zapffe and Sims, insufficient time was allowed for the attainment of equilibrium.

Hilty and Crafts[55] have carried out an extensive study of the silicon-oxygen equilibrium based on the slag-metal technique and using magnesia, alumina and silica crucibles together with a rotating crucible furnace. Heats were made at 1550°C, 1600° and 1650°C and metal samples analysed for silicon and oxygen.

Although it was found that the change in oxygen content of the metal with silicon content could be represented on a logarithmic plot by a straight line for each temperature, Hilty and Crafts stated that the data could be represented better by two intersecting curves. In addition, it was postulated that the intersection of the curves represented an invariant point which corresponded to an equilibrium between the three phases, liquid metal, liquid slag and solid silica. Darken[56] has pointed out, however, that the gradient of the curves at the point of intersection violates the law of heterogeneous equilibria, in that the metastable extensions pass into the homogeneous field of liquid iron.

The results of this study were reported in the form of an empirical deoxidation constant given by:

$$\log K_1' = \log [\%Si][\%O]^2 = -18,050/T + 5{\cdot}10$$

Gokcen and Chipman[22] have made a detailed study of the influence of silicon on the oxygen content of liquid iron in equilibrium with pure silica and water-vapour/hydrogen gas mixtures. In order to minimise thermal diffusion the inlet gases, with argon added in the ratio 4 : 1, were preheated to about 1500°C. On account of the slow approach to equilibrium, heats were continued for periods extending up to 18 hours. The melts were then quenched in a stream of hydrogen and subsequently analysed for silicon and oxygen. Although most of the work was carried out at 1600°C, several heats were made at 1545° and 1650°C.

From the results obtained, a study was made of the equilibria represented by the following reactions.

$$SiO_2\ (crist) = \underline{Si} + 2\,\underline{O}$$

$$K_1 = [a_{Si}][a_O]^2 \quad ; \quad K_1' = [\%Si][\%O]^2$$

$$SiO_{2(crist)} + 2H_2(g) = \underline{Si} + 2H_2O(g)$$

$$K_2 = [a_{Si}](p_{H_2O}/p_{H_2})^2 ; \quad K_2' = [\%Si](p_{H_2O}/p_{H_2})^2$$

$$H_2(g) + \underline{O} = H_2O_{(g)}$$

$$K_3 = p_{H_2O}/(p_{H_2} \cdot [a_O]) \quad ; \quad K_3' = p_{H_2O}/(p_{H_2} \cdot [\%O])$$

Although the results when plotted in the form log [%O] v log [%Si] do not confirm the apparent break in the curve reported by Hilty and Crafts, in general the two sets of data are in good agreement.

An attempt was made by Gokcen and Chipman to measure the effect of silicon on the activity coefficient of oxygen and hence the effect of oxygen on the activity coefficient of silicon. This involved the introduction of complex relationships between activity coefficient and concentration terms. However, in view of the results obtained from an analogous study of the Fe-Al-O system[56], these relationships were subsequently withdrawn[57]. Qualitatively the following conclusions appeared to be valid.

(1) The activity coefficient of oxygen is reduced by the addition of silicon.

(2) In dilute solutions the activity coefficient of silicon increases with its concentration.

(3) With respect to the equilibrium between silicon and oxygen in liquid iron the above effects are approximately compensating, and the product $[\%Si][\%O]^2$ remains almost constant in the range 0·02 to 15 per cent silicon. As a good approximation $K_1 = K_1'$.

Matoba, Gunjii and Kuwana[58] using the same type of experimental technique have restudied the various equilibria investigated by Gokcen and Chipman, and recently Chipman and Pillay[50] have published some results for the following reaction at 1600°C.

$$SiO_2(s) + 2H_2(g) = \underline{Si} + 2H_2O(g)$$

The three sets of data for this reaction are in good

agreement for silicon concentrations up to 1 per cent and are adequately represented by the equations proposed by Matoba et alia.

$$\log K_2 = \log [a_{Si}](p_{H_2O}/p_{H_2})^2 = -15,640/T + 4{\cdot}85$$

$$\Delta G_2^\circ = 71,540 - 22{\cdot}17\ T\ cal$$

The reference state for the activity of silicon is the infinitely dilute solution and $\log K_2$ was taken as the limiting value of $\log K_2'$ at 0 per cent Si for temperatures 1570°, 1625° and 1680°C.

The values obtained by Matoba et alia for the equilibrium constant $K_1 = [a_{Si}][a_O]^2$, are only slightly smaller than those of Gokcen and Chipman. At 1600°C the values are $2{\cdot}3$ and $2{\cdot}8 \times 10^{-5}$ respectively. Chipman and Pillay have calculated values for this constant by combining the data of Floridis and Chipman[11] with that of Matoba et alia.

$$H_2(g) + \underline{O} = H_2O(g)$$

$$\Delta G_3^\circ = -32,200 + 14{\cdot}63\ T_{cal}\ \text{(Floridis and Chipman)}$$

$$SiO_2(s) + 2H_2(g) = \underline{Si} + 2H_2O(g)$$

$$\Delta G_2^\circ = 71,540 - 22{\cdot}17\ T_{cal}\ \text{(Matoba et alia)}$$

Combining these equations.

$$SiO_2 = \underline{Si} + 2\,\underline{O}$$

$$\Delta G_1^\circ = +135,940 - 51{\cdot}43\ T\ cal$$

$$\log K_1 = -29,700/T + 11{\cdot}24$$

Values for K_1 calculated from the above equation are compared with experimental values in Table 4. It is evident that the data of Matoba et alia are in very good agreement with the calculated data of Chipman and Pillay.

Table 4 Comparison of Experimental Values for the Product $[\%Si][\%O]^2 \times 10^5$ with calculated Values for the Product $[a_{Si}][a_O]^2 \times 10^5$.

Temperature, °C.	1550	1600	1650
Körber and Oelsen[53]	1·3	3·6	10·6
Hilty and Crafts[55]	1·6	3·0	5·3
Gokcen and Chipman[22]	1·2	2·8	5·5
Matoba et alia[58]	0·8	2·3	6·1
Calculated Values[60]	0·9	2·3	6·0

Matoba and co-workers have derived values for the parameters $e_o^{(Si)}$ and $e_{Si}^{(Si)}$ assuming, in each case, that the influence of oxygen on the activity coefficients is negligible. Their value for $e_o^{(Si)} = \partial \log f_O / \partial[\%Si]$ was -0·13 valid for the temperature range 1570°C - 1680°C. The relationship between $e_{Si}^{(Si)}$ and the absolute temperature was reported to be

$$e_{Si}^{(Si)} = \partial \log f_{Si} / \partial[\%Si] = 3,910/T - 1·77$$

At 1600°C this corresponds to a value of about 36 for the

parameter $\epsilon_{Si}^{(Si)} = \partial \ln \gamma_{Si} / \partial N_{Si}$ compared to the value of approximately 13 derived from the data of partition experiments[51,52].

In Chapter VIII the results of Gokcen and Chipman and Matoba et alia are re-examined in the light of the results obtained from the present work and an attempt is made to explain the above discrepancy in the data for the activity of silicon in liquid iron.

8. The Effect of Silicon on the Activity Coefficient of Aluminium in Liquid Iron-Silicon-Aluminium Alloys

In an extension of their work on the distribution of aluminium between liquid iron and liquid silver at 1600°C Chipman and Floridis[27] have studied the distribution of aluminium between:- (a) Fe-C alloys and silver and (b) Fe-C-Si alloys and silver. The effect of silicon on the activity coefficient of aluminium, $\gamma_{Al}^{(Si)}$ was given by:-

$$\log \gamma_{Al}^{(Si)} = \log \gamma_{Al} - \log \gamma_{Al}^{(C)} - \log \gamma'_{Al}$$

where γ_{Al} is the activity coefficient of aluminium in Fe-Al-C-Si alloys,

$\gamma_{Al}^{(C)}$ represents the effect of carbon on the activity coefficient of aluminium,

and γ'_{Al} represents the activity coefficient of aluminium in the binary Fe-Al solution of the same aluminium concentration.

When the results were plotted in the form $\log \gamma_{Al}^{(Si)}$ v N_{Si} a straight line was obtained for silicon concentrations up to about 0·23 N_{Si}. At higher silica concentrations a slight curvature was evident. It was suggested that this might be due in part to

interaction effects in the silver layer where the atom fraction of silicon was as high as 0·08.

This suggestion was later confirmed by Chipman and Langenberg[38] who applied a correction for the effect of silicon on the activity coefficient of aluminium in the silver layer corresponding to $\epsilon_{Al}^{(Si)} = 7{\cdot}0$.

From this work it was found that for silicon concentrations up to 0·4 N_{Si} in iron, the parameter $\epsilon_{Al}^{(Si)} = \partial \ln \gamma_{Al} / \partial N_{Si}$ had the value + 6·9 at 1600°C.

This data was later recalculated by Wilder and Elliott[32] on the basis of their results for the activity of aluminium in liquid silver. This procedure yielded a value for $\epsilon_{Al}^{(Si)}$ of + 7·0 at 1600°C.

C H A P T E R IV

SOME EXPERIMENTAL CONSIDERATIONS

1. Effect of Thermal Diffusion on Gas-Metal Equilibrium Studies.

2. The Determination of the Water Vapour Pressure above Saturated Lithium Chloride Solutions.

3. Temperature Measurements with a Disappearing Filament Optical Pyrometer.

SOME EXPERIMENTAL CONSIDERATIONS

1. Effect of Thermal Diffusion on Gas-Metal Equilibrium Studies

When two gases of unlike molecular weight enter a tube in which there is a temperature gradient, a partial separation occurs, the heavier gas molecules tending to concentrate in the cooler zone, while the lighter molecules move towards the hotter zone. This phenomenon, known as thermal diffusion, is probably one of the most significant, though least obvious, sources of error occurring in the determination of equilibrium between a gas mixture and a condensed phase at an elevated temperature.

In the study of equilibrium between molten iron and a gas mixture of hydrogen and water vapour, one of the simplest ways of stirring the melt and thus hastening the approach to equilibrium is to use high frequency induction heating. However, this method of heating has the disadvantage that a sharp temperature gradient is set up at the gas-metal interface. with the result that the actual water-vapour/hydrogen ratio immediately above the melt surface is lower than the inlet ratio used in the computation of K values. Because of this effect, the oxygen content of the metal is lower than that which would be in equilibrium with gas of the inlet composition.

The phenomenon of thermal diffusion, predicted in 1911

by Enskog[59] and independently by Chapman in 1916[60], was first observed by Chapman and Dootson[61] in 1917. More recently, detailed investigations of the effect have been made by:-

Emmett and Schultz[62], who pointed out errors of as much as 40 per cent in the water-vapour/hydrogen ratios used in some of the earlier static determinations of equilibria.

Darken and Gurry[63], who described conditions for avoiding errors due to thermal diffusion in gaseous mixtures flowing into or out of a vertical tube furnace.

Dastur and Chipman[64], who investigated methods for eliminating the error under experimental conditions similar to those existing during the present study.

In the last mentioned work, two methods were used to minimise errors due to thermal diffusion. The first, and more obvious, method was to eliminate as far as possible, the sharp temperature gradient existing at the gas-metal interface by pre-heating the incoming gases. The second method was based on a kinetic approach to the problem, developed by Gillespie[65], in which it was shown that the relative separation of two gases by thermal diffusion was inversely proportional to the square root of the mean molecular weight of the mixture, and could, therefore, be decreased by the addition of a third gas of high molecular weight. Dastur and Chipman concluded that the error could be eliminated

by adequate preheating of the incoming gases, and in the absence of sufficient preheat, diminished by the addition of a heavy inert gas.

In recent studies of gas-metal equilibria in the temperature range 1550° to 1870°C, the gas preheater has been run at 1550 to 1600°C and argon added to the hydrogen in ratios between 4 • 1 and 6 • 1. In the present work several heats were made in the absence of preheat and a comparison of the results obtained is given in Table 5.

TABLE 5 Effects of Thermal Diffusion

With Preheat		Inlet Gas Composition	No Preheat	
Heat No.	Al, wt. pct	$P_{H_2O}/P_{H_2} \times 10^3$	Heat No	Al, wt pct
21	0·067	3·6	19	0·068
22	0·049	5·1	17	0·065
20	0·034	6·7	18	0·062

From consideration of the reaction

$$Al_2O_3(s) + 3\ H_2(g) = 2\ \underline{Al} + 3\ H_2O(g)$$

it is evident that the higher aluminium concentrations in the melts made without preheat indicate that the oxygen potential of the gas phase at the gas-metal interface was lower than that in the corresponding heats made with preheat.

Thus throughout the present study in order to minimise

errors arising from thermal diffusion, the gas mixture was preheated to about 1550°C and argon added in the approximate ratio 6 : 1.

2. The Determination of the Water Vapour Pressure above Saturated Lithium Chloride Solutions

To obtain the very low water vapour pressures required for the present study, by bubbling hydrogen through pure water, would necessitate rather awkward temperature control in the range -15 to + 18°C. However the same vapour pressures can be obtained by bubbling the hydrogen through a series of saturated lithium chloride solutions held at temperatures between 20 and 50°C. Because of the disagreement between reported values[66,67,68] for the vapour pressure of water above saturated lithium chloride solutions, it was decided to make an independent determination of the vapour pressure curve. A diagram of the apparatus used is shown in Fig. 6.

Cylinder hydrogen, via a calibrated flowmeter, was bubbled through a system of four glass vessels containing saturated lithium chloride solutions together with excess crystals of the salt. The vessels were immersed in a large water bath, the temperature of which was automatically controlled to with ± 0·05°C. The temperatures were measured with a thermometer, calibrated at the National Physical Laboratory.

From preliminary experiments it was found that the bubbler in the first vessel tended to choke up after about twenty-four hours due to crystallisation of lithium chloride; however, this difficulty

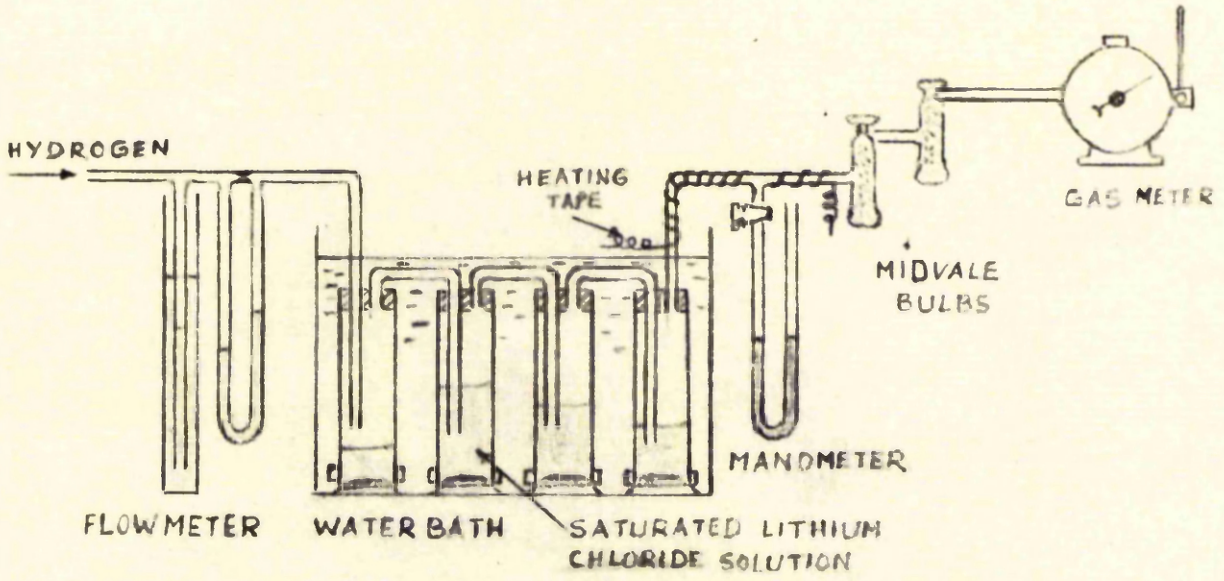

FIG.6 APPARATUS FOR THE DETERMINATION OF THE WATER VAPOUR PRESSURE ABOVE SATURATED LITHIUM CHLORIDE SOLUTIONS

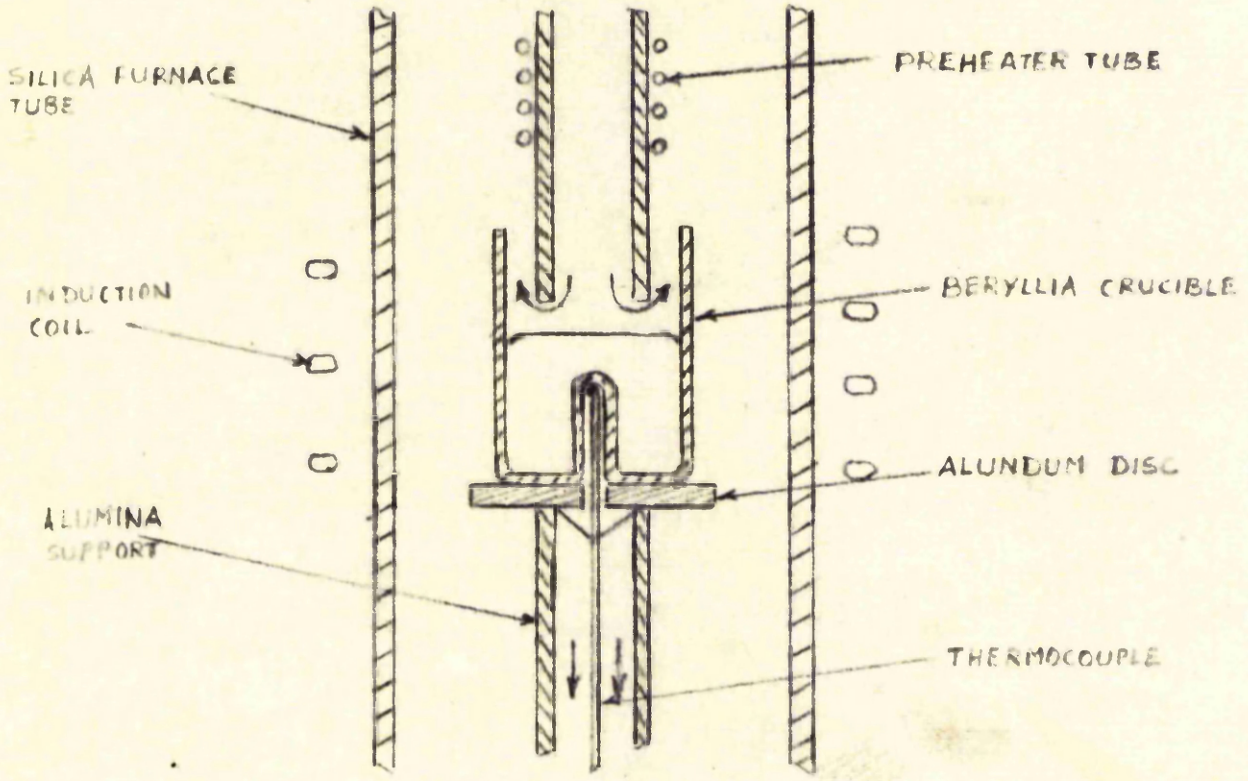

FIG 8 FURNACE ARRANGEMENT FOR CALIBRATION OF OPTICAL PYROMETER

was overcome by keeping the entrant tube about half an inch above the surface of the solution. After saturation, the pressure was measured on a manometer and the gas mixture led off through a glass tube which, in order to prevent condensation, was maintained at about 70°C by an "Isothermal" heating tape. The water vapour was absorbed by leading the gases through two weighed midvale bulbs containing magnesium perchlorate and the total volume of hydrogen passing through the system in a given time measured with a wet-type laboratory gas meter.

The performance of the saturator system was checked using distilled water in place of the lithium chloride solutions and the results were within ± 0·2 per cent of the theoretical values. A number of runs were made using lithium chloride solutions with gas flow rates varying from 75 to 300 cc/minute, and under the experimental donditions described, the results were reproducible to within ± 0·03 mm Hg. In the calculation of vapour pressures, it was assumed that water vapour had the properties of an ideal gas since the correction for deviation from ideality in the pressure range covered here is less than 0·07 per cent[66].

The vapour pressure data used throughout the present study together with the results of previous workers are shown in Fig. 7. At lower temperatures the present results agree well with those of Gokcen[66], Huttig[67] et al, and, when extrapolated, with the single determination by Lannung[68], although in this case there is some doubt

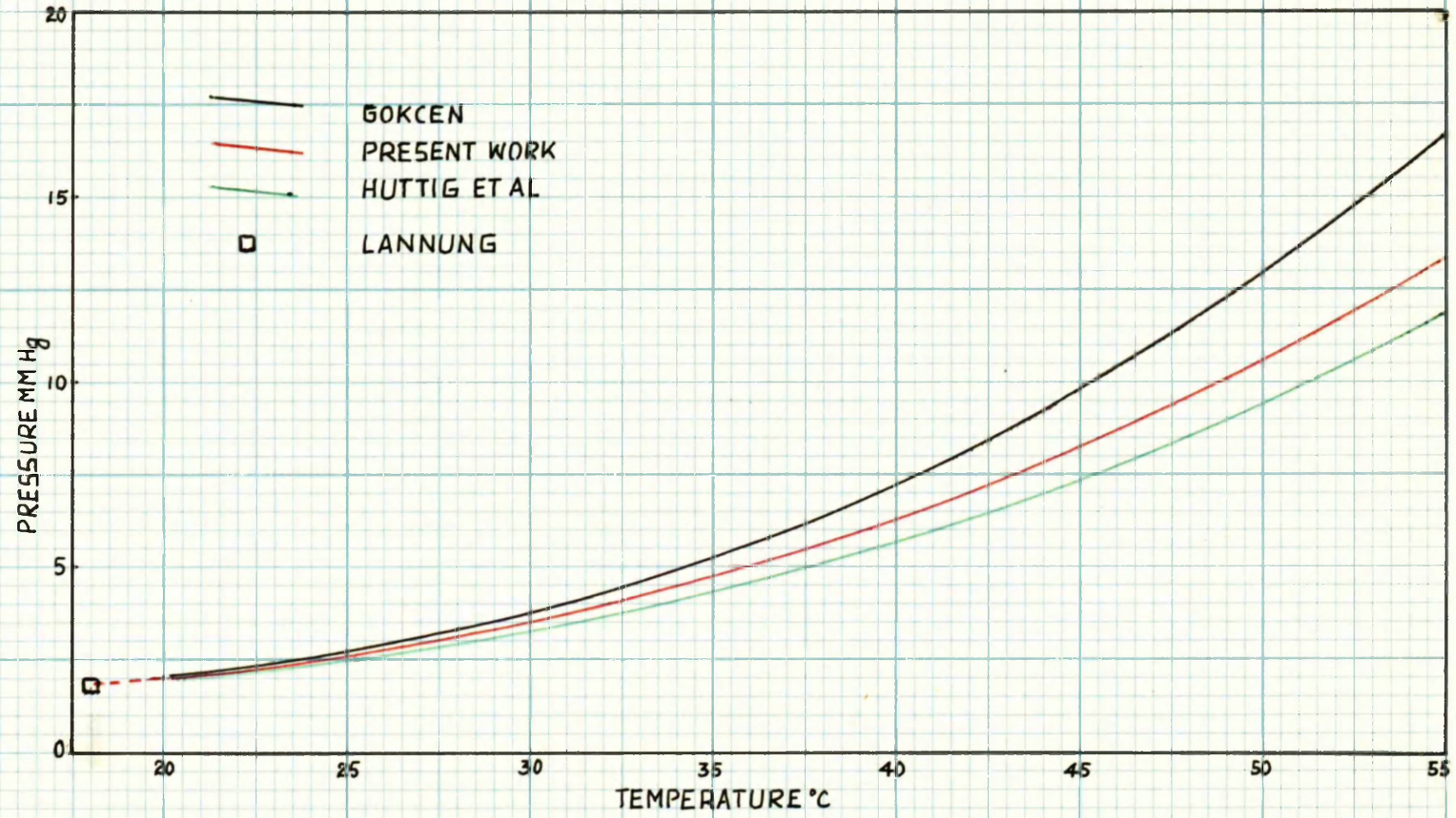

FIG 7 VAPOUR PRESSURE OF SATURATED LITHIUM CHLORIDE SOLUTIONS

as to the composition of the solid phase present, due to the fact that lithium chloride undergoes the following transformations, according to measurements made by Appleby and Cook[69]

$$LiCl \cdot 2H_2O \xrightarrow{19 \cdot 1^\circ C} LiCl \cdot H_2O + H_2O$$

and $$LiCl \cdot H_2O \xrightarrow{93 \cdot 55^\circ C} LiCl + H_2O$$

As the temperature increases, the curves gradually diverge. In this respect it is perhaps worth noting that the results of the earlier investigation by Huttig showed poor reproducibility in comparison with those of Gokcen, which were reproducible to within $\pm$ 0·02 mm Hg. One reason for the lack of consistency in the data may be the presence of different impurities in the lithium chloride. For the lithium chloride used in the present work the maximum limits of impurities were as follows:-

0·02 per cent sulphate (SO_4), 0·002 per cent iron, 0·001 per cent lead, 0·0001 per cent arsenic.

Other errors may occur if insufficient time is allowed for the lithium chloride solutions to come to equilibrium with solid lithium chloride at any particular temperature. Thus in the present work erratic results were obtained when runs were made about two hours after altering the water bath temperature by about 10°C. In the procedure adopted, therefore, the thermostat was adjusted to the desired value, and the solutions left overnight before measuring the vapour pressure at that temperature.

3. Temperature Measurements with a Disappearing Filament Optical Pyrometer

During the experimental runs temperature measurements were made at frequent intervals by means of an Evershed High Precision Disappearing Filament Optical Pyrometer sighted on the clean surface of the melt. A calibration curve for the instrument was obtained in the following way. A charge of 20 g of electrolytic iron contained in a specially designed beryllia crucible having a re-entrant tube at the bottom was held in the furnace under exactly the same conditions as those prevailing during the equilibrium determinations, i.e. in a preheated gas stream of purified argon and hydrogen containing a small controlled amount of water vapour [Fig. 8]. This gas stream, sweeping across the surface of the molten iron minimised errors resulting from the presence of iron vapour. A 5 per cent Rh-Pt/20per cent Rh-Pt thermocouple, previously checked against the melting point of palladium was pushed up through the central crucible support until the bead junction was positioned inside the re-entrant tube.

By careful adjustment of the power input from the high frequency unit, it was possible to check both the optical pyrometer and the thermocouple against the melting point of the electrolytic iron, taken as 1535°C. The power input was then increased slightly and when a constant and steady temperature had been obtained, simultaneous readings were taken on the optical pyrometer and the thermocouple-potentiometer. This procedure was repeated a number of times and readings taken at intervals during heating agreed

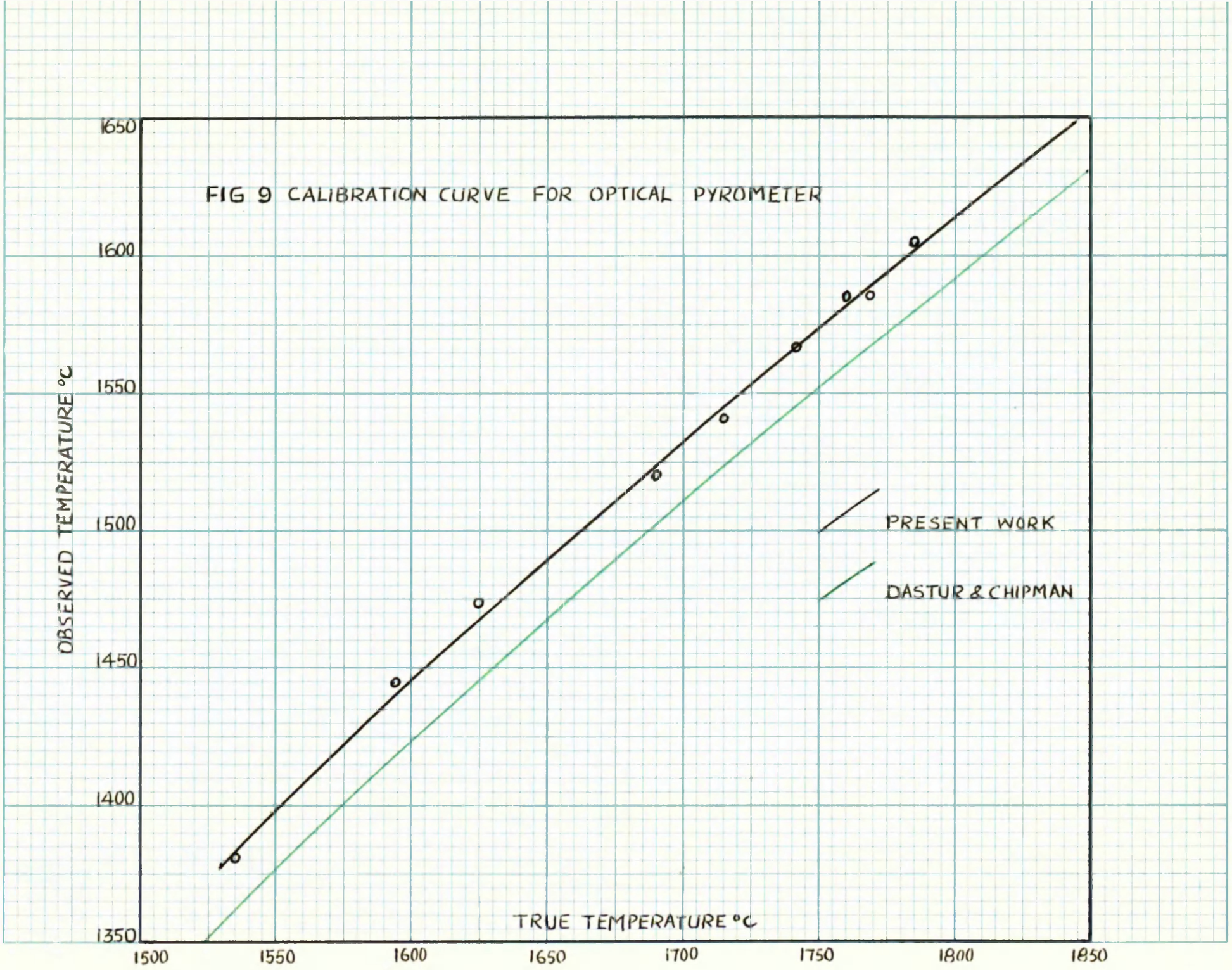
FIG 9 CALIBRATION CURVE FOR OPTICAL PYROMETER
OBSERVED TEMPERATURE °C
1650
1600
1550
1500
1450
1400
1350
TRUE TEMPERATURE °C
1500
1550
1600
1650
1700
1750
1800
1850
PRESENT WORK
DASTUR & CHIPMAN

well with those taken at intervals during cooling, thus indicating the absence of a temperature gradient between the molten metal and thermocouple.

The observation by Schofield and Grace[70], that platinum-rhodium alloy thermocouple readings were unaffected by the field present in a high frequency induction coil was confirmed during the calibration experiments when it was found that momentarily cutting off the input supply had no effect on the potentiometer readings.

From a number of measurements made with the gas preheating coil cold, it was concluded that the optical readings were independent of the preheater temperature. This is in agreement with the findings of Dastur and Gokcen[71] who calibrated an optical pyrometer under somewhat similar conditions.

The results of true (thermocouple) and observed (optical) temperature readings are plotted in Fig. 9 to give the calibration curve which was used throughout this study. This takes into account the emissivity of the iron as well as the absorption of the optical system. Strictly speaking this curve refers to pure iron, but Gokcen and Chipman[22] have shown that the emissivity of iron is unaffected by the addition of silicon up to 13·6 per cent provided the melt surface is not covered by scum. This was confirmed in the present work by checking the melting point of the various iron-silicon alloys used at the beginning of a heat. It was assumed from observations made on the melting points of iron-chromium alloys that the data was also unaffected by the presence of chromium up

to 10 per cent.

Actual reading on the pyrometer were reproducible to within $\pm$ 3°C and the temperature during equilibrium runs could be kept constant within $\pm$ 10°C by controlling the power input from the generator. The estimated uncertainty in the calibration curve is also of this order.

C H A P T E R V

APPARATUS AND EXPERIMENTAL TECHNIQUE

1. The Gas System

2. The Furnace Arrangement

3. Materials

4. Experimental Procedure

5. Approach to Equilibrium

6. The Determination of Aluminium

7. The Determination of Oxygen.

APPARATUS AND EXPERIMENTAL TECHNIQUE

1. The Gas System

A diagram of the gas system is shown in Fig. 10. High purity hydrogen containing less than 10 parts/million oxygen was led through

a calibrated flowmeter (A),

soda asbestos (B) to remove any carbon dioxide present,

anhydrone (C) to remove moisture,

platinised asbestos at 450°C (D) to convert any oxygen present in the hydrogen to water vapour, and

saturated lithium chloride solutions (E).

Finally, purified argon was added in the ratio 6 : 1 and the ternary mixture introduced into the furnace.

In the argon purification line, the gas was passed through

a calibrated flowmeter (A),

soda asbestos (B) to remove carbon dioxide,

anhydrone (C) and phosphorous pentoxide (G) to dry the gas, and

calcium turnings at 700°C (H) to take up any oxygen present.

A by-pass (J) was provided so that the hydrogen line could be flushed out with argon whenever required. The two flowmeters were calibrated by displacement of water from an inverted litre flask and the calibration curves checked with a wet-type laboratory gas meter.

FIG 10 THE GAS SYSTEM

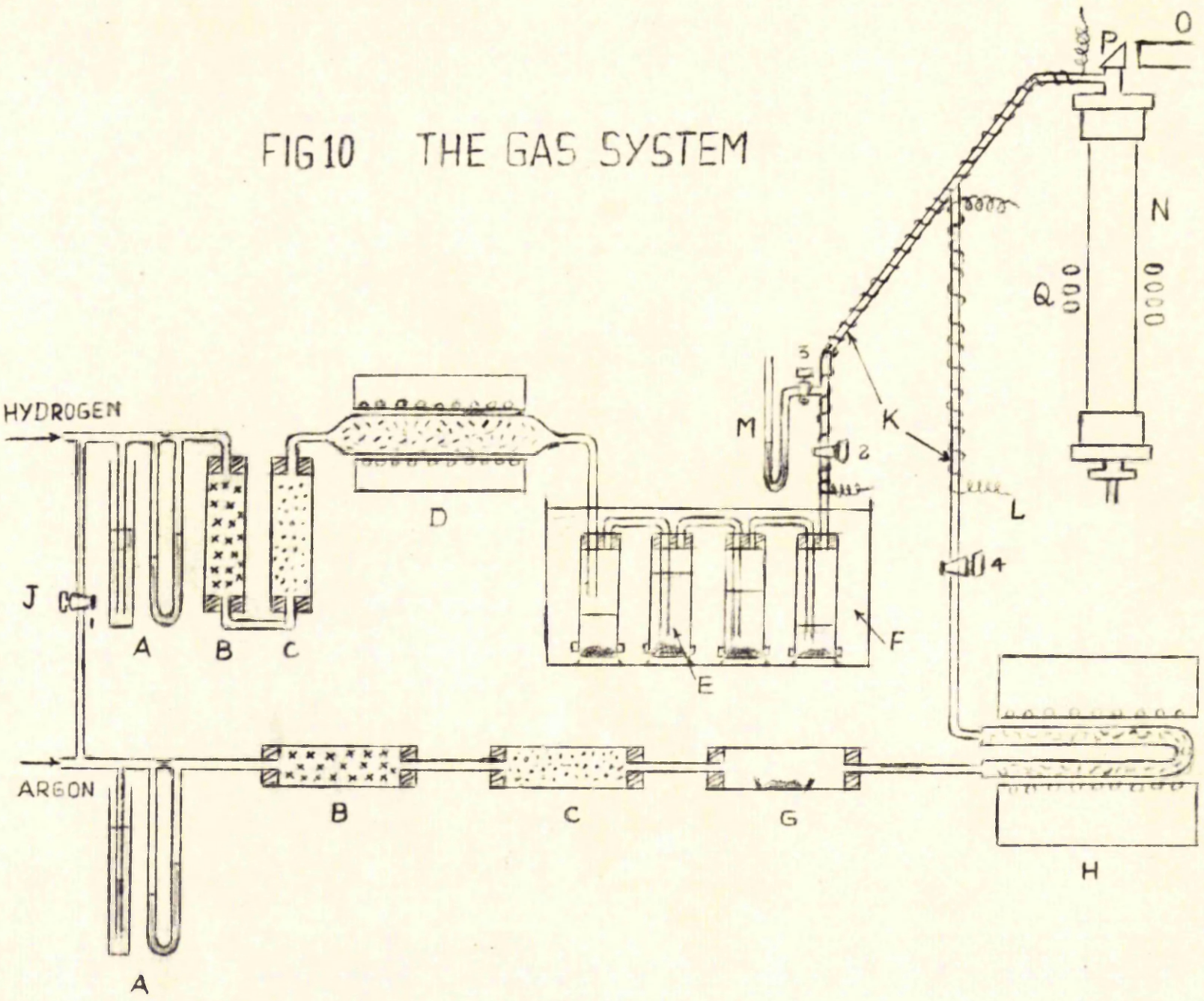

A FLOW METER
B SODA ASBESTOS
C ANHYDRONE
D PLATINISED ASBESTOS (450°c)
E SATURATED LiCl SOLUTIONS
F WATER BATH
G PHOSPHOROUS PENTOXIDE
H CALCIUM TURNINGS (700°
J BY-PASS
K COPPER TUBE
L HEATING TAPE
M MANOMETER
N REACTION FURNACE
O OPTICAL PYROMETER
P PRISM
Q INDUCTION COIL

Copper tubing was used to convey the argon from the calcium furnace, and the Hydrogen from the saturator system into the reaction chamber. This tubing was heated by an "Isothermal" heating tape to about 70°C to prevent condensation of water vapour. The pressure within the system was measured with a small manometer connected by a tap to the gas line in the position shown in Fig. 10, and was usually of the order of 5 mm mercury.

2. The Furnace Arrangement

(a) The Reaction Chamber - The reaction chamber, a diagram of which is shown in Fig. 11, was similar to that used by Chipman and co-workers for the study of a number of gas-metal reactions[22,36]. It consisted of a glazed surface silica tube (K) 24 inches long and 2 inches internal diameter with water cooled brass end plates (H). The top plate was fitted with a gas inlet, a small sight glass (A) to allow temperature measurements to be made with an optical pyrometer, and a preheater tube (G) cemented into position with water glass.

The alumina crucible (M) was positioned on an alundum disc (O) which rested on an alumina tube (P) which was in turn supported by a stainless steel tube (Q). This support system, which also served as a gas outlet, could be moved up or down inside the furnace as desired by means of an asbestos gasket (U) set into the brass base plate (T). This plate was also fitted with two copper tubes (R) pierced at intervals with small holes so that the melt could be quenched in a stream of hydrogen when lowered into position between

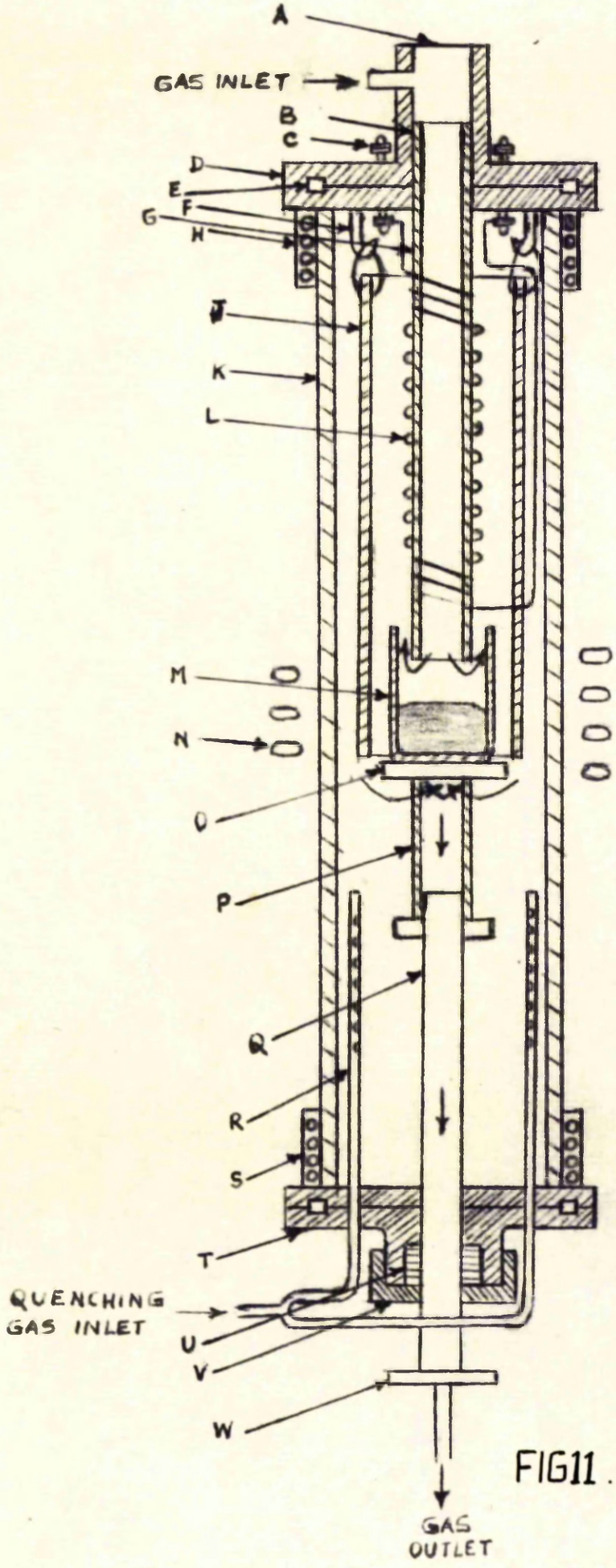

A	SIGHT GLASS
B	WATER GLASS CEMENT SEAL
C	PREHEATER TERMINALS
D	BRASS TOP
E	RUBBER GASKET
F	SUSPENDING HOOK
G	PREHEATER TUBE
H, S	WATER COOLING COIL
J	ALUNDUM INSULATING SLEEVE
K	GLAZED QUARTZ TUBE
L	PREHEATER COIL
M	RECRYSTALLISED ALUMINA CRUCIBLE CONTAINING MELT
N	INDUCTION COIL
O	ALUNDUM SUPPORT
P	RECRYSTALLISED ALUMINA TUBE
Q	STAINLESS STEEL TUBE
R	COPPER QUENCHING TUBE
T	BRASS BOTTOM
U	ASBESTOS PLUG
V	BRASS CAP
W	STEEL HANDLE

FIG11. THE REACTION CHAMBER.

the jets at the end of a heat.

The power required for melting was supplied by a 20 kilo-watt, 400 kilo-cycles/sec Philips high frequency generator.

(b) The Preheater - A recrystallised alumina tube 14 inches long and 0·5 inches internal diameter was wound over a distance of 10 inches at 10 turns per inch with 22 gauge platinum -10 pct rhodium wire and the wire leads connected to ceramic coated terminals soldered into the brass top. A thin coating of silica-free alumina cement held the winding in position on the alumina tube. As shown in Fig. 11, the preheater was enclosed by an alundum insulating sleeve, 12 inches long and 1·25 inches internal diamter suspended with iron wire from two hooks screwed into the brass cap. The preheater temperature was controlled by means of a variable transformer and measured by focussing the optical pyrometer on the inner walls of the tube.

Under the experimental conditions, contamination and subsequent failure of the winding occurred after about 100 hours at 1550°C. The fractured sections of the wire were brittle, coarsely granular and adhered strongly to the alumina protective coating. This effect has also been observed by Gokcen and Chipman[22] who suggested that localised impurities in the alumina were reduced by hydrogen at very low water vapour-hydrogen ratios, and then absorbed by the wire, thus making it very brittle. In a subsequent investigation by the same authors[36] the preheater was run at a lower

temperature in an attempt to prolong the life of the coil.

In the present work, after the failure of two platinum-rhodium alloy windings, it was decided to replace them with a 24 gauge molybdenum wire. This proved to be much more successful in that the coil had a working life in excess of 500 hours at 1550°C.

(c) Quenching Technique - At the end of a heat, the melt was lowered to a position just below the upper jet holes in the copper tubes and quenched in a stream of hydrogen at 15 to 20 p s i, a technique introduced by Gokcen and Chipman[23]. The time required for freezing was usually about 5 to 10 seconds. On a few occasions, when the crucible support was pulled down, the crucible was left sticking to the end of the preheater tube due to the presence of an iron deposit caused by volatilisation of the melt. In such cases, the solidification time was about 15 to 20 seconds. During the quenching treatment, tap 2 (Fig. 10) was closed to prevent "blow-back" of the lithium chloride solutions into the platinised asbestos furnace.

2. The Materials Used

Metal charges weighing 20 g were prepared from the following materials mixed together in the required proportions and compressed into cylindrical shaped pellets 14 mm in diameter and 10 mm high.

(a) "Sintrex" electrolytic iron powder supplied by G. Cohen, Sons and Co., Ltd., London(containing a maximum of 0·015 pct carbon, 0·040 pct manganese, 0·010 pct silicon, 0·020 pct sulphur and 0·015 pct phosphorus.

(b) Grade A electrolytic lump chromium (containing a maximum of 0·015 pct carbon, 0·010 pct sulphur and 0·040 pct silicon.

and (c) High purity silicon metal (containing a maximum of 0·1 pct aluminium.

Both (b) and (c) were supplied by Union Carbide and Carbon Corporation.

The pellets were contained in cylindrical, recrystallised, alumina crucibles (height 33 mm, outside diameter 22 mm, wall thickness 1 mm) supplied by Morgan Refractories, Ltd.

4. Experimental Procedure

The metal charge, weighing about 20 g and contained in an alumina crucible was positioned by means of the movable crucible support, such that the exit end of the preheater tube was 0·3 inches inside the crucible. The apparatus was checked to ensure the absence of leaks by passing gas through the system at a slow flow rate, closing the gas outlets from the furnace and observing the behaviour of the flowmeters. The water bath thermostat was set, the purification furnaces and heating tape switched on, the gas flow rate adjusted to approximately 15 cc per min hydrogen and 90 cc per min argon, the preheater brought up to about 1200°C over a period of about one hour in order to avoid excessive thermal shock, and the apparatus left overnight.

Next day, the gas flow rate was increased to 150 cc per min. hydrogen and 900 cc per min argon, the preheater temperature brought

up to about 1550°C, the high frequency induction furnace switched on and the metal heated to the required temperature within two minutes. Heats were made at the two temperature levels 1723° and 1823°C.

During a heat, the temperature of the melt was observed with the optical pyrometer and controlled to within ± 10°C of the required temperature by altering the circuit induction. After holding the melt at constant temperature for sufficient time to ensure the attainment of equilibrium, usually between ten and twelve hours, it was quenched in a stream of hydrogen as described previously.

5. Approach to Equilibrium

Several heats were made at 1723° and 1823°C in order to establish the approximate times required for the attainment of equilibrium. Data for these heats are given in Table 6 and Fig. 12.

TABLE 6 Approach to Equilibrium

Heat No	Temp °C	Hours at Temp	P_{H_2O}/P_{H_2} x 10^3	Al, wt pct
1	1823	6·0	4·98	0·0265
2	1823	10·0	4·98	0·0328
3	1823	1·0	3·48	0·0193
4	1823	4·5	3·48	0·0467
5	1823	12·0	3·48	0·0666
6	1723	6·0	3·54	0·0174
7	1723	12·0	3·54	0·0217

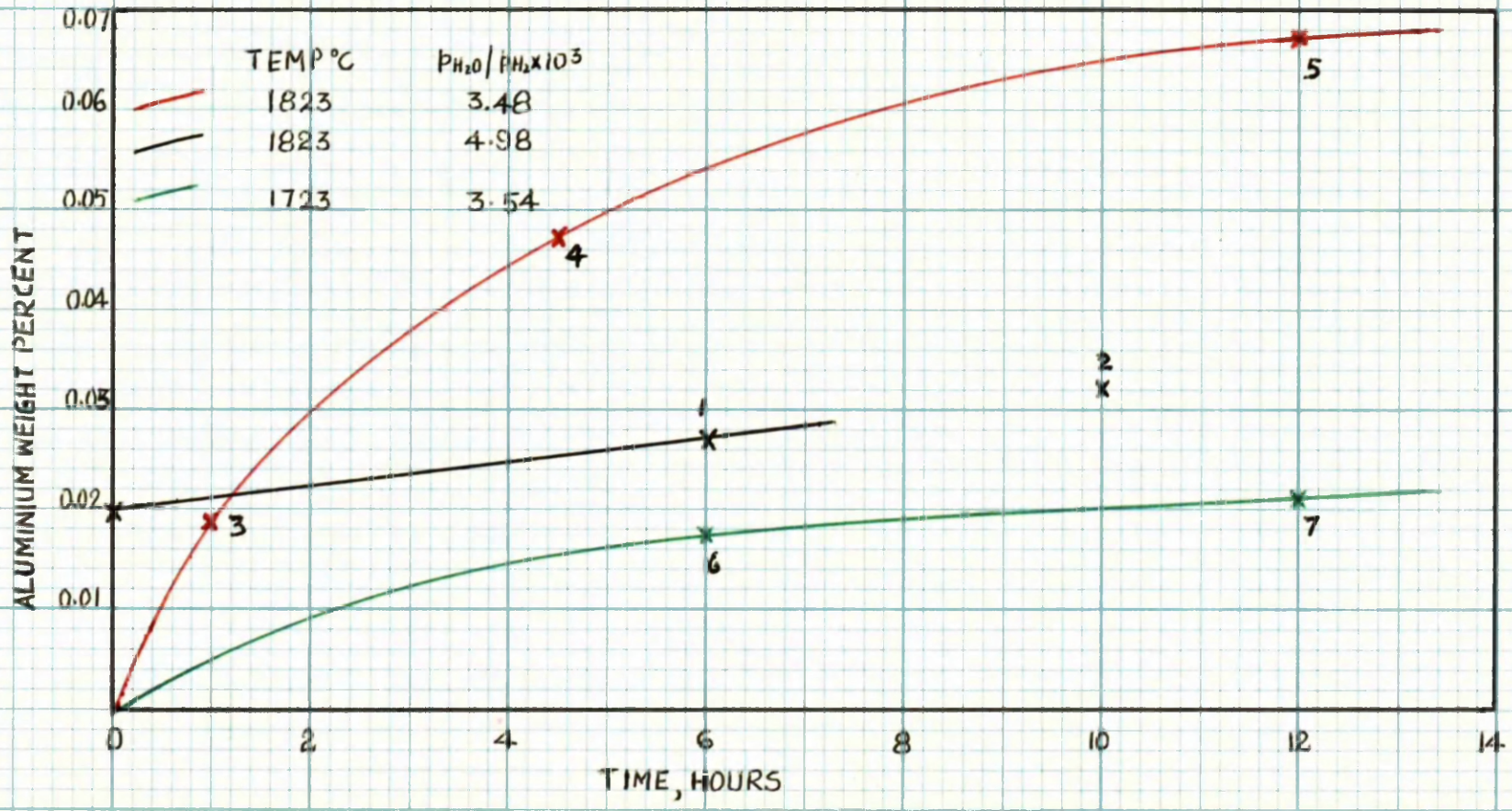

FIG 12. APPROACH TO EQUILIBRIUM

In Heat 1, 0·02 per cent aluminium was added to the charge in the form of a 10 per cent Fe-Al alloy. In the remainder of the heats the intiial charge consisted of pure iron.

From the various data it is evident that a period of between ten and twelve hours is required for equilibrium. Longer times are not justified since the analysis for aluminium is not sufficiently precise to detect small the changes involved.

6. The Determination of Aluminium

The aluminium content of the iron samples was determined by a colorimetric technique based on a method described by Hill[72] for carbon and low alloy steels. This method depends on the fact that when ascorbic acid is added to an acid solution of trivalent iron, an oxidised derivative of ascorbic acid is formed which complexes the iron and minor amounts of other reducible elements present in the steel.

"Solochrome Cyanine R" was used in the nitrated condition to form a coloured complex with the aluminium. The nitrated dye solution was made up by adding 2 cc of 1·20 specific gravity nitric acid to 0·3500 g of solochrome cyanine R in a dry beaker, the solution swirled for 2 minutes at room temperature until orange-red, 75 cc of water added followed by 0·25 g of urea to remove the nitrous acid formed during the nitrating treatment and which would otherwise decrease the dye stability. After swirling again the solution was diluted to 1 litre. In this condition the dye was stable for a period of at least six months.

The coloured aluminium complex is most stable at a pH of 5·5 and this condition was obtained with the aid of a sodium acetate buffer made up by dissolving 400 g of sodium acetate trihydrate in a litre of water and adjusting the pH with either sodium hydroxide or acetic acid to give a value of 6·5, which, under the experimental conditions described, gives a pH of 5·5 in the test solutions.

A 0·5000 g sample was dissolved in 10 cc of 10 per cent sulphuric acid, 25 cc of 3N nitric acid added, the nitrogen oxides boiled off, a small excess of saturated potassium permanganate solution added, the solution boiled for a further 2 minutes to ensure complete oxidation and the excess permanganate reduced by a dropwise addition of 10 per cent sodium nitrite solution and 2 drops added in excess. The oxides of nitrogen were again boiled off, the solution cooled, transferred to a 250 cc volumetric flask, diluted to volume and well shaken.

To a 5 cc aliquot in a 25 cc volumetric flask were added 5cc of 1 per cent ascorbic acid together with 5 cc of the dye solution followed after 1 minute by 5 cc of the buffer solution. After standing for 3 minutes to allow the coloured complex to form, the solution was diluted to volume, well shaken and the absorbance measured against an aluminium free, pure iron blank, carried through all the steps of the above procedure at 535 mμ in 1 or 2 cm cells on a Unicam S.P. 600 spectrophotometer.

The per cent aluminium present in the sample was determined from a calibration curve previously constructed by adding known

amounts of aluminium in the form of aluminium ammonium sulphate to 0·5000 g of pure iron and processing these samples as described previously. The calibration curve was checked against standard steel samples issued by the Bureau of Analysed Samples, Ltd. The two standards M.S. 271 and M.S. 272 had aluminium contents of 0·008 and 0·064 per cent respectively. Average deviation in duplicate analyses was usually of the order ± 0·0005 per cent.

It is worth noting that the ascorbic acid solution must be made up fresh for each determination and that the coloured test solution should be examined within 30 minutes of making up the ascorbic acid after which time the colour of the solution gradually changes. In the present work test solutions were examined 20 minutes after making up the ascorbic acid and steady readings were then obtained on the spectrophotometer over a period of about 10 minutes.

Although the above procedure was satisfactory for iron-aluminium alloys and even iron-silicon-aluminium alloys, at least within the range of silicon contents studied, it was found that 2 per cent chromium and above, blocked the formation of the aluminium complex. Thus, in the case of the iron-chromium-aluminium alloys, the chromium, and incidentally the iron, was first removed by a mercury cathode electrolysis separation.

The sample was dissolved as before by warming with 10 cc of 10 per cent sulphuric acid, the solution diluted to 100 cc and electrolysed using a mercury cathode and a platinum disc anode. After

about 30 minutes the green colour of the solution gradually disappeared as more and more chromium was taken up in the mercury. After a further 15 minutes spot tests made on the electrolyte for chromium and iron confirmed their absence and the electrolyte was then rapidly transferred to another beaker, and the remaining mercury washed by decantation. The minute quantity of chromium or iron which might be returned to the solution during this treatment is small and can readily be complexed later by the ascorbic acid. The solution was boiled to reduce its bulk, treated with 3N nitric acid and the estimation completed as previously described.

7. The Determination of Oxygen

The oxygen content of the metal was determined by a vacuum fusion technique. A schematic diagram of the apparatus is shown in Fig. 13 and 14. The furnace side of the equipment is similar to that described by Murad[73], but the pumping and gas analysis systems have been altered.

The Pumping System

Evacuation of the apparatus was carried out by means of an Edwards "Speedivac" rotary pump, type 1S50 with an integral phosphorous pentoxide moisture trap, backing an Edwards mercury diffusion pump, type 2 M 4. An Edwards "Speedivac" 1/2" magnetic valve at the rotary pump end of the backing line acted as a safety device in case of electrical failure by isolating the vacuum system and admitting air to the rotary pump and so preventing flooding of the system with pump oil.

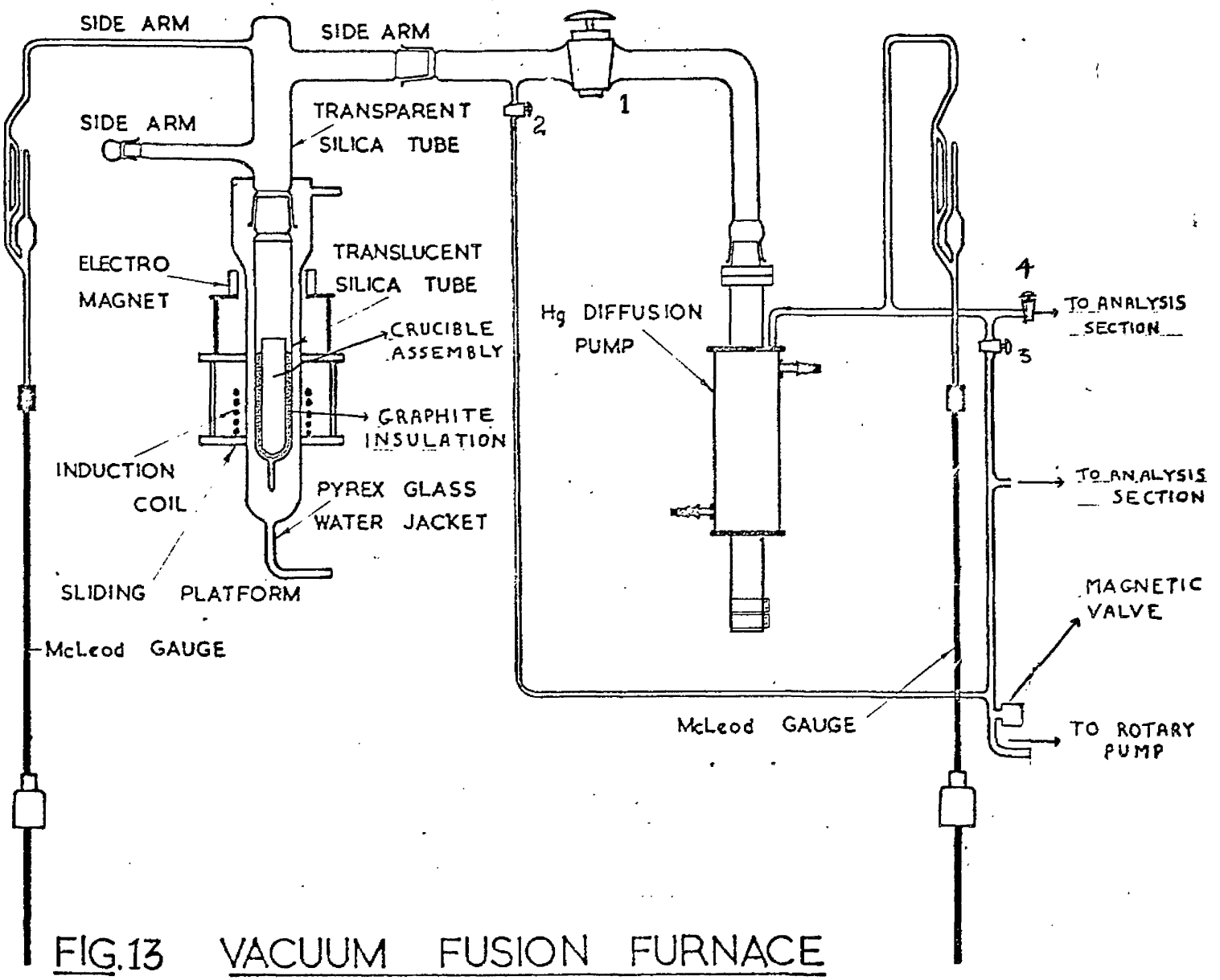

FIG.13 VACUUM FUSION FURNACE

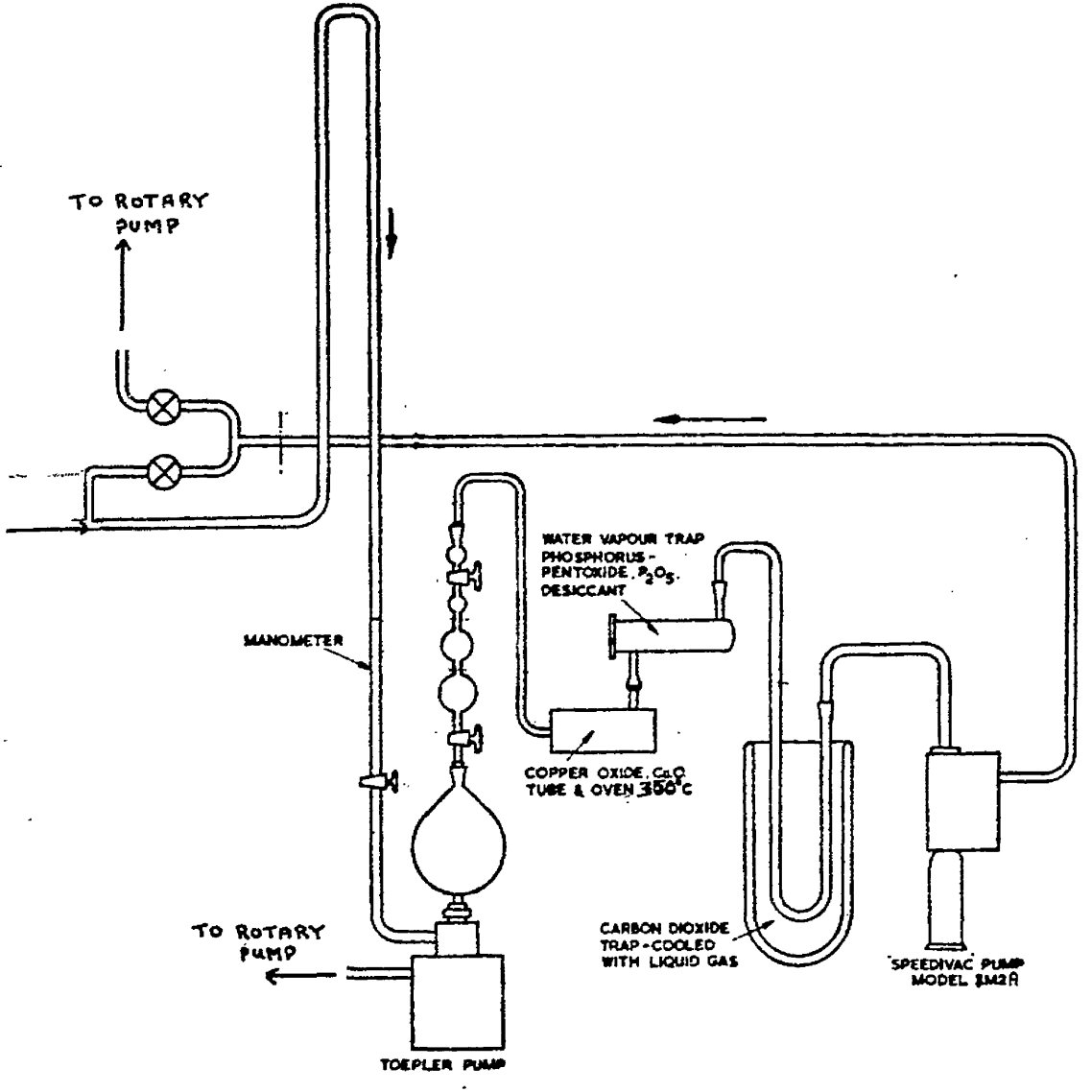

FIG-14 ANALYSIS SECTION

The diffusion pump gave an ultimate pressure of 10^{-6} mm of Hg and the rotary pump gave a backing pressure of 5×10^{-3} mm of Hg. An Edwards "Speedivac" rotary pump, type 1S150 was used to operate the McLeod gauges and also the Toepler pump on the gas analysis side of the equipment

The Gas Analysis System

The gas collection space consisted of a 90 cm glass manometer mounted beside a Toepler pump having an approximate volume of 1000 cc together with a series of calibrated bulbs giving total volumes of 1·26, 5·21, 20·66 and 51·76 cc.

The gas collected from the metal samples was mainly carbon monoxide and hydrogen and after compression to a known volume in the calibrated bulbs, its pressure was read on the manometer by using the Toepler pump as a form of McLeod gauge. The various taps were then set so that the gas could be drawn through the analysis system by means of an Edwards "Speedivac" mercury diffusion pump, type 1 M 2 A which gave an ultimate pressure of 10^{-6} mm of Hg. The carbon monoxide and hydrogen were oxidised at 350°C over cupric oxide, formed by heating copper powder in air. The water vapour formed was absorbed by passing the gases over phosphorous pentoxide and the remaining gas once again collected in the calibrated bulbs, compressed to the same volume as before and its pressure noted. Simple

subtraction of the two pressure readings gave the partial pressure of the hydrogen. The gas was again circulated in this instance with liquid oxygen in the cold trap, thereby freezing out the carbon dioxide. The remaining gas was collected, compressed, the pressure noted and the partial pressure of carbon dioxide obtained by subtraction.

From the partial pressures, volumes and temperatures of the gases, their respective volumes at N.T.P. can be calculated, which, together with a knowledge of the blank for the apparatus, allows the gas content of the metal to be determined.

Some Notes on the Experimental Technique

(i) Preparation of the Samples

Samples were taken from the metal by means of a fine toothed hacksaw and the surfaces and edges abraded with a fine-cut file to give specimens roughly cylindrical in shape with rounded ends, about 15 mm long, 5 mm in diameter and weighing 2 to 3 g. They were then cleaned in benzene and acetone, dried, weighed and introduced into the sample arm of the apparatus.

(ii) Evacuation of the Furnace Chamber

The furnace tube was packed with -200 mesh high grade graphite powder and sealed in position with Apiezon Wax W-40. The initial pump down of the furnace side was carried out by means of the rotary pump with tap 2 open and tap 1 closed. In this way the

diffusion pump was bypassed and could therefore be kept under high vacuum except when taps 1, 3 and 4 required cleaning, after which about 100 hours continuous running were necessary to degas the pump.

In order to avoid puffing of the graphite powder with consequent loss of insulation and carry-over of carbon into other parts of the equipment, the air inlet on the magnetic valve, fully open at the start of the pump-down, was gradually closed over a period of about 15 minutes. As a further precaution against puffing, fresh graphite powder was always dried overnight at 200°C before use.

(iii) Degassing Procedure

With the diffusion pump in operation, tap 2 was closed, taps 1 and 3 opened and the crucible assembly heated slowly to red heat and then more rapidly to about 2250°C. In general/the higher the degassing temperature, the shorter the time required for degassing. However, a number of runs made in the range 2300 to 2500°C brought to light a number of disadvantages:-

(a) Volatilisation of graphite from the hotter regions and its condensation on the cooler parts of the apparatus was quite marked. Sometimes this led to the welding together of the ball stopper and the funnel of the crucible assembly, but this could be prevented by raising the stopper occasionally during the degassing period. A more serious effect of volatilisation was the formation of a fairly thick graphite film on the silica furnace tube walls. On a few occasions, runs had to be abandoned due to gas evolution from

particles of this film which dropped into the crucible when the ball stopper, raised for sample admission or temperature measurement, came into contact with the tube walls.

(b) Occasionally, there was a loss of insulation with the consequent development of hot spots in the packing due to sintering of the graphite powder.

(c) The working life of the crucible assembly was greatly reduced.

In the present work a satisfactory blank could usually be obtained after degassing for 7 to 8 hours at a temperature somewhere in the range 2200 to 2300°C. Thirty minute blank collections made over the temperature range covered during actual sample analysis, i.e. 1400 to 1650°C, were of the order 0·06 cc per hour at N.T.P. and contained about 72 per cent carbon monoxide, 21 per cent hydrogen and 7 per cent nitrogen by volume. This data is compared with that from other sources[20] in Table 7.

Table 7 Comparison of Vacuum Fusion Data

Source	Degassing Temp °C	Degassing Time-Hrs	Working Temp	Blank cc/Hr
National Physical Lab.	2600	2-2.1/2	1550-1600	0·004
United Steel Cos.Ltd.	2000	2	1650	0£3 - 0·4
Sheffield Univeristy	2100	3	1650	0·9
Brown-Firth Research Lab.	2100	2	1650	0·5 - 1
Present Work	2200-2300	7-8	1650	0·06

Temperature measurements were made by raising the ball stopper and focussing the previously mentioned optical pyrometer on the base of the inner crucible.

(iv) The Extraction Period

During the extraction period if the evolution of gas from the sample takes place too rapidly, there is a tendency for the metal bath to spatter, and this can lead to low results due to imcomplete gas extraction from metal particles adhering to the crucible assembly and ball stopper. In order to avoid this spattering effect, the temperature was always lowered to about 1400°C before dropping a sample, and then gradually increased to the final extraction temperature, which, from the point of view of keeping the extraction period, and therefore the blank correction to a minimum, should be as high as possible. However, if the extraction temperature is too high there is a possibility of metal volatilising from the bath and condensing on the cooler parts of the furnace tube, and this also can be the cause of low results due to adsorption of gas on the freshly deposited and highly reactive metal film.

In the present work it was found that an extraction temperature of 1650°C yielded reproducible results while a number of runs made at 1750°C did not yield any more gas. During preliminary tests on the apparatus with standard steels of known oxygen content, it was found that gas evolution from the first sample was very slow and

that the final result was always low sometimes by as much as 25 per cent. To avoid errors from this source, 4 to 6 g of Armco iron were always added to the crucible and degassed, prior to the addition of the first sample. In this way a pool of molten metal was obtained which enable complete solution and carburisation of the samples to take place much more rapidly. By this technique gas evolution from most samples was usually complete after about 15 to 20 minutes.

The performance of the equipment was checked at frequent intervals with standard steel samples supplied by the Gases and Non-Metallic Sub-Committee of the British Iron and Steel Research Association. The two standards used, No. 8652/4 and No 784/4 had oxygen contents of 0·0145 and 0·0105 per cent respectively. In general reproducibility was of the order ± 0·0005 per cent. (Table 8)

Table 8 Standard Steels

Standard	Oxygen Content	Analysed Oxygen Content		
8652/4	0·0145	0·0139	0·0142	0·0147
784/4	0·0105	0·0102	0·0107	0·0107

C H A P T E R VI

ALUMINIUM-OXYGEN EQUILIBRIA IN LIQUID IRON

1. Introduction

2. Activity Coefficients in the Iron-Oxygen and Iron-Aluminium Binary Systems

3. Aluminium-Oxygen Interaction in Liquid Iron

4. Equilibrium Study of the Reaction $H_2(g) + \underline{O} = H_2O(g)$

5. Equilibrium Study of the Reaction $Al_2O_3(s) + 3H_2(g) = 2\,\underline{Al} + 3H_2O(g)$

6. Equilibrium Study of the Reaction $Al_2O_3(s) = 2\,\underline{Al} + 3\,\underline{O}$

ALUMINIUM OXYGEN EQUILIBRIA IN LIQUID IRON

1. Introduction

Experimental investigations of the relationship existing between aluminium and oxygen in liquid iron have been hampered by many of the difficulties common to studies at high temperatures, for example, control of the furnace atmosphere, measurement and control of temperature, adequate contact between the different phases present and retention of the equilibrium composition of the different phases at room temperature. In addition, the value of experimental work on aluminium deoxidation is largely dependent upon accurate analytical techniques. This factor has particular relevance where experiments have been conducted at about 1600°C, at which temperature the concentrations of both oxygen and aluminium at equilibrium are extremely low.

In the present investigation, analytical uncertainties have been reduced by carrying out the experiments at 1723° and 1823°C. At these temperatures the equilibrium aluminium and oxygen concentrations in the melts were high enough for accurate analysis. Extrapolation of the data to 1600°C yields a value for the deoxidation constant which is probably more reliable than could have been obtained by a direct experimental determination at 1600°C using the present technique.

The experimental method consisted of melting electrolytic iron in pure alumina crucibles under a controlled water-vapour/hydrogen atmosphere and holding it at constant temperature until equilibrium was established between solid, liquid and gas phases. The melts

were then quenched in a stream of cold hydrogen to retain at room temperature the equilibrium concentrations of aluminium and oxygen. Subsequently the melts were analysed for these elements and on the basis of the results obtained, a study was made of the equilibria represented by the following equations:-

$$Al_2O_{3(s)} = 2\,\underline{Al} + 3\,\underline{O} \qquad K_1' = [Al]^2[\%O]^3 \quad ...(1)$$

$$Al_2O_{3(s)} + 3H_{2(g)} = 2\,\underline{Al} + 3H_2O_{(g)} \qquad K_2' = [\%Al]^2\left(\frac{p_{H_2O}}{p_{H_2}}\right)^3 \quad ...(2)$$

$$H_{2(g)} + \underline{O} = H_2O_{(g)} \qquad K_3' = \frac{p_{H_2O}}{p_{H_2}}\cdot\frac{1}{[\%O]} \quad ..... \quad (3)$$

Data for a number of melts which are believed to have reached equilibrium at 1723° and 1823°C are shown in Table 9 together with corresponding values for K_1', K_2' and K_3'. The apparent equilibrium ratios are related to the true equilibrium constants for the three reactions through the activity coefficients f_{Al} and f_o, where f_{Al} is the activity coefficient of aluminium and f_o is the activity coefficient of oxygen in the ternary Fe-Al-O melts. In each case the standard state is such that the activity approaches the weight per cent at infinite dilution.

TABLE 9 - EQUILIBRIUM DATA AT 1723° and 1823°C

Temperature	Heat No	p_{H_2O}/p_{H_2} x 10^3	Al, Wt Pct x 10^3	O, Wt Pct x 10^3	$K_1' = [\%Al]^2[\%O]^3$	$K_2' = [\%Al]^2\left(\frac{p_{H_2O}}{p_{H_2}}\right)^3$	$K_3' = \frac{p_{H_2O}}{p_{H_2}}\frac{1}{[\%O]}$
1723°C	7	3·54	21·7	2·7	$9·27 \times 10^{-12}$	$2·09 \times 10^{-11}$	1·31
	12	4·92	19·5 +	3·5	$4·72 \times 10^{-12}$	$1·31 \times 10^{-11}$	1·41
	31	6·56	6·0 +	4·1	$2·48 \times 10^{-12}$	$1·02 \times 10^{-11}$	1·60
	15	8·61	3·0	5·0	$1·13 \times 10^{-12}$	$0·58 \times 10^{-11}$	1·72
1823°C	5	3·48	66·6	4·2	$3·28 \times 10^{-10}$	$1·87 \times 10^{-10}$	0·83
	2	4·98	32·8	5·5	$1·79 \times 10^{-10}$	$1·33 \times 10^{-10}$	0·91
	8	6·51	22·7	7·0	$1·77 \times 10^{-10}$	$1·42 \times 10^{-10}$	0·93
	9	8·72	9·8	8·6	$0·61 \times 10^{-10}$	$0·64 \times 10^{-10}$	1·02
	10	11·62	7·3	10·7	$0·65 \times 10^{-10}$	$0·84 \times 10^{-10}$	1·09

+ Average Deviation about 0·001

Thus,

$$K_1 = [a_{Al}]^2 \cdot [a_O]^3$$

$$= [f_{Al} \times \%\,Al]^2 \cdot [f_O \times \%\,O]^3$$

$$= K_1' \cdot f_{Al}^2 \cdot f_O^3 \qquad \ldots\ldots\ldots (4)$$

$$K_2 = [a_{Al}]^2 \cdot \left(\frac{p_{H_2O}}{p_{H_2}}\right)^3$$

$$= K_2' \cdot f_{Al}^2 \qquad \ldots\ldots\ldots (5)$$

and $$K_3 = \frac{p_{H_2O}}{p_{H_2}} \frac{1}{[a_O]}$$

$$= K_3' / f_O \qquad \ldots\ldots\ldots (6)$$

Adopting the method developed by Chipman et alia[3] and discussed in Chapter II, each of the coefficients f_{Al} and f_O can be expressed as a product of two factors:-

i.e. $f_{Al} = f_{Al}^{(Al)} \cdot f_{Al}^{(O)}$

and $f_O = f_O^{(O)} \cdot f_O^{(Al)}$

where $f_{Al}^{(Al)}$ is the activity coefficient of aluminium in the binary iron aluminium solution of the same aluminium concentration as the ternary solution;

$f_o^{(O)}$ is the activity coefficient of oxygen in the binary iron-oxygen solution of the same oxygen concentration as the ternary solution;

$f_{Al}^{(O)}$ is a factor representing the effect of oxygen on the activity coefficient of aluminium;

and $f_o^{(Al)}$ is a factor representing the effect of aluminium on the activity coefficient of oxygen.

In the following section a brief study is made of the relevant data for the iron-aluminium and the iron-oxygen binary

systems and it is found that in the present case no great error is introduced by taking each of the coefficients $f_{Al}^{(Al)}$ and $f_{O}^{(O)}$ as unity.

2. Activity Coefficients in the Iron-Aluminium and the Iron-Oxygen Binary Systems

(a) The Iron-Aluminium Binary System. From the data of Chipman and Floridis[27] on the distribution of aluminium between iron and silver, Wilder and Elliott[32] have calculated a value of 5·3 for the parameter $\epsilon_{Al}^{(Al)}$, with reference to iron-aluminium alloys at 1600°C. The value of this parameter at higher temperatures can be calculated on the assumption that $\epsilon_{Al}^{(Al)}$ is inversely proportional to the absolute temperature. At 1723° and 1823°C, $\epsilon_{Al}^{(Al)}$ takes the values shown in Table 10.

TABLE 10 Extrapolated Values for the Parameters $\epsilon_{Al}^{(Al)}$ and $e_{Al}^{(Al)}$.

Parameter	1600°C	1723°C	1823°C
$\epsilon_{Al}^{(Al)} = \dfrac{\partial \ln \gamma_{Al}^{(Al)}}{\partial N_{AL}}$	5·3	5·0	4·7
$e_{Al}^{(Al)} = \dfrac{\partial \log f_{Al}^{(Al)}}{\partial [\%Al]}$	0·048	0·045	0·042

The largest deviation from ideality will occur in those melts containing the greatest amounts of aluminium, i.e. in heat 7 at 1723° and heat 5 at 1823°C. The activity of aluminium in binary iron-aluminium alloys, of the same aluminium concentrations as in melts 7 and 5, is calculated in Table 11, from which it can be seen that the maximum effect of $f_{Al}^{(Al)}$ results in a change of activity, which

is well within the accuracy limits of the aluminium determinations. In view of this fact, $f_{Al}^{(Al)}$ is taken as unity, throughout the experimental range of the present study.

Table 11 Activity of Aluminium in Binary Fe-Al Alloys

Temperature	Al, Wt Pct	$e_{Al}^{(Al)}$	$\log f_{Al}^{(Al)} = e_{Al}^{(Al)}[\%Al]$	$f_{Al}^{(Al)}$	$a_{Al} = f_{Al}^{(Al)}[\%Al]$
1723°C	0·0217	0·045	0·0010	1·002	0·0218
1823°C	0·0666	0·042	0·0028	1·007	0·0670

(b) The Iron-Oxygen Binary System. Floridis and Chipman[11] have found that the activity coefficient of oxygen in iron at 1600°C is given by:-

$$\log f_o^{(o)} = -0{\cdot}20[\%O]$$

Assuming that $e_o^{(o)}$ is inversely proportional to the absolute temperature, the value of the parameter at 1723° and 1823°C is -0·19 and -0·18 respectively. In this case the largest deviations from ideality will occur in those melts containing the greatest amounts of oxygen, i.e. in heat 15 and 10. In Table 12 oxygen activities are calculated for two binary iron-oxygen alloys of the same oxygen content as melts 15 and 10. The results of these calculations show that the maximum effect of $f_o^{(o)}$ is very much less than the error limits placed on the oxygen analyses. In the oxygen concentration range of the present study therefore, the error introduced by taking $f_o^{(o)}$ as unity is negligible.

TABLE 12 Activity of Oxygen in Binary Fe-O Alloys

Temperature	O, Wt Pct	$e_O^{(O)}$	$\log f_o^{(O)} = e_O^{(O)}[\%O]$	$f_o^{(O)}$	$a_O = f_o^{(O)}[\%O]$
1723°C	0·0050	-0·19	-0·0010	0·9977	0·00499
1823°C	0·0107	-0·18	-0·0019	0·9956	0·01065

Thus within the range of composition of iron-aluminium-oxygen alloys encountered in the present work, variations in the activity coefficient of oxygen have been ascribed entirely to the effect of aluminium, and variations in the activity coefficient of aluminium entirely to the effect of oxygen.

$$\text{i.e. } f_O = f_O^{(Al)}$$
$$\text{and } f_{Al} = f_{Al}^{(O)}$$

and equations 4, 5 and 6 may be rewritten in the form:-

$$\log K_1 = \log K_1' + 2 \log f_{Al}^{(O)} + 3 \log f_O^{(Al)} \quad \ldots\ldots(7)$$

$$\log K_2 = \log K_2' + 2 \log f_{Al}^{(O)} \quad \ldots\ldots(8)$$

$$\log K_3 = \log K_3' - \log f_O^{(Al)} \quad \ldots\ldots(9)$$

3. Aluminium-Oxygen Interaction in Liquid Iron

The equilibrium constant for the reaction:-

$$H_2(g) + \underline{O} = H_2O(g)$$

may be expressed in the form:

$$\log K_3 = \log K_3' - \log f_O^{(Al)}$$
$$= \log K_3' - e_O^{(Al)}[\%Al]$$
$$\text{i.e. } \log K_3' = e_O^{(Al)}[\%Al] + \log K_3$$

In Fig. 15 a graph is presented of log K_3' v [%Al]. A curve, implying a variation in $e_o^{(Al)}$ with aluminium concentration would be a possible representation of the data, but the latter is not sufficiently precise to warrant this treatment. The gradients of the two lines yield values for the parameter $e_o^{(Al)}$ of -3·45 and -2·04 at 1723° and 1823°C respectively. The intercept at zero per cent aluminium represents log K_3, but a more accurate value will be obtained after establishing average values for the parameter $e_o^{(Al)}$.

The data of Floridis and Chipman[11] for K_3 in aluminium free melts are also included in Fig. 15. According to equation [9], the activity coefficient of oxygen, $f_o^{(Al)}$, could be determined quite simply by dividing each experimental value for K_3' by K_3. Using the values of Floridis and Chipman for K_3 gives the very low values for $f_o^{(Al)}$ shown in Table 13. Their points, therefore, at zero per cent aluminium are ignored in drawing the lines and values for $f_o^{(Al)}$ are determined independently on the basis of the present work.

Table 13 Calculation of $f_o^{(Al)}$ Using the Expression: $\log f_o^{(Al)} = \log K_3' - \log K_3$

Temperature	Heat No	Log K_3'	log K_3	log $f_o^{(Al)}$	$f_o^{(Al)}$
1723°C	7	0·118	0·335	-0·217	0·61
	12	0·149	0·335	-0·186	0·65
	31	0·204	0·335	-0·131	0·74
	15	0·236	0·335	-0·099	0·80
1823	5	-0·081	0·170	-0·251	0·56
	2	-0·043	0·170	-0·213	0·61
	8	-0·032	0·170	-0·202	0·63
	9	+0·006	0·170	-0·164	0·69
	10	+0·037	0·170	-0·133	0·74

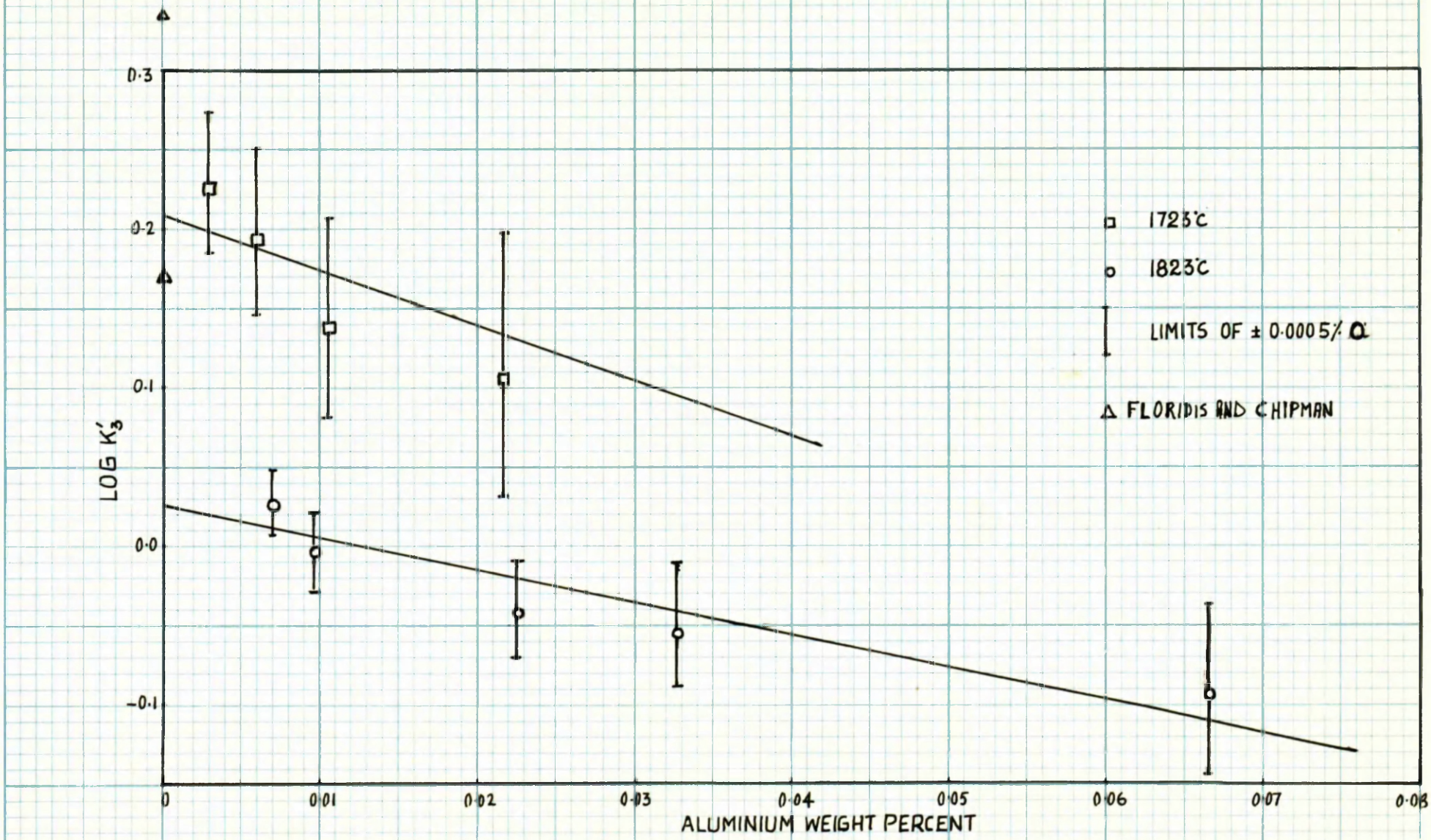

FIG 15. EXPERIMENTAL VALUES OF LOG p_{H_2O}/p_{H_2} [% O]

To illustrate the sensitivity of the plot, limits are shown which represent errors of ± 0·0005 per cent in the oxygen analyses. The effect of an error of ±0·03 mm.Hg in the partial pressure of water vapour would lead to a maximum error of only ±0·005 in log K_3' and since this maximum would occur in melts at the lowest oxygen levels, where the error limits for log K_3' are greatest, the effect is disregarded.

Values for the parameter $e_o^{(Al)}$ can also be determined from consideration of the results obtained for the reaction represented by equation [1]

$$\text{i.e.} \quad Al_2O_{3(s)} = 2\,\underline{Al} + 3\underline{O}$$

The equilibrium constant for this reaction, $K_1 = [a_{Al}]^2 \cdot [a_O]^3$ may be expressed in the following way[36], with the aid of equation 7:-

$$\log K_1 = \log K_1' + 2 \log f_{Al}^{(O)} + 3 \log f_O^{(Al)}$$
$$= \log K_1' + 2e_{Al}^{(O)}[\%O] + 3e_O^{(Al)}[\%Al]$$

And from equation [8] of Chapter II

$$M_3 e_2^{(3)} = M_2 e_3^{(2)} \text{ where Mi is the atomic weight of i}$$
$$e_{Al}^{(O)} = \frac{27}{16} e_O^{(Al)} \qquad \text{.....(10)}$$
$$\text{Thus } \log K_1 = \log K_1' + 3{\cdot}375 e_O^{(Al)}[\%O] + 3e_O^{(Al)}[\%Al]$$
$$\text{i.e. } \log K_1' = -3e_O^{(Al)}(1{\cdot}125\,[\%O] + [\%Al]) + \log K_1 \text{ .....(11)}$$

Values for the expression (1·125 [%O] + [%Al]) are calculated in Table 14, and a graph of log K_1' v (1·125 [%O] +[%Al]) is shown in Fig. 16.

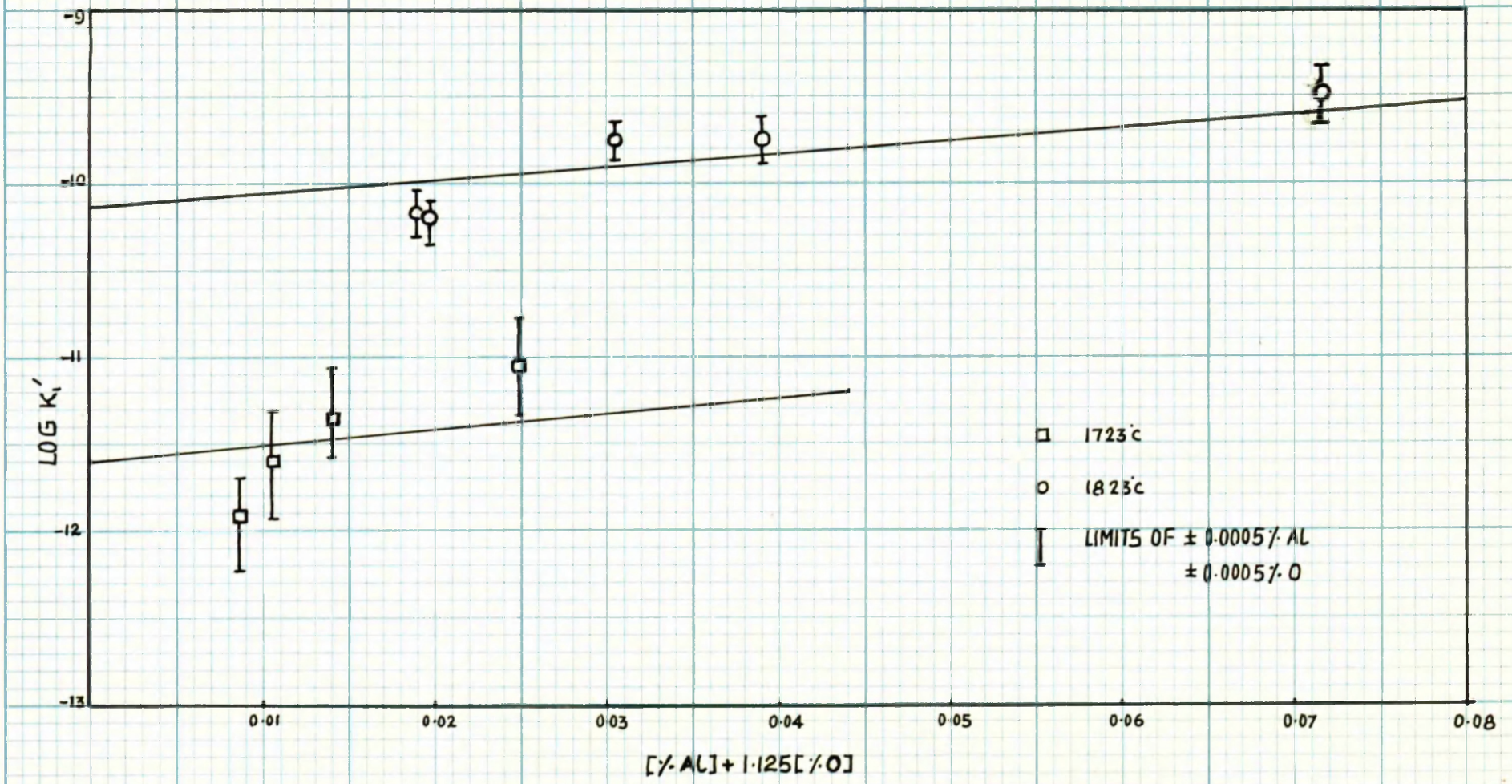

FIG 16 EFFECT OF CONCENTRATION ON THE EQUILIBRIUM PRODUCT $[\%AL]^2[\%O]^3$

TABLE 14 Data for Plot of log K_1' against (1·125 [%O] + [%Al])

Temperature	Heat No.	O, Wt Pct	1·125[%O]	Al, Wt Pct	(1·125[%O]+[%Al])	log K_1'
1723°C	7	0·0027	0·0030	0·0217	0·0247	-11·03
	12	0·0035	0·0039	0·0105	0·0144	-11·33
	31	0·0041	0·0046	0·0060	0·0106	-11·61
	15	0·0050	0·0056	0·0030	0·0086	-11·95
1823	5	0·0042	0·0047	0·0666	0·0713	- p·48
	2	0·0055	0·0062	0·0328	0·0390	- 9·75
	8	0·0070	0·0079	0·0227	0·0306	- 9·75
	9	0·0086	0·0097	0·0098	0·0195	-10·21
	10	0·0107	0·0120	0·0073	0·0193	-10·19

The limits shown on the graph represent errors of (±·0005%O, ±·0005%Al) except in the case of heats 12 and 31, where the possible error in the aluminium analyses is ± ·001 per cent. The gradient of the lines is equivalent to $-3e_O^{(Al)}$ and yields values for $e_O^{(Al)}$ of -3·15 and -2·73 at 1723° and 1823°C respectively. Again a value for the equilibrium constant, in this case K_1, could be obtained from the intercept of the lines at zero per cent aluminium and oxygen, however, as before, a more accurate value will be obtained after establishing average values for the parameters $e_O^{(Al)}$ and $e_{Al}^{(O)}$.

In Fig. 17, the two sets of values which have now been obtained for $e_O^{(Al)}$ are plotted against the reciprocal of the absolute

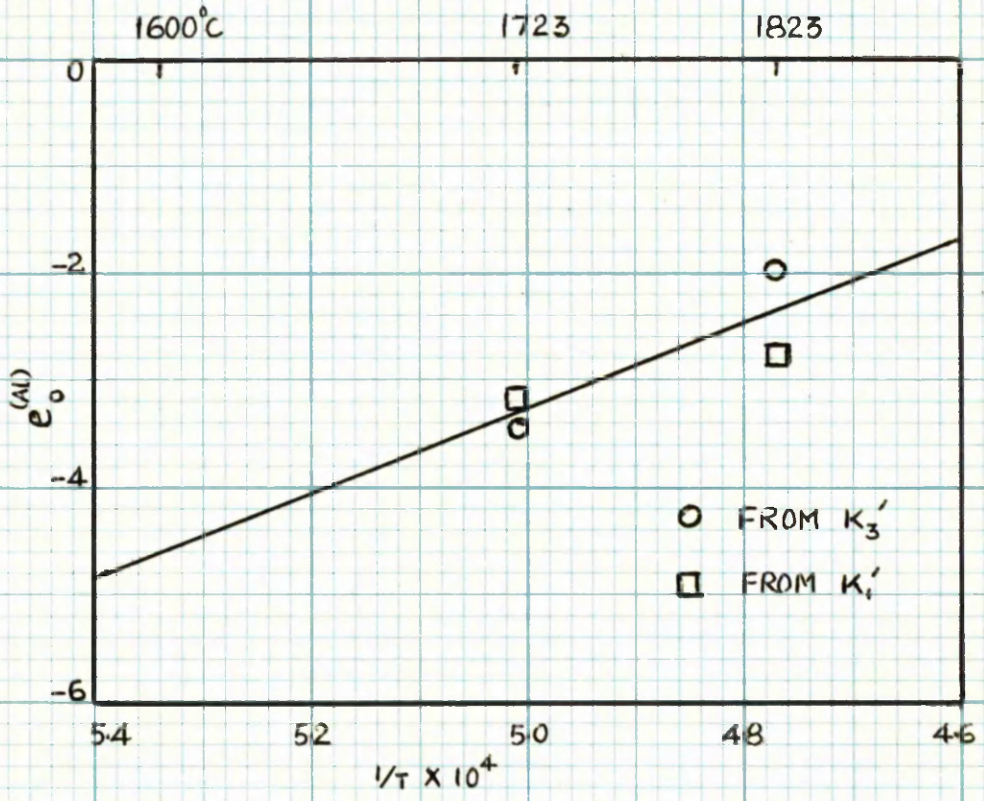

FIG 17 EFFECT OF TEMPERATURE ON THE INTERACTION PARAMETER $e_0^{(Al)} = \partial \log f_0 / \partial [\%Al]$

temperature and the best straight line drawn through them. Although the two sets of data are not entirely independent in that both involve oxygen analyses, the first set, derived from Fig. 15, demands a knowledge of the gas composition, while the second does not.

Substitution of the average values obtained for $e_O^{(Al)}$ in equation [10], i.e. $e_{Al}^{(O)} = 27e_O^{(Al)}/16$, yields values for the parameter $e_{Al}^{(O)}$ of -5·56 and -4·03 at 1723° and 1823°C respectively. Information on the parameter $e_{Al}^{(O)}$ could also be obtained from consideration of the reaction:-

$$Al_2O_{3(s)} + 3H_{2(g)} = 2\,\underline{Al} + 3H_2O_{(g)}$$

since, according to equation [8], the equilibrium constant for this reaction, can be expressed in the form:-

$$\log K_2 = \log K_2' + 2 \log f_{Al}^{(O)}$$

$$\text{i.e.} \quad \log K_2' = -2e_{Al}^{(O)}[\%O] + \log K_2$$

A graph of $\log K_2'$ v $[\%O]$ is shown in Fig. 18. The limits shown on this graph take into account the effect of errors from two sources:

(i) Analytical errors of ± 0·005 per cent in the determination of aluminium except in heats 12 and 31, where the error is about ± 0·001 per cent.

(ii) Errors of ± 0·03 mm mercury in the partial pressure of water-vapour.

The second factor is included within the limits, since in this instance the effect of such an error in the gas composition, would be greatest at low water-vapour/hydrogen ratios, i.e. in heats where the aluminium concentrations are greatest and the errors associated with the aluminium analyses, least significant.

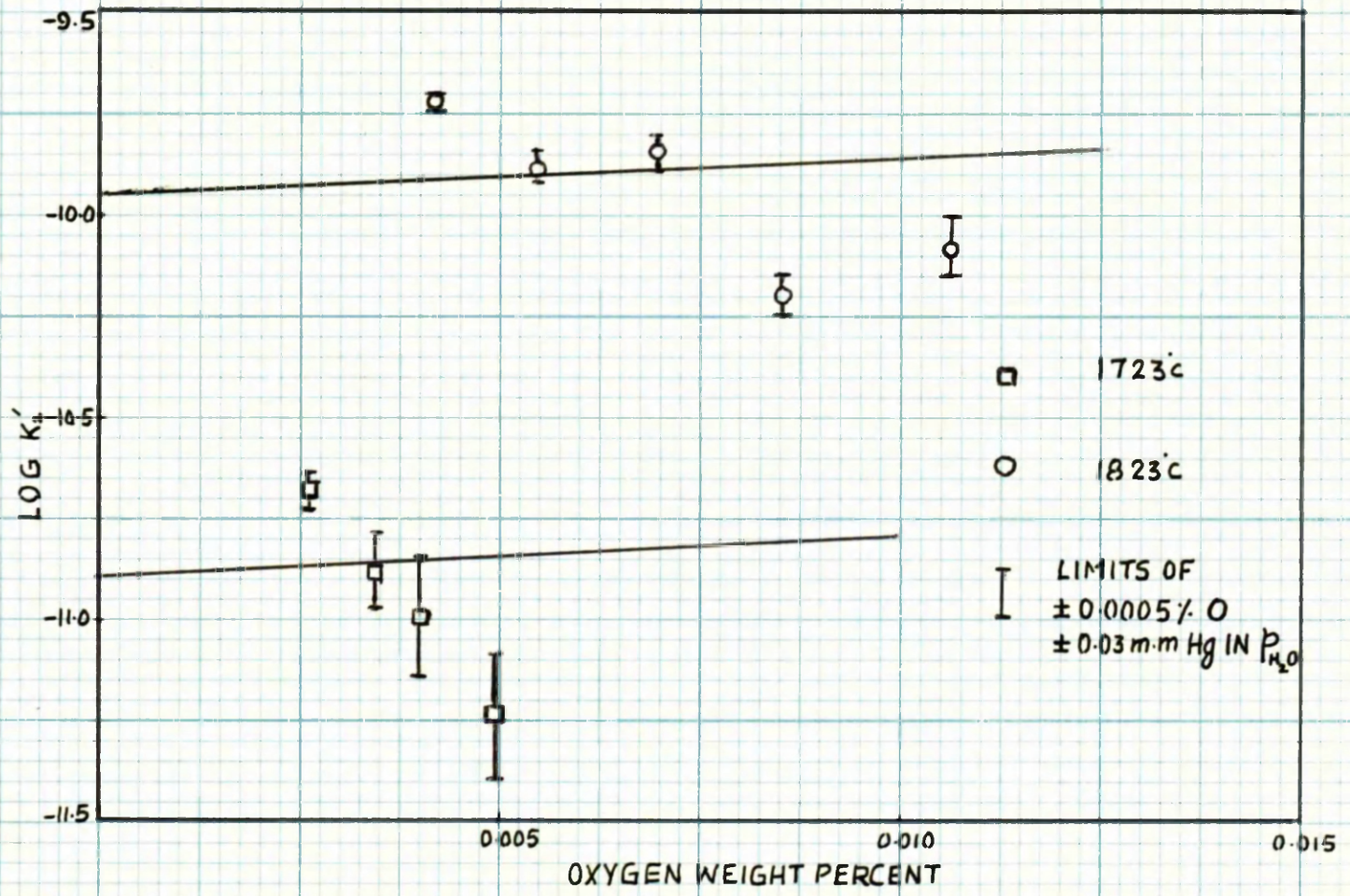

FIG 18 EXPERIMENTAL VALUES OF LOG $[\%Al]^2 (P_{H_2O})^3/(P_{H_2})^3$

The lines drawn through the data in Fig. 18 have gradients which are equivalent to $-2\varepsilon_{Al}^{(O)}$, where $\varepsilon_{Al}^{(O)}$ has the values calculated previously. It is evident, however, that the data when presented in this form, does not yield accurate values for the parameter $\varepsilon_{Al}^{(O)}$. In the following sections therefore the values adopted for the parameter $\varepsilon_{Al}^{(O)}$ are those derived from the average values for $\varepsilon_{O\%}^{(Al)}$.

In Fig. 19, the data for $\varepsilon_{O}^{(Al)}$ and $\varepsilon_{Al}^{(O)}$ are extrapolated to 1600°C, and the average values for the parameters at several temperatures are collected in Table 15. The corresponding values obtained by Gokcen and Chipman[36] for the various parameters are also included in Fig 19 and Table 15. From the various results it is

TABLE 15 Interaction Parameters of Aluminium and Oxygen in Liquid Iron

Parameter	1600°C		1723°C		1823°C	
	Gokcen and Chipman	Present Work	Gokcen and Chipman	Present Work	Gokcen and Chipman	Present Work
$\varepsilon_{O}^{(Al)} = \partial \log f_O / \partial [\%Al]$	-12	-4.60	-7.9	-3.30	-4.9	-2.39
$\varepsilon_{Al}^{(O)} = \partial \log f_{Al} / \partial [\%O]$	-20	-7.75	-13.2	-5.56	-8.2	-4.03
$\epsilon_{O}^{(Al)} = \partial \ln f_O / \partial N_{Al}$	-1340	-512	-880	-367	-545	-266

evident that the data from the present study yield values for the different parameters which are not quite so large as those of Gokcen and Chipman. Both sets of data agree that there is a large negative deviation from Henry's Law in the Fe-Al-O system, which is indicative of a high Al-O bonding energy. The discrepancy between the two sets of data can be attributed mainly to the experimental difficulties at

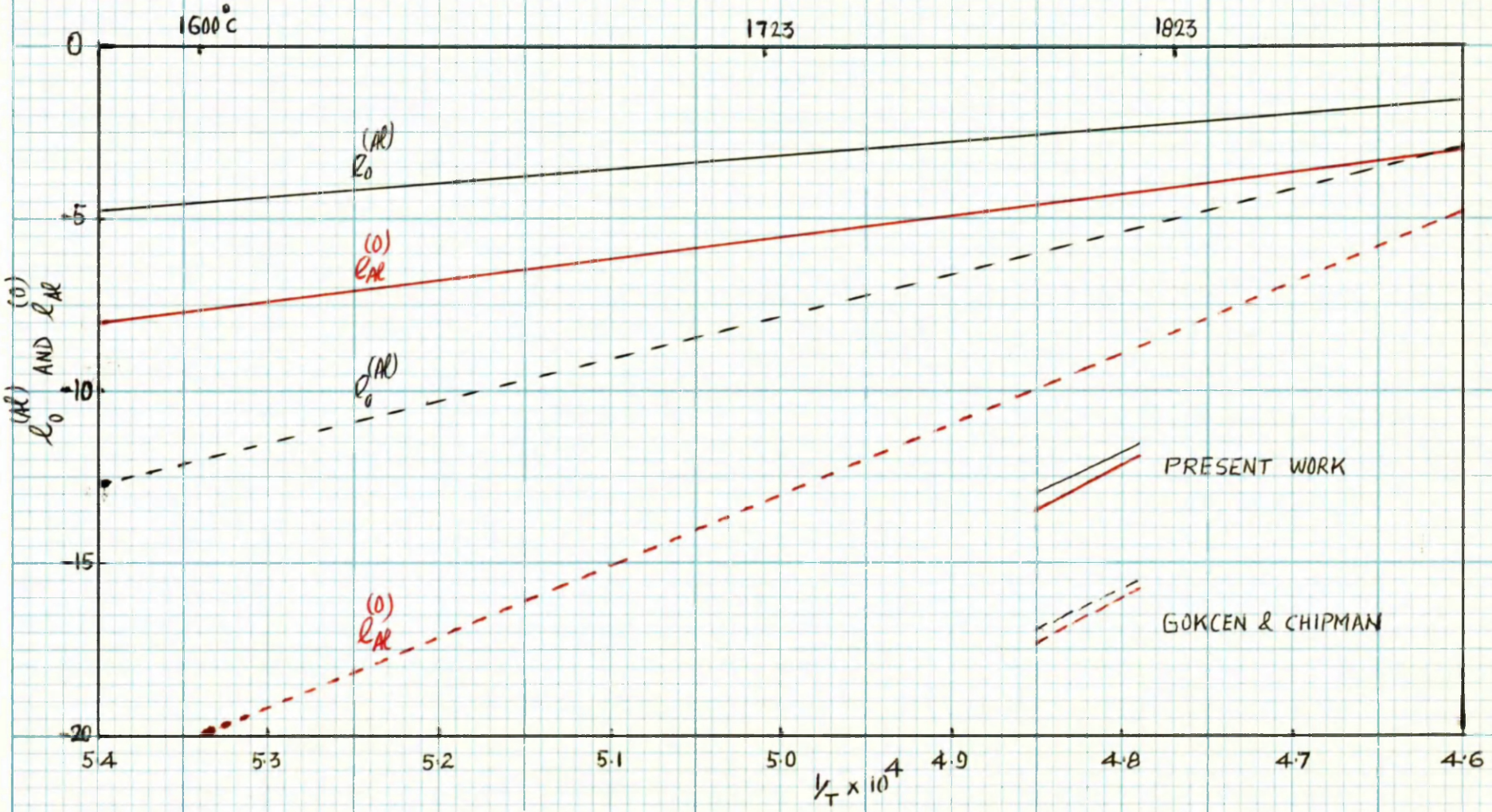

FIG. 19 EFFECT OF TEMPERATURE ON THE PARAMETERS $e_o^{(Ar)}$ & $e_{Ar}^{(o)}$

very low concentrations of aluminium and oxygen.

The negative values for the parameter $e_o^{(Al)}$ imply that as the aluminium concentration increases, the activity coefficient of oxygen decreases, from which it follows that aluminium does not function so well as a deoxidiser at higher concentrations as one might expect from consideration of its behaviour at lower concentrations. From a physical standpoint, this phenomenon can be explained in terms of an association between the aluminium and oxygen solute atoms.

In the case of a simple iron-oxygen solution, each oxygen atom is surrounded by a certain number of iron atoms which share the iron-oxygen bonding energy. When aluminium is present, the bonding energy between the aluminium and oxygen is greater than that between the iron and oxygen with the result that the ratio of aluminium atoms to iron atoms is greater in the vicinity of oxygen atoms than in the bulk of the solution. As the aluminium concentration increases, this effect becomes more significant, and as the oxygen atoms become more and more firmly bonded, the oxygen activity decreases.

Another factor which probably contributes to the large negative deviation from ideality is associated with the large Al-Fe bonding energy, an indication of which is the high positive value of 5·3 obtained for $\epsilon_{Al}^{(Al)}$ from a study of iron-aluminium alloys at 1600°C [32]. In such alloys, as the aluminium concentration increases, the competition for iron atoms in the neatest neighbour shells, also increases, with the result that the activity of aluminium gradually increases.

In Fe-Al-O solutions, this effect is concealed by Al-O intersolute attraction, but must still be present and it has been suggested[45] that in such ternary solutions, the surrounding of aluminium atoms by iron atoms occurs, as well as the surrounding of oxygen atoms by aluminium and iron atoms. The strong attraction between any two such atomic groupings, or possible even their coming together, which might be considered as a solution of AlO would account for the large negative value of $\epsilon_O^{(Al)}$.

4. Equilibrium Study of the Reaction:- $H_2(g) + \underline{O} = H_2O(g)$

The values for the equilibrium constant K_3, shown in Table 16, are calculated using the following equations:-

From equation [9] $\log K_3 = \log K_3' - \log f_O^{(Al)}$

$$\text{i.e.} \log K_3 = \log K_3' - e_O^{(Al)}[\%Al]$$

From Section 3, at 1723°C $\log K_3 = \log K_3' + 3{\cdot}3\ ]\%Al]$

and at 1823°C $\log K_3 = \log K_3' + 2{\cdot}39\ [\%Al]$

From Table 16 it can be seen that at 1723° and 1823°C, $\log K_3$ has the values 0·21 and 0·04 respectively with an estimated uncertainty of $\pm$ 0·06 in the first case and $\pm$ ·03 in the second. Extrapolation of the lines in Fig. 15 to zero per cent aluminium yields values of 0·22 and 0·04 at the same temperature levels.

TABLE 16 Calculation of the Equilibrium Constant $K_3 = \frac{1}{[a_O]} \frac{P_{H_2O}}{P_{H_2}}$

Temperature	Heat No.	Al, Wt Pct	$-\log f_O^{(Al)}$	Log K_3'	log K_3
1723°C	7	0·0217	0·072	0·118	0·190
	12	0·0105	0·035	0·149	0·184
	31	0·0060	0·020	0·204	0·224
	15	0·0030	0·010	0·236	0·246
					Average 0·21
1823°C	5	0·0666	0·159	-0·081	0·078
	2	0·0328	0·078	-0·043	0·035
	8	0·0227	0·054	-0·032	0·022
	9	0·0098	0·023	+0·006	0·029
	10	0·0073	0·017	+0·037	0·054
					Average 0·04

In Fig. 20 the average values for log K_3 from Table 16 are plotted against the reciprocal of the absolute temperature. Also included for comparison, are the results of a number of other studies. The earlier data shown, that of Dastur and Chipman[10] were based on a number of heats made in the temperature range 1563° to 1760°C, in which the oxygen concentrations did not exceed 0·06 per cent. Slightly lower values for log K_3 were obtained by Floridis and Chipman[11] from several heats at 1550° and 1600°C. They found that the effect of temperature on the equilibrium constant was adequately represented, by a line drawn through their data parallel to that of Dastur and Chipman. In Gokcen's[12] investigation the maximum experimental temperature was 1600°C and in the case of Samarin et al[14] 1645°C.

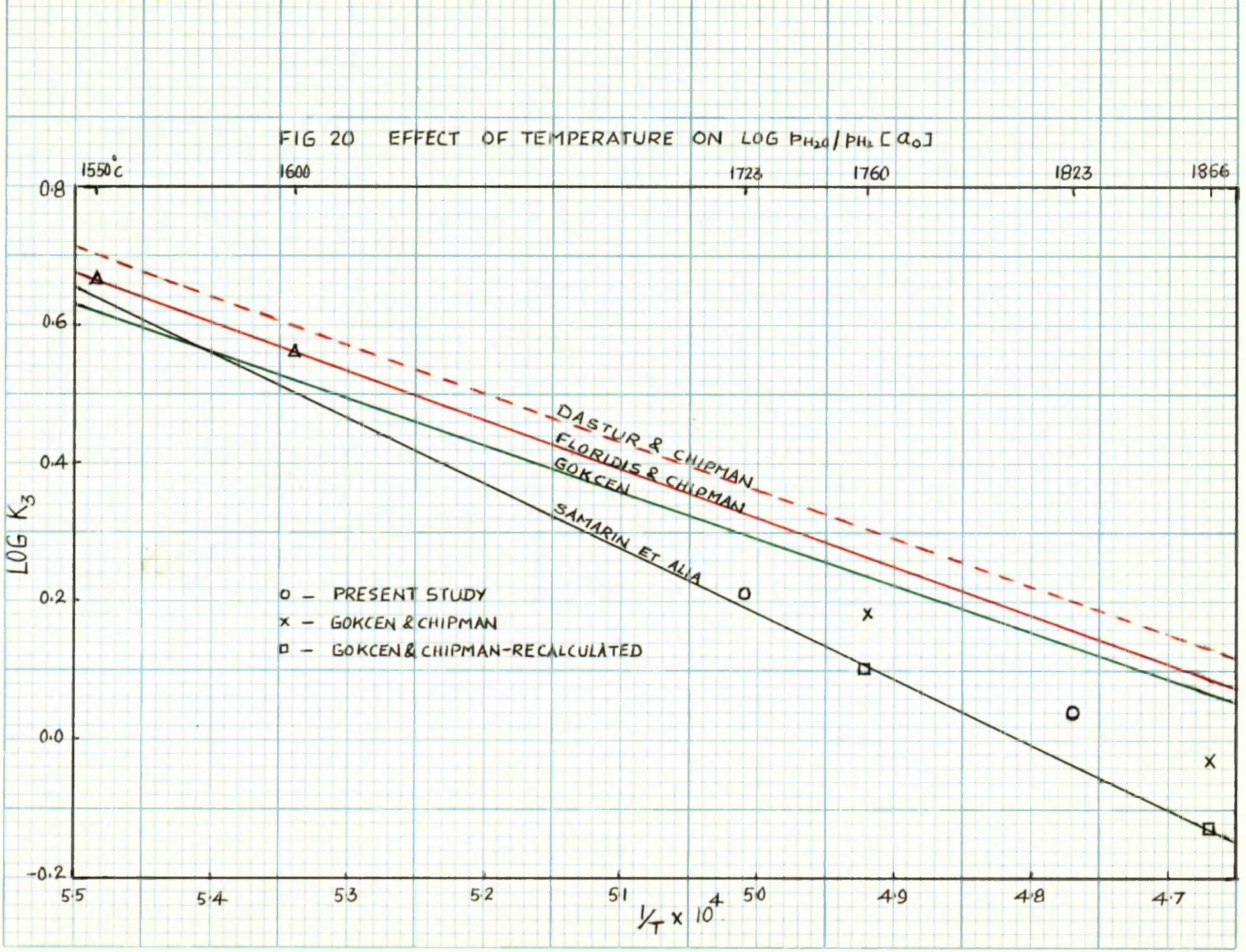
FIG 20 EFFECT OF TEMPERATURE ON LOG P_{H_2O}/P_{H_2} [a_o]
1550°C
1600
1723
1760
1823
1866
0.8
0.6
0.4
0.2
0.0
-0.2
LOG K_3
DASTUR & CHIPMAN
FLORIDIS & CHIPMAN
GOKCEN
SAMARIN ET ALIA
o – PRESENT STUDY
x – GOKCEN & CHIPMAN
□ – GOKCEN & CHIPMAN-RECALCULATED
5·5
5·4
5·3
5·2
5·1
5·0
4·9
4·8
4·7
$1/T \times 10^4$

When the various data are extrapolated to higher temperatures as shown in Fig. 20, it is found that the values for log K_3 derived from the present work are about 0·13 lower than those of Floridis and Chipman. On the other hand they exceed the values of Samarin et al by only 0·02 at 1723° and 0·08 at 1823°C. The greater difference between the values at the higher temperature, despite the slightly closer limits placed on the value of log K_3 at 1823°C, may be due in part to magnification of errors introduced by extrapolation of the data from 1645°C.

Also included in Fig. 20 are two sets of values for log K_3 at 1760° and 1866°C deduced from the data of Gokcen and Chipman[36]. The higher values represent the limiting values of log K_3 at zero per cent aluminium obtained from a graph of log K_3' v. [%Al]. When compared with the best data available at that time for log K_3, namely the data of Dastur and Chipman[10], their values of 0·18 and -0·03 were low to the extent of 0·12 and 0·16 at 1760° and 1866°C respectively. Although the authors were unable to assign definite causes for the deviations, they did point out the possibility that their results, which were all at very low oxygen concentrations, might contain some small systematic error which could make their values for log K_3, slightly lower than they should be.

In Table 17 average values are calculated for log K_3, using the experimental data of Gokcen and Chipman for log K_3' together with values for the activity coefficient of oxygen, $f_O^{(Al)}$, based on the values derived for the parameter $e_O^{(Al)}$ in the previous section.

TABLE 17 Calculation of the Equilibrium Constant K_3, using Values for K_3' from Ref. (36).

Temperature	Al, Wt Pct	$-\log f_O^{(Al)}$	$\log K_3'$	$\log K_3$
1760°C	0.008	0.024	0.167	0.191
	0.008	0.024	0.057	0.081
	0.0150	0.044	0.057	0.101
	0.023	0.068	0.000	0.068
	0.019	0.056	0.021	0.077
				Average 0.10
1866°C	0.0085	0.017	-0.097	-0.080
	0.0086	0.017	-0.208	-0.191
	0.0230	0.046	-0.051	-0.005
	0.0260	0.052	-0.167	-0.115
	0.0570	0.114	-0.366	-0.252
				Average -0.13

As can be seen from Fig. 20 these average values for $\log K_3$ are in very good agreement with the extrapolated data of Samarin et alia[14] which is represented by the equation

$$\log K_3 = 9440/T - 4.536$$

At temperatures of approximately 1550° - 1600°C, the data of Floridis and Chipman and Samarin et alia are in reasonable agreement. The data of the latter, however, indicate a greater temperature dependence for $\log K_3$, so that as the temperature increases, the difference between the two sets of values for $\log K_3$ becomes increasingly significant.

From the results of the present study, together with

the recalculated data of Gokcen and Chipman, it is apparent that for temperatures above 1700°C the equation proposed by Samarin et alia is in better agreement with the present experimental data than that of Floridis and Chipman.

5. Equilibrium Study of the Reaction: $Al_2O_3(s) + 3H_2(g) = 2\,\underline{Al} + 3H_2O(g)$

The effect of oxygen on the equilibrium ratio for the above reaction, i.e. K_2', is shown in Fig. 18. Extrapolation of the data to zero per cent oxygen yields values for log K_2 which are subject to an uncertainty of ±0.5. More accurate values for the equilibrium constant can be calculated from the experimental values for log K_2' with the aid of the following equations. The results of this calculation are shown in Table 18, and Fig. 21.

From equation [8], $\log K_2 = \log K_2' + 2 \log f_{Al}^{(O)}$

$= \log K_2' + 2\, e_{Al}^{(O)}[\%O]$

From Section 3, at 1723°C $\log K_2 = \log K_2' - 11.12\ [\%O]$

and at 1823°C $\log K_2 = \log K_2' - 8.06\ [\%O]$

The only experimental data published for this reaction is that of Gokcen and Chipman[36]. Their values for log K_2 were taken as the limiting values of log K_2' at zero per cent oxygen from a graph similar to that shown in Fig. 18 and were subject to an uncertainty of ± 0.5. Using their data for log K_2' at 1695, 1760 and 1866°C

TABLE 18 Calculations of the Equilibrium Constant $K_2 = [a_{Al}]^2 \left(p_{H_2O}/p_{H_2}\right)^3$

Temperature	Heat No	O, Wt Pct	$-2 \log f_{Al}^{(O)}$	$-\log K_2'$	$-\log K_2$
1723°C	7	0·0027	0·03	10·68	10·71
	12	0·0035	0·04	10·88	10·92
	31	0·0041	0·05	10·99	11·04
	15	0·0050	0·06	11·24	11·30
				Average Value =	10·99
1823°C	5	0·0042	0·03	9·73	9·76
	2	0·0055	0·04	9·88	9·92
	8	0·0070	0·06	9·85	9·91
	9	0·0086	0·07	10·20	10·27
	10	0·0107	0·09	10·08	10·17
				Average Value =	10·01

together with values for $e_{Al}^{(O)}$ deduced from Fig. 19, average values for the equilibrium constant are redetermined (Table 19) and included in Fig. 21.

The straight line drawn through the data in Fig. 21 is represented by the equation:-

$$\log K_2 = \frac{-43,600}{T} + 10·9$$

which was calculated from available thermodynamic data in the following way:- From data for the heat and free energy of formation of alumina given by Elliott and Gleiser[74] for the temperature range 1800° to 2300°K:-

$$Al_2O_{3(s)} = 2Al_{(\ell)} + \tfrac{3}{2} O_{2(g)} \qquad \Delta G° = 400,900 - 76·6\ T \text{ cal....[12]}$$

TABLE 19 Calculation of the Equilibrium Constant K_2, using Values for K_2' from Ref (36)

Temperature	O, Wt Pct	$-2 \log f_{Al}^{(o)}$	$-\log K_2'$	$-\log K_2$
1695°C	0.0065	0.078	10.889	10.967
	0.0052	0.062	11.153	11.215
	0.0038	0.046	11.126	11.172
	0.0032	0.038	11.278	11.316
	0.0026	0.031	11.472	11.503
			Average Value =	11.23
1760°C	0.0065	0.065	10.250	10.315
	0.0062	0.062	10.650	10.712
	0.0046	0.046	10.487	10.533
	0.0038	0.038	10.538	10.576
	0.0036	0.036	10.710	10.746
			Average Value =	10.58
1866°C	0.0164	0.115	9.799	9.914
	0.0155	0.109	10.187	10.296
	0.0080	0.056	9.719	9.775
	0.0076	0.053	10.022	10.075
	0.0057	0.040	10.319	10.359
			Average Value =	10.08

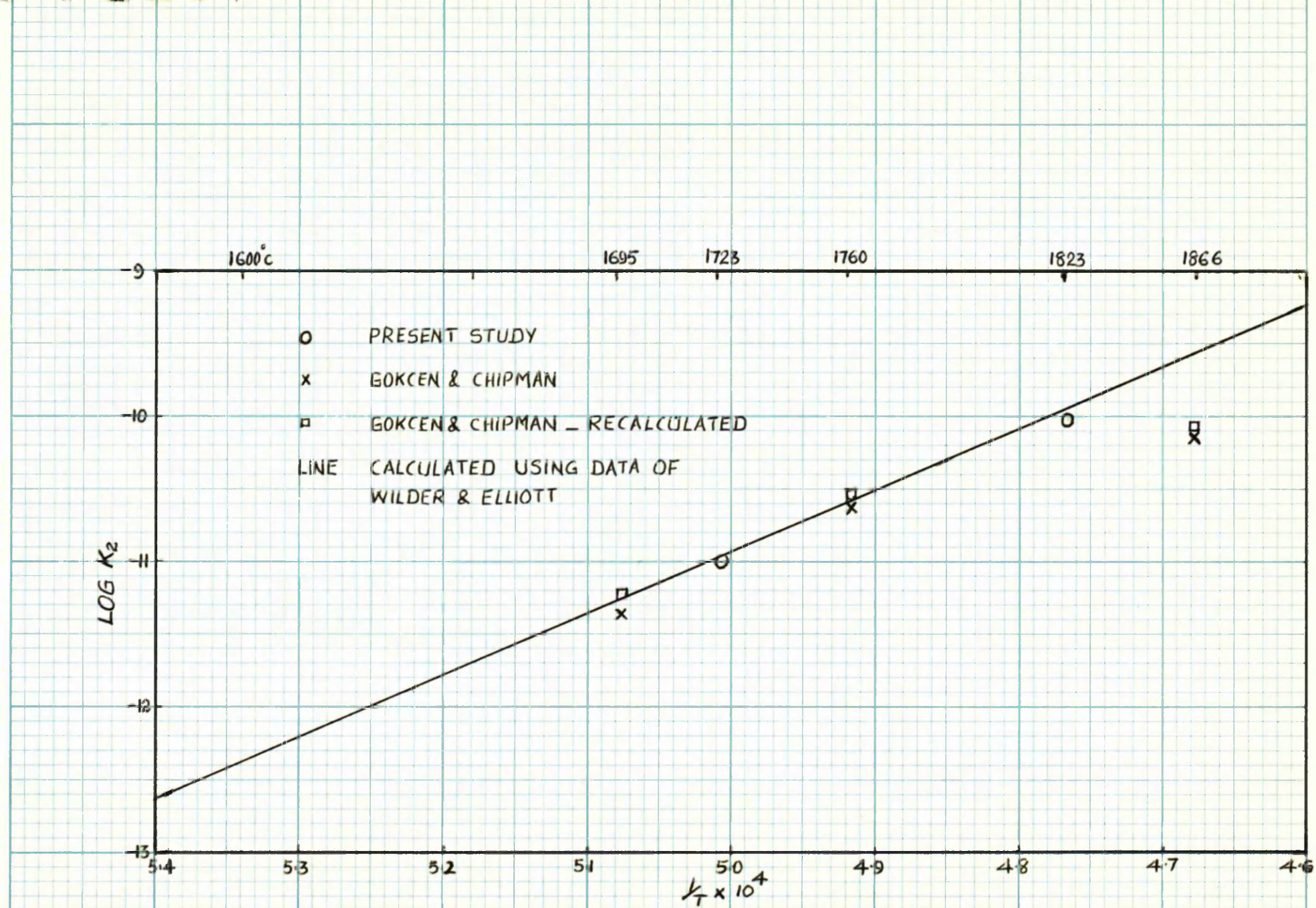

FIG 21 EFFECT OF TEMPERATURE ON LOG $[a_{Al}]^2(p_{H_2O})^3/(p_{H_2})^3$

Wilder and Elliott[22] gave the activity coefficient of aluminium in liquid iron, at infinite dilution, on a mole fraction basis as $\gamma^{\circ}_{Al} = 0.064$ at 1600°C. Conversion from a standard state of unit mole fraction to one of unit weight per cent involves a change in standard free energy, given by[75] :-

$$Al_{(\ell)} = \underline{Al}\ (\%)\ ;\ \Delta G^{\circ} = 4.575\ T \log \frac{0.5585 \times 0.064}{27}\ cal$$

$$= -10,200 - 7.7\ T\ cal\ assuming\ regular\ behaviour$$

$$For\ 2\ Al_{(\ell)} = 2\underline{Al}(\%)\ ;\ \Delta G^{\circ} = -20,400 - 15.4\ T\ cal.....[13]$$

The free energy of formation of water vapour in the temperature range 1800° - 2300°K is given by[74] :-

$$H_2(g) + \tfrac{1}{2}\ O_2(g) = H_2O_{(g)}\ ;\ \Delta G^{\circ} = -60,285 + 14.0T\ cal...[14]$$

$$\therefore\ 3H_2(g) + \tfrac{3}{2}O_2(g) = 3H_2O_{(g)}\ ;\ \Delta G^{\circ} = -180,855 + 42.0\ T\ cal..[15]$$

Combining equations [12], [13] and [15] gives:-

$$Al_2O_3(s) + 3H_2(g) = 2\ \underline{Al} + 3H_2O_{(g)};\Delta G^{\circ} = +199,645 - 50.0\ T\ cal$$

$$and\quad \log K_2 = \frac{-43,600}{T} + 10.9.....[16]$$

As can be seen from Fig 21, with the possible exception of the points at 1866°C, there is good agreement between the two sets of experimental data and the straight line represented by equation [16] derived from thermodynamic data. Even at 1866°C, the recalculated value for log K_2 differs from that of the equation by only 0.5 which is still within the limits placed on the original data by Gokcen and Chipman.

6. Equilibrium Study of the Reaction:- $Al_2O_{3(s)} = 2\,\underline{Al} + 3\,\underline{O}$

Approximate values for the deoxidation constant of aluminium at 1723° and 1823°C, could be obtained from the limiting values of log K_1' at zero oxygen and aluminium concentrations on the graph shown in Fig. 16. However, more accurate values can now be calculated as shown in Table 20 using the values established for $e_{Al}^{(O)}$ and $e_O^{(Al)}$, together with equation [7]:-

$$\text{i. e. } \log K_1 = \log K_1' + 2\log f_{Al}^{(O)} + 3\log f_O^{(Al)}$$
$$= \log K_1' + 2e_{Al}^{(O)}[\%O] + 3e_O^{(Al)}[\%Al]$$

From Section 3

at 1723°C, $\log K_1 = \log K_1' - 11{\cdot}12\,[\%O] - 9{\cdot}90\,[\%Al]$

at 1823°C, $\log K_1 = \log K_1' - 8{\cdot}06\,[\%O] - 7{\cdot}17\,[\%Al]$

TABLE 20 Calculation of the Equilibrium Constant $K_1 = [a_{Al}]^2 \cdot [a_O]^3$

Temperature	Heat No	O, Wt Pct	Al Wt Pct	$-3\log f_O^{(Al)}$	$-2\log f_{Al}^{(O)}$	$-\log K_1'$	$-\log K_1$
1723°C	7	0·0027	0·0217	0·22	0·03	11·03	11·28
	12	0·0035	0·0105	0·10	0·04	11·33	11·47
	31	0·0041	0·0060	0·06	0·05	11·61	11·72
	15	0·0050	0·0030	0·03	0·06	11·95	12·04
				Average Value = 11·63			
1823°C	5	0·0042	0·0666	0·48	0·03	9·48	9·99
	2	0·0055	0·0328	0·24	0·04	9·75	10·03
	8	0·0070	0·0227	0·16	0·06	9·75	9·97
	9	0·0086	0·0098	0·07	0·07	10·21	10·35
	10	0·0107	0·0073	0·05	0·09	10·19	10·33
				Average Value = 10·13			

A graph of $\log K_1$ v $\frac{1}{T^{\circ}K}$ is shown in Fig. 22. The line drawn through the data of the present study corresponds to the equation:-

$$\log K_1 = \frac{-62,500}{T} + 19.67 \quad \ldots\ldots\ldots [17]$$

Also included in Fig 22 for comparison, are the results of a number of other investigations. The results of three of the earlier studies, all of which have been mentioned in Chapter III, can be represented by the following equations:-

Wentrup and Hieber[33], $\log K_1' = \frac{-71,200}{T} + 27.98$ .... [18]

Geller and Dicke[34], $\log K_1' = \frac{-58,600}{T} + 18.90$ .... [19]

Hilty and Crafts[35], $\log K_1' = \frac{-58,600}{T} + 22.75$..... [20]

It should be noted that in each of the above equations, the deoxidation product is expressed in terms of weight concentrations and not activities. In each case the equations are valid for the temperature range 1600° - 1700°C.

In the more recent work reported by Gokcen and Chipman[36], average values for K_1 were calculated from experimental values of $\log K_1'$, by a method similar to that used in Table 20. Their values were in good agreement with an equation calculated from thermodynamic data[37], although they did indicate a slightly smaller temperature coefficient. However the experimental data were not sufficiently precise to justify altering the slope of the calculated line which was represented by the following equation:-

$$\log K_1 = \frac{-64,000}{T} + 20.48 \quad \ldots\ldots\ldots\ldots [21]$$

FIG 22 COMPARISON OF ALUMINIUM DEOXIDATION DATA

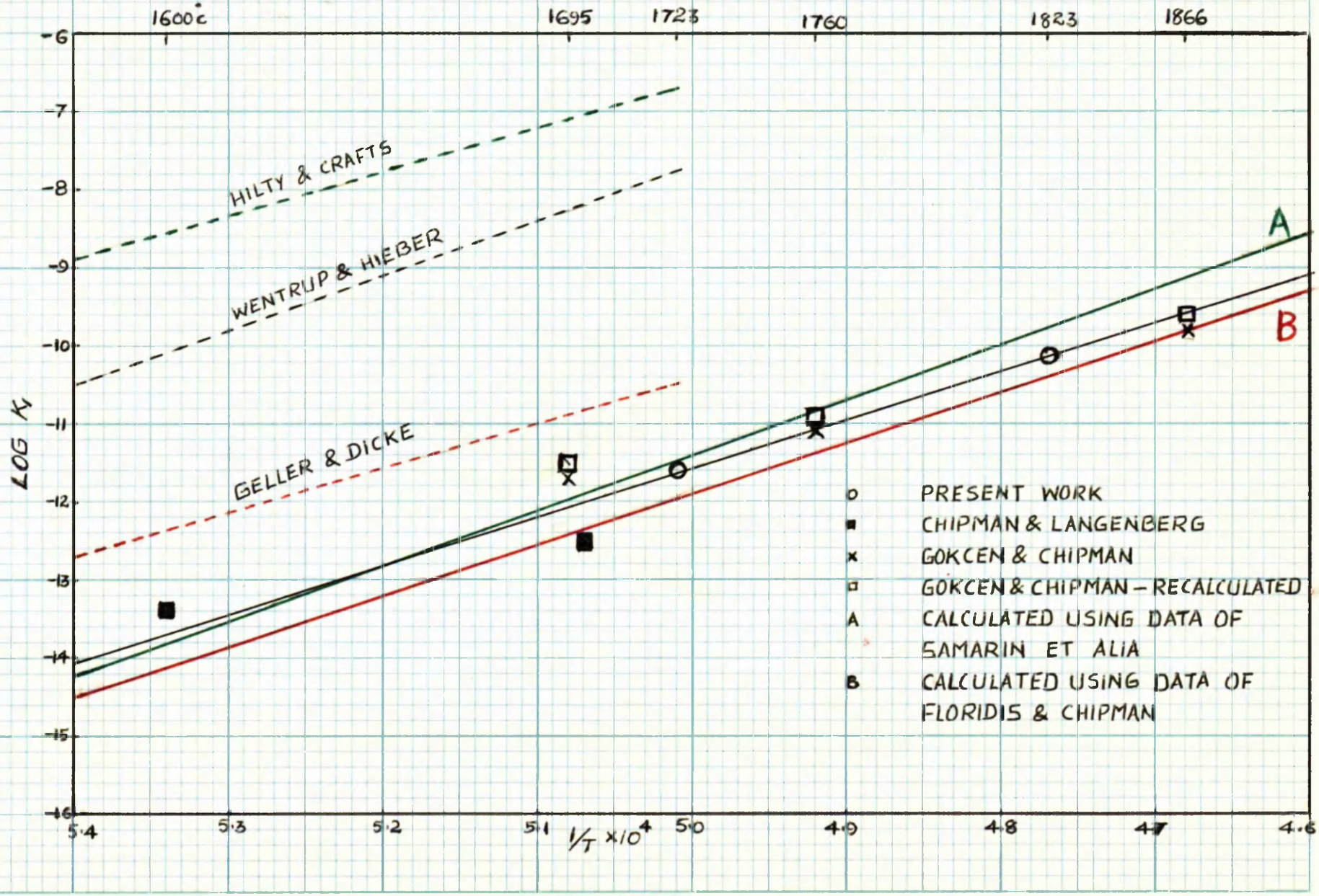

In this case the deoxidation product is expressed in terms of activities. The chief uncertainty in the calculation of equation [21], was the activity coefficient of aluminium in liquid steel, γ°_{Al}. The best data then available was that of Chou and Elliott[26] who estimated a value for γ°_{Al} of 0.043 at 1600°C. In Table 21, Gokcen and Chipman's average values for log K_1 are recalculated using the values for $e_o^{(Al)}$ and $e_{Al}^{(O)}$ from the present study.

The two sets of data, the original and the recalculated, are included in Fig. 22. Also shown are two values for the deoxidation constant at 1600° and 1700°C calculated by Langenberg and Chipman[38] from the results of their study on the aluminium content of carbon saturated iron in equilibrium with pure alumina.

The two calculated lines given in Fig. 22 are based on the known heat of formation of alumina[74], the activity coefficient of aluminium in iron-aluminium alloys[33], and the free energy of solution of oxygen in liquid iron as deduced from the data of (a) Samarin et al[14] and (b) Floridis and Chipman[11]. The equations for the two lines were calculated in the following manner.

From the data collected by Elliott and Gleiser[74], the free energy of formation of Al_2O_3 in the temperature range 1800° - 2300°K, is given by:-

$$Al_2O_3(s) = 2\,Al_{(l)} + \tfrac{3}{2}\,O_2(g); \quad \Delta G^{\circ} = 400{,}900 - 76{\cdot}6\,T \text{ cal} \quad \ldots\ldots[12]$$

From equation [13], $2Al_{(l)} = 2\,\underline{Al}(\%)$; $\Delta G^{\circ} = -20{,}400 - 15{\cdot}4\,T$ cal $\ldots\ldots[13]$

TABLE 21 Calculation of the Equilibrium Constant K_4, using Value for K_4' from Ref. (36)

Temperature	O, Wt Pct	Al, Wt Pct	$-3 \log f_O^{(Al)}$	$-2 \log f_{Al}^{(O)}$	$-\log K_4'$	$-\log K_4$
1695°C	0.0065	0.0038	0.041	0.078	11.41	11.53
	0.0052	0.0045	0.049	0.0622	11.55	11.66
	0.0038	0.0073	0.079	0.046	11.54	11.66
	0.0032	0.0125	0.135	0.038	11.29	11.46
	0.0026	0.0164	0.177	0.031	11.32	11.53
				Average =	11.57	
1760°C	0.0065	0.008	0.071	0.065	10.75	10.89
	0.0062	0.008	0.071	0.062	10.82	10.95
	0.0046	0.015	0.133	0.046	10.66	10.84
	0.0038	0.023	0.204	0.038	10.54	10.78
	0.0036	0.019	0.168	0.036	10.79	10.99
				Average =	10.89	
1866°C	0.0164	0.0085	0.051	0.115	9.50	9.67
	0.0155	0.0086	0.052	0.109	9.56	9.72
	0.0080	0.0230	0.138	0.056	9.57	9.76
	0.0076	0.0260	0.156	0.053	9.53	9.74
	0.0057	0.0570	0.342	0.040	9.22	9.60
				Average =	9.70	

[A] From the data of Samarin et al[14]

$$H_2(g) + \underline{O} = H_2O_{(g)} \quad ; \quad \Delta G^\circ = -43,200 + 20{\cdot}8\ T \text{ cal} \quad \ldots\ldots [22]$$

From equation [14], $H_{2(g)} + \frac{1}{2} O_{2(g)} = H_2O_{(g)}$; $\Delta G^\circ = -60,285 + 14{\cdot}0\ T$ cal ..... [14]

Combining equations [22] and [14] gives the following expression for the free energy of solution of oxygen in liquid iron, where the standard state is taken as the 1 per cent dilute solution:-

$$\tfrac{1}{2} O_{2(g)} = \underline{O}\ (\%) \quad ; \quad \Delta G^\circ = -17,085 - 6{\cdot}8\ T \text{ cal}$$

$$\tfrac{3}{2} O_{2(g)} = 3\ \underline{O}(\%) \quad ; \quad \Delta G^\circ = -51,255 - 20{\cdot}4\ T \text{ cal} \ldots [23]$$

Combining equations [12], [13] and [23] gives:-

$$Al_2O_{3(s)} = 2\ \underline{Al}\ (\%) + 3\ \underline{O}(\%) \; ; \; \Delta G^\circ = 329,245 - 112{\cdot}4\ T \text{ cal}$$
$$\text{and } \log K_1 = \frac{-71,900}{T} + 24{\cdot}6 \ldots\ldots [24]$$

[B] From the data of Floridis and Chipman[11]

$$H_2(g) + \underline{O} = H_2O_{(g)} \quad ; \quad \Delta G^\circ = -32,200 + 14{\cdot}63\ T \text{ cal} \ldots [25]$$

From equation [14], $H_{2(g)} + \frac{1}{2}O_{2(g)} = H_2O_{(g)}$; $\Delta G^\circ = -60,285 + 14{\cdot}0\ T$ cal ... [14]

Combining equations [25] and [14]:-

$$\tfrac{1}{2}O_{2(g)} = \underline{O}\ (\%) \quad ; \quad \Delta G^\circ = -28,085 - 0{\cdot}63\ T \text{ cal}$$

$$\tfrac{3}{2}O_{2(g)} = 3\ \underline{O}(\%) \quad ; \quad \Delta G^\circ = -84,255 - 1{\cdot}89\ T \text{ cal} \ldots [26]$$

Combining equations [12], [13] and [26] gives:-

$$Al_2O_{3(s)} = 2\ \underline{Al}\ (\%) + 3\ \underline{O}(\%) \; ; \; \Delta G^\circ = 296,245 - 93{\cdot}89\ T \text{ cal}$$
$$\text{and } \log K_1 = \frac{-64,700}{T} + 20{\cdot}5$$
$$\ldots\ [27]$$

The two equations for log K_1, [24] and [27], calculated from thermodynamic data, are represented in Fig. 22 by lines A and B respectively. From the various data recorded in Fig. 22, values are deduced for log K_1 or log K_1' as the case may be at 1600°, 1700° and 1800°C and presented in Table 22.

TABLE 22 Values of Log $K_1 = \text{Log } [a_{Al}]^2 \cdot [a_O]^3$

Temperature	Hilty and Crafts +	Wentrup and Hieber +	Geller and Dicke +	Langenberg and Chipman	Gokcen and Chipman	Present Study	Line "A"	Line "B"
1600	-8·6	-10·0	-12·4	-13·4	-13·7	-13·7	-13·6	-14·1
1700	-7·0	-8·1	-10·9	-12·6	-11·9	-12·0	-11·9	-12·3
1800	-	-	-	-	-10·4	-10·5	-10·1	-10·7

+ Log $K_1' = \log [\%Al]^2 \cdot [\%O]^3$

From the data given in Fig. 22 and Table 22, it can be seen that the results of the present study are in good agreement with the values of Gokcen and Chipman, which in the above Table are based on the calculated equation of Ref. (37). They also agree fairly well with the results of Langenberg and Chipman. With reference to the calculated lines, the data is in better agreement with equation [24] corresponding to line A at temperatures below 1770°C and with equation [27] corresponding to line B above 1770°C.

The divergence of the two lines A and B, as the temperature increases, is due entirely to the different data used for computation of the free energy of solution of oxygen in liquid iron.

With regard to the earlier data of Hilty and Crafts, Wentrup and Hieber, and Geller and Dicke, it is clear that discrepancies exist between them and the various other data mentioned in the previous paragraphs. It is possible to account for these discrepancies in several ways.

In all three investigations under consideration, the deoxidation products are expressed in terms of weight concentrations, whereas the various other data are given in terms of activities. The magnitude of the effect of the activity coefficients of aluminium and oxygen on the deoxidation product can be determined with the aid of the equation:-

$$\log K_1 = \log K_1' + 2 \log f_{Al} + 3 \log f_O$$

Of the three sets of data, that of Geller and Dicke comes closest to the calculated values for $\log K_1$. During their investigation the equilibrium studied was that between dissolved carbon (0·4 to 1·1%) and aluminium in liquid iron contained in an alumina crucible. The oxygen concentration was calculated from a knowledge of the carbon content and published data on the equilibrium $\underline{C} + \underline{O} = CO_{(g)}$[76]. In this case in order to calculate values for $\log K_1$, it is necessary to take into account the effect of carbon on the activity coefficients of aluminium and oxygen.

Elliott[77] has derived an equation for the effect of carbon on the activity coefficient of oxygen, based on the data of Marshall and Chipman[76]:-

$$\log f_O^{(C)} = -0{\cdot}42\ [\%C] + 0{\cdot}008\ [\%C]^2 \qquad \ldots\ldots[28]$$

This equation is really only valid for carbon concentrations up to 2 per cent at 1540°C. Elliott has stated however that the error involved in its use at 1600°C is probably quite small in comparison with the uncertainty inherent in its derivation.

Using the distribution data of Chipman and Floridis[27], Wilder and Elliott[33] have calculated a value of +5·3 for the parameter $\epsilon_{Al}^{(C)}$ at 1600°C, which yields the following expression for the effect of carbon on the activity coefficient of aluminium, valid for carbon concentrations up to about 5 per cent.

$$\log f_{Al}^{(C)} = + 0{\cdot}107\ [\%C] \qquad \ldots\ldots\ldots \qquad [29]$$

Taking Geller and Dicke's value for $\log K_1'$ at 1600°C, i.e. -12·4, values can be calculated for $\log K_1$, using the equation

$$\log K_1 = \log K_1' + 2 \log f_{Al} + 3 \log f_O$$

where $$\log f_{Al} = \log f_{Al}^{(O)} + \log f_{Al}^{(C)}$$

and $$\log f_O = \log f_O^{(Al)} + \log f_O^{(C)}$$

Values for $\log f_{Al}^{(O)}$ and $\log f_O^{(Al)}$ can be determined using the parameters $e_{Al}^{(O)}$ and $e_O^{(Al)}$ from the present work and $\log f_O^{(C)}$ and $\log f_{Al}^{(C)}$ can be calculated from equations [28] and [29] respectively.

For carbon concentrations of 0·4 and 1·0 per cent the corresponding oxygen concentrations at 1600°C are 0·0075 and 0·004 per cent[77]; when combined with the above data this yields values for $\log K_1$ of -13·0 and -13·5 respectively.

Thus, when the results of Geller and Dicke are expressed in terms of activities, the discrepancy which exists between them and the data obtained from the more recent studies, is probably of

the same order as the uncertainty inherent in:-(a) the experimental work, which would involve the determination of very small quantities of aluminium, and (b) the theoretical treatment of the data.

If the values obtained by Hilty and Crafts and Wentrup and Hieber for log K_1' are used to compute values for log K_1 , as shown in Table 23, it is found that the correction provided by the use of activities rather than weight concentrations is small when compared with the discrepancy which exists between the experimental and calculated data.

TABLE 23 Calculation of Log K_1 Values

Data at 1600°C	O, Wt Pct	Al, Wt Pct	2 $\log f_{Al}$	3 $\log f_O$	log K_1'	log K_1	log K_1 (line A)
Hilty and Crafts	0·010	0·005	-0·152	-0·069	-8·6	-8·8	-13·8
Wentrup and Hieber	0·010	0·010	-0·152	-0·138	-10·0	-10·3	-13·8

Thus in these two investigations, the major part of the discrepancy must be accounted for by some factor or factors other than activity coefficients.

Hilty and Crafts have pointed out that during their experimental heats, extreme difficulty in attaining equilibrium was experienced, due to extensive reaction between the liquid metal and the alumina crucible, particularly at aluminium concentration below 0·1 per cent. Due to this reaction, the inner surfaces of their crucibles were covered with a layer of material of variable composition,

but containing both iron oxide and alumina. By means of X-ray diffraction, material removed from one of the crucibles was identified as a mixture of the spinel hercynite ($FeO \cdot Al_2O_3$), and alumina.

When aluminium was added to a high oxygen, low aluminium melt, excessive amounts were required to give even a slight increase in the aluminium concentration of the metal. Bell[78] has suggested that this could have been due to the fact, that the first additions of aluminium served only to reduce the metal-crucible surface layer. The alumina formed during this reaction would separate out from the melt and the aluminium content of the metal remain unchanged. It was also observed, that when ferric oxide was added to high aluminium, low oxygen melts, excessive amounts were again required to effect an incremental lowering of the aluminium content, probably because the first oxide added, was used up in the formation of the surface layer.

Although it is not certain that the metal was in equilibrium with the surface layer, it is quite clear that it was not in equilibrium with pure alumina. Thus the activity of alumina in the experiments was not unity, as might be expected from the use of alumina crucibles, but in fact something less than unity. Chipman[79] has pointed out that if the free energy of formation of hercynite is taken into account in the calculation of the deoxidation product, the difference between the calculated and experimental values is of the same order as the experimental uncertainty.

Wentrup and Hieber in their study, added aluminium to molten iron of high oxygen content and considered a period of ten

minutes sufficient for the removal of the products of deoxidation from the melt. Ten minutes after adding the aluminium a sample was taken by pouring a portion of the melt into a copper mould to freeze the equilibrium. The sample was then analysed for aluminium and oxygen and the assumption made, that any oxide inclusions present in the sample had been in solution when the melt was sampled. If, however, the time allowed for separation of alumina from the melt was insufficient, then the assumption was unjustified and consequently the values obtained for the deoxidation product would be higher than those expected from theoretical considerations.

Another possible source of error in the same investigation was the furnace atmosphere, which consisted almost entirely of air at 10 - 20 mm mercury pressure, and as such formed a potential source for continuous oxidation of the melt. It is quite possible, therefore, that the oxygen values used in their calculations of the deoxidation product were too high.

Thus the discrepancies which exist in the data of Geller and Dicke, Hilty and Crafts and Wentrup and Hieber can be explained on the basis of the following factors.

(a) In all three investigations, the use of actual weight concentrations rather than activities.

(b) In the study by Hilty and Crafts, a lack of equilibrium with pure alumina.

(c) In the study by Wentrup and Hieber, (i) insufficient time allowed for the removal of the products of deoxidation from

the melts, and (ii) continuous oxidation of the melt by the furnace atmosphere.

From the results obtained in the present work for the deoxidation constant, K_1, at 1600°, 1723° and 1823°C, corresponding aluminium and oxygen activities can be calculated. A graph showing the relationship between these two quantities at three temperature levels is given in Fig 23. Data are also given for actual concentrations of aluminium and oxygen. These were obtained by substituting the appropriate values of log K_1 and $e_o^{(Al)}$ in equation [11]

$$\text{i.e. } \log K_1 = \log K_1 + 3e_O^{(Al)}(1{\cdot}125\ [\%O] + [\%Al])$$
$$= 2 \log [\%Al] + 3 \log [\%O] + 3e_O^{(Al)}(1{\cdot}125[\%O]+[\%Al])$$

Included in Fig 23 are three lines representing the data at 1600°C of Hilty and Crafts, Wentrup and Hieber and Geller and Dicke.

An interesting feature of the data from the present study is that above a certain percentage of aluminium, the activity coefficient of oxygen is lowered to such an extent, that the oxygen concentrations actually increase with further additions of aluminium. A similar trend was pointed out by Gokcen and Chipman, and their results for 1600° C are also included in Fig 23. At 1600°C their value for K_1 is the same as that obtained from the present work and so the two lines representing activities are the same. Since the values used for the parameter $e_o^{(Al)}$ are different, the two lines representing the corresponding percentages are slightly different. Thus the data of Gokcen and Chipman indicate that a turning point occurs at 0·02 per cent aluminium, whereas the new data shows the turning

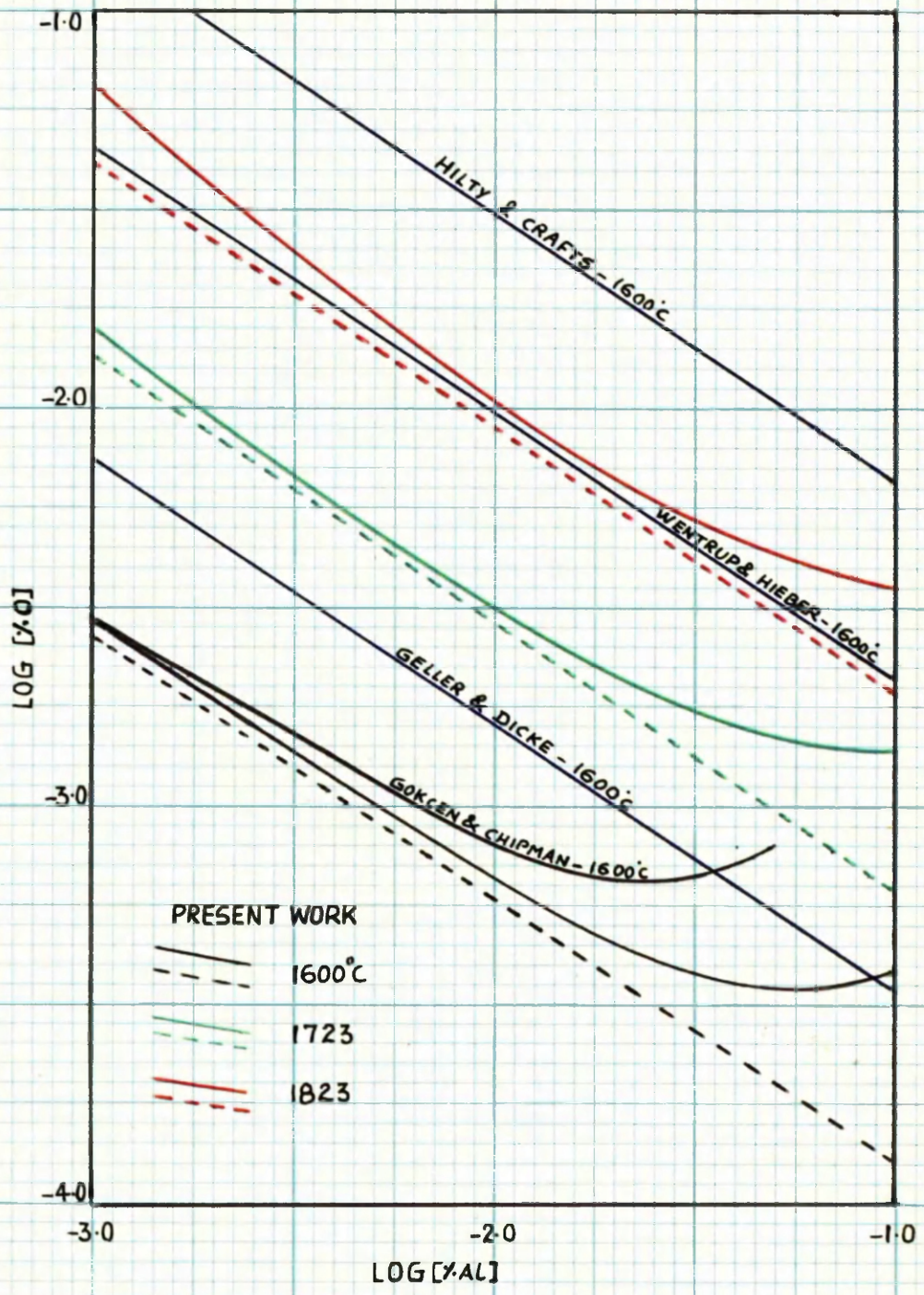

FIG 23 COMPARISON OF ALUMINIUM DEOXIDATION DATA. BROKEN LINES SHOW ACTIVITIES - SOLID LINES ARE CORRESPONDING PERCENTAGES.

point at 0·06 per cent aluminium.

It can also be seen from Fig. 23 that as the temperature increases from 1600° to 1723°C the aluminium concentration at the turning point increases from 0·06 to 0·08 per cent. This effect is due to the fact that as the temperature increases, the deviation from ideality, and therefore the aluminium-oxygen interaction, gradually decreases.

Summary

An experimental study has been made at 1723° and 1823°C of the equilibria involved between pure alumina, liquid iron containing aluminium and oxygen and controlled water-vapour/hydrogen gas mixtures.

From the data obtained, values have been calculated for the parameters $e_O^{(Al)}$ and $e_{Al}^{(O)}$ (Table 15) which indicate that the activity coefficient of oxygen in liquid iron is greatly reduced in the presence of aluminium and the activity coefficient of aluminium is greatly reduced in the presence of oxygen.

With the aid of the above parameters, values have been calculated for the equilibrium constants of the following reactions:-

$$Al_2O_3(s) = 2\,\underline{Al} + 3\,\underline{O}$$

$$Al_2O_3(s) + 3H_2(g) = 2\,\underline{Al} + 3\,H_2O(g)$$

$$H_2(g) + \underline{O} = H_2O(g)$$

Extrapolation of the various data to 1600°C yields values which are probably more accurate than a direct experimental determination would be at that temperature. Wherever possible these values have been compared with other experimental data and also values deduced from available thermodynamic data.

C H A P T E R VII

CHROMIUM-ALUMINIUM-OXYGEN EQUILIBRIA IN LIQUID IRON

1. Introduction

2. Calculation of Equilibrium Ratios and Related Functions

3. Chromium-Oxygen Interaction in Liquid Iron

4. Chromium-Aluminium Interaction in Liquid Iron

5. Chromium-Aluminium-Oxygen Interaction in Liquid Iron

CHROMIUM-ALUMINIUM-OXYGEN EQUILIBRIA IN LIQUID IRON

1. Introduction

In this chapter a study is made of the effect of chromium on the activity coefficients of aluminium and oxygen in liquid iron. 20 g samples containing the required amounts of electrolytic iron and chromium were made up in the form of pellets. Heats were made at 1723°C with chromium concentrations of 2, 6 and 10 per cent by weight.

The melts, contained in pure alumina crucibles, were held at constant temperature for 12 hours under controlled water-vapour/hydrogen atmospheres, quenched with cold hydrogen and analysed. In the determination of aluminium using solochrome cyanine R, chromium causes interference and it was therefore necessary to remove the chromium from the test solution before attempting to measure the aluminium concentration. This was accomplished by means of a mercury cathode separation. Under these conditions it was found that duplicate analyses were not quite as close together as they were in the absence of chromium. For this reason slightly wider limits ($\pm$ 0·001 rather than $\pm$ 0·0005) are placed on the aluminium results.

2. Calculation of Equilibrium Ratios and Related Functions

In Table 24, equilibrium ratios are given for the following reactions together with experimental data from a series of heats which are thought to have reached equilibrium at 1723°C.-

$$Al_2O_{3(s)} = 2\,\underline{Al} + 3\,\underline{O} \;;\; K_1' = [\%Al]^2 \cdot [\%O]^3$$

$$Al_2O_3(s) + 3H_{2(g)} = 2\,\underline{Al} + 3H_2O_{(g)} \;;\; K_2' = [\%Al]^2 (p_{H_2O}/p_{H_2})^3$$

$$H_{2(g)} + \underline{O} = H_2O_{(g)} \;;\; K_3' = p_{H_2O}/p_{H_2} \cdot [\%O]$$

In Table 25 the interaction parameters $e_o^{(Al)}$ and $e_{Al}^{(O)}$ which were determined in the previous chapter, are used to calculate values for the coefficients $f_o^{(Al)}$ and $f_{Al}^{(O)}$. These coefficients are combined with the equilibrium products of Table 24 to give three functions, which, when plotted against per cent chromium, yield values for the parameters $e_o^{(Cr)}$ and $e_{Al}^{(Cr)}$ as described in the following sections.

3. Chromium -Oxygen Interaction in Liquid Iron

The effect of chromium on the activity of oxygen in liquid iron was determined as follows from the reaction:-

$$H_{2(g)} + \underline{O} = H_2O_{(g)}$$

The equilibrium constant for this reaction, K_3 may be expressed as:-

$$K_3 = \frac{p_{H_2O}}{p_{H_2}} \cdot \frac{1}{[f_o \cdot \%O]}$$

$$= K_3'/f_o$$

In this instance, $f_o = f_o^{(O)} f_o^{(Al)} f_o^{(Cr)}$

where f_o represents the activity coefficient of oxygen in Fe-Cr-Al-O melts,

$f_o^{(O)}$ represents the activity coefficient of oxygen in binary Fe-O melts of the same oxygen concentration. As explained in the previous chapter, since the concentrations of oxygen involved were small, $f_o^{(O)}$ may be taken as unity.

TABLE 24 Computation of the Equilibrium Ratios K_1', K_2', and K_3'

Heat No	$P_{H_2O}/P_{H_2} \times 10^3$	Al, Wt Pct x_3 10	O, Wt Pct x_3 10	$K_1' = [\%Al]^2[\%O]^3$	$K_2' = \frac{[\%Al]^2}{(P_{H_2O}/P_{H_2})^3}$	$K_3' = \frac{(P_{H_2O}/P_{H_2})^3}{[\%O]}$
0 Pct Cr						
7	3.54	21.7	2.7	9.27×10^{-12}	2.09×10^{-11}	1.31
12	4.92	10.5	3.5	4.72×10^{-12}	1.31×10^{-11}	1.41
31	6.56	6.0	4.1	2.48×10^{-12}	1.02×10^{-11}	1.60
2 Pct Cr						
49	3.53	31	3.2	3.14×10^{-11}	4.23×10^{-11}	1.104
44	4.78	13	5.1	2.24×10^{-11}	1.85×10^{-11}	0.937
43	6.55	5	6.7	7.52×10^{-12}	0.70×10^{-11}	0.979
6Pct Cr						
51	3.53	24	6.0	1.24×10^{-10}	2.54×10^{-11}	0.590
47	4.84	8	7.9	3.16×10^{-11}	0.73×10^{-11}	0.612
48	6.75	2	9.0	2.92×10^{-12}	1.23×10^{-12}	0.750
10 Pct Cr						
50	3.56	20	9.0	2.92×10^{-10}	1.81×10^{-11}	0.396
45	4.82	5	10.5	2.90×10^{-11}	0.28×10^{-11}	0.458
46	6.58	1	11.4	1.48×10^{-12}	0.03×10^{-11}	0.577

TABLE 25 - Computation of Functions for Determination of Parameters $e_o^{(Cr)}$ and $e_{Al}^{(Cr)}$

Heat No	Al Wt Pct x 10^3	O Wt Pct x 10^3	$-\log f_o^{(Al)}$	$-2\log f_{Al}^{(O)}$	$-\log K_1'$	$-\log K_2'$	$-\log K_3'$	$-[\log K_3' - \log f_o^{(Al)}]$	$-[\log K_2' + 2\log f_{Al}^{(O)}]$	$-[\log K_1' + 2\log f_{Al}^{(O)} + 3\log f_o^{(Al)}]$
0 pct Cr										
7	21·7	2·7	0·07	0·03	11·03	10·68	-0·12	-0·19	10·71	11·28
12	10·5	3·5	0·03	0·04	11·33	10·88	-0·15	-0·18	10·92	11·47
31	6·0	4·1	0·02	0·05	11·61	10·99	-0·20	-0·22	11·04	11·72
						Average values taken from previous Chapter:-		-0·21	10·99	11·6
2 pct Cr										
49	31	3·2	0·10	0·04	10·50	10·37	-0·04	-0·14	10·41	10·85
44	13	5·1	0·04	0·06	10·65	10·73	+0·03	-0·01	10·79	10·84
43	5	6·7	0·02	0·07	11·12	11·15	+0·01	-0·01	11·22	11·24
						Average values		-0·05	10·81	10·9
6 pct Cr										
51	24	6·0	0·08	0·07	9·91	10·60	0·23	0·15	10·67	10·22
47	8	7·9	0·03	0·09	10·50	11·14	0·21	0·18	11·23	10·67
48	2	9·0	0·01	0·10	11·53	11·91	0·12	0·11	12·01	11·65
						Average values		0·15	11·30	10·8
10 pct Cr										
50	20	9·0	0·07	0·10	9·53	10·74	0·40	0·33	10·84	9·83
45	5	10·5	0·02	0·12	10·54	11·55	0·34	0·32	11·67	10·71
46	1	11·4	0·00	0·13	11·83	12·55	0·24	0·24	12·68	11·97
						Average values		0·30	11·73	10·8

$f_O^{(Al)}$ represents the effect of aluminium on the activity coefficient of oxygen,

and $f_O^{(Cr)}$ represents the effect of chromium on the activity coefficient of oxygen.

Thus $\log K_3 = \log K_3' - \log f_O^{(Al)} - \log f_O^{(Cr)}$

Thus

$$\text{i.e. } \log K_3' - \log f_O^{(Al)} = \log f_O^{(Cr)} + \log K_3$$

$$= e_O^{(Cr)}[\%Cr] + \log K_3$$

From the data in Table 25, for the function $\log K_3' - \log f_O^{(Al)}$

From the data in Table 25, for the function $\log K_3 - \log f_O^{(Cr)}$

a graph is constructed as shown in Fig. 24. The line drawn through the data is such that the intercept at zero per cent chromium corresponds to the average value calculated for $\log K_3$, in the previous chapter. The gradient of the line is equivalent to the parameter $e_O^{(Cr)}$, and yields a value for this parameter of -0·057 at 1723°C. Assuming regular behaviour this corresponds to a value for $e_O^{(Cr)}$ at 1600°C, of -0·061. This value is compared with data from other investigations in Table 26, from which it is evident that the data from all the studies, except that of Chen and Chipman, are in reasonable agreement.

TABLE 26 Chromium-Oxygen Interaction in Liquid Iron at 1600°C

Parameter	Chen and Chipman[41,45]	Turkdogan[47]	Charlton[44]	Present Study
$e_O^{(Cr)} = \partial \log f_O / \partial [\%Cr]$	-0·041	-0·064	-0·058	-0·061
$\epsilon_O^{(Cr)} = \partial \ln f_O / \partial N_{Cr}$	-8·8	-13·7	-12·4	-13·1

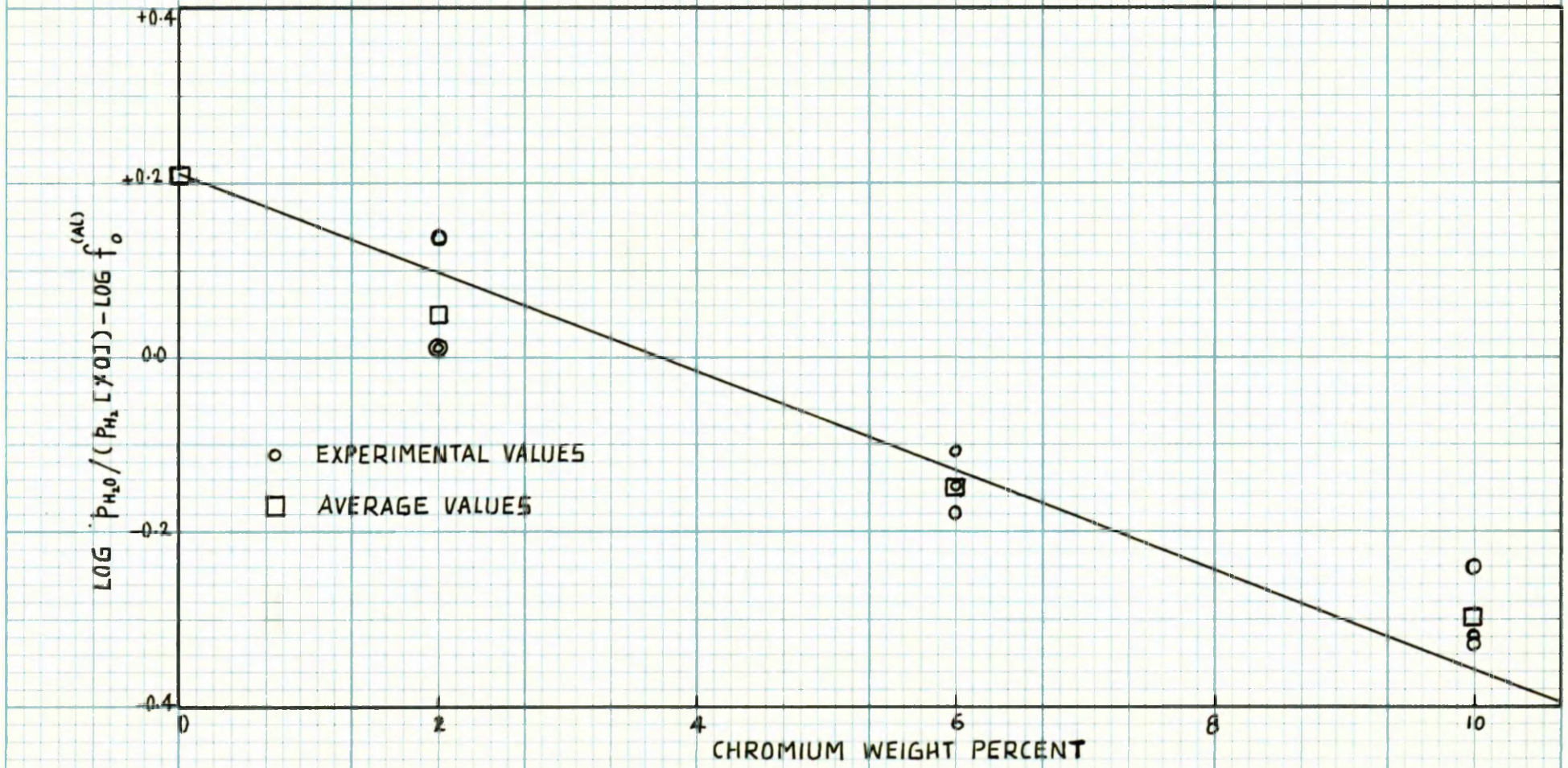

FIG 24 EFFECT OF CHROMIUM ON LOG K_3'

4. Chromium-Aluminium Interaction in Liquid Iron

The effect of chromium on the activity coefficient of aluminium can be deduced from the data recorded in Tables 24 and 25 with reference to the following reactions.

$$Al_2O_3(s) + 3\,H_2(g) = 2\,\underline{Al} + 3\,H_2O(g)$$

The equilibrium constant for this reaction may be expressed in terms of the equilibrium product K_2' and activity coefficients.-

$$\text{i.e. } K_2 = [f_{Al} \times \%Al\,]^2 \left(\frac{p_{H_2O}}{p_{H_2}}\right)^3$$

$$= f_{Al}^2 \cdot K_2'$$

and in this case $f_{Al} = f_{Al}^{(O)} \cdot f_{Al}^{(Cr)}$

where $f_{Al}^{(O)}$ represents the effect of oxygen, and $f_{Al}^{(Cr)}$ the effect of chromium on the activity coefficient of aluminium. As in the previous chapter $f_{Al}^{(Al)}$ is assumed to be unity.

$$\text{Thus } \log K_2 = \log K_2' + 2 \log f_{Al}^{(O)} + 2 \log f_{Al}^{(Cr)}$$

$$\text{i.e. } \log K_2' + 2 \log f_{Al}^{(O)} = -2\,e_{Al}^{(Cr)}[\%Cr] + \log K_2$$

In Fig 25, a graph is presented of $\log K_2' + 2 \log f_{Al}^{(O)}$ v $[\%Cr]$. Limits shown on this graph illustrate the effect of an error of $\pm$ 0·001 per cent in the aluminium analysis. There is a degree of scatter in the data which is greatest in those melts which have a very low aluminium content. At this level, the error limits are greatest, e.g. heats 48 and 46, where the aluminium concentrations are 0·002 and 0·001 per cent respectively.

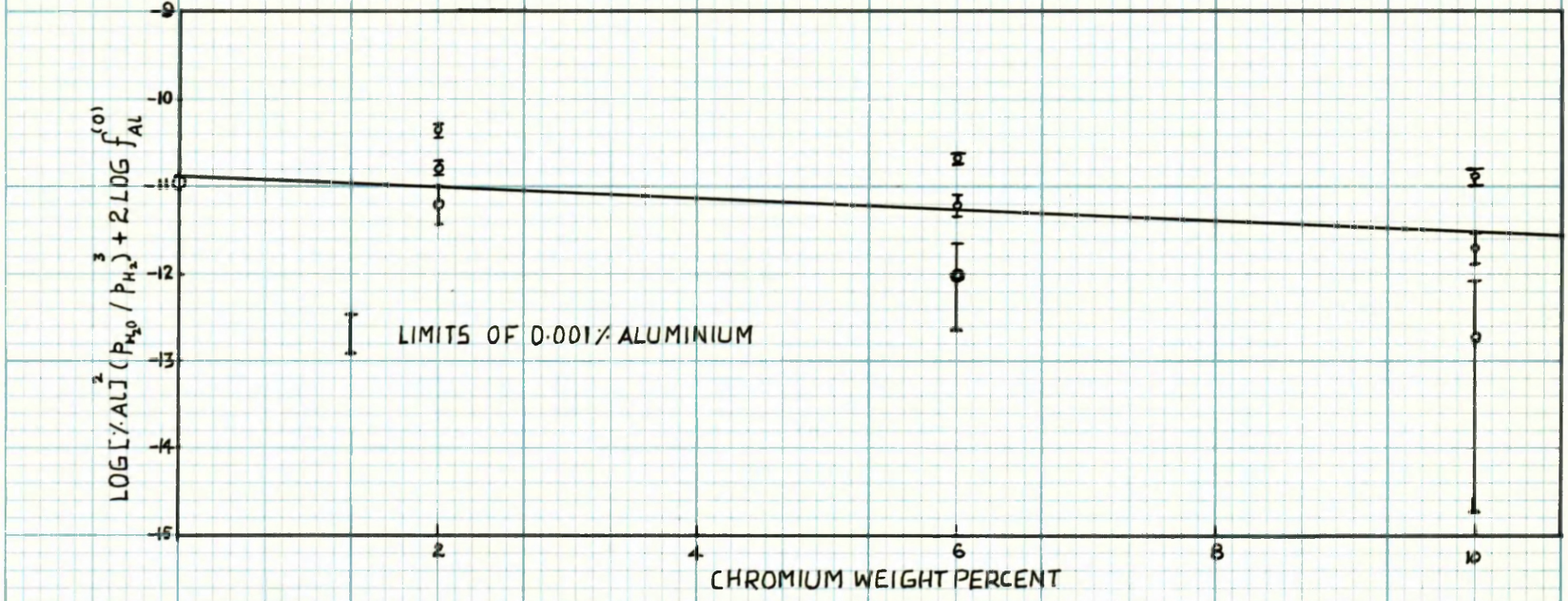

FIG 25 EFFECT OF CHROMIUM ON LOG K_2'

The line drawn through the data is such that the intercept at zero per cent chromium corresponds to the value determined for log K_3 in the previous chapter. The gradient of the line is of opposite sign to the parameter $\epsilon_{Al}^{(Cr)}$, and twice its magnitude. From this data $\epsilon_{Al}^{(Cr)}$ has the value + 0·025 at 1723°C, which corresponds to a value of +5·36 for the parameter $\epsilon_{Al}^{(Cr)}$ at the same temperature. At 1600°C, $\epsilon_{Al}^{(Cr)}$ will have the value + 5·7, assuming regular behaviour.

These values for the parameter $\epsilon_{Al}^{(Cr)}$ are of particular interest from the point of view that no experimental data appear to have been published for the effect of chromium on the activity coefficient of aluminium in liquid iron.

Recently Wada, Kawai and Saito[43] reported data for the activity of chromium in liquid iron-chromium alloys. From their results a value of about + 6 is obtained for the parameter $\epsilon_{Cr}^{(Cr)} = \partial \ln \gamma_{Cr} / \partial N_{Cr}$ at 1600°C and for concentrations up to about 0·1 N_{Cr}. For iron-aluminium alloys at the same temperature, Wilder and Elliott[32] have calculated a value of + 5·3 for the parameter $\epsilon_{Al}^{(Al)} = \partial \ln \gamma_{Al} / \partial N_{Al}$

With the aid of equation [12] from Chapter II$_b$, and the above data for Fe-Cr and Fe-Al binary solutions, a value can be deduced for the effect of chromium on the activity coefficient of aluminium in ternary Fe-Cr-Al solutions.

From Chapter II, equation [12]: $\epsilon_3^{(2)} = \epsilon_2^{(3)} \cong \pm \left[\epsilon_2^{(2)} \cdot \epsilon_3^{(3)}\right]^{1/2}$

i.e. $\epsilon_{Al}^{(Cr)} \cong \pm \left[\epsilon_{Cr}^{(Cr)} \cdot \epsilon_{Al}^{(Al)}\right]^{1/2}$

$\cong \pm \left[6 \times 5.3\right]^{1/2} \cong \pm 5.6.$

Wagner[3] has pointed out that in a ternary solution, the activity of solute metal 2, will be increased by the presence of solute metal 3, provided metals 2 and 3 change the electron/atom ratio in the same direction. For this reason the negative value in the above expression is rejected and $\epsilon_{Al}^{(Cr)}$ taken as + 5·6. This value is in very good agreement with that of + 5·7 obtained from the present study.

Using the distribution data of Chipman and Floridis[27], Wilder and Elliott[33] have also shown that at 1600°C, $\epsilon_{Al}^{(C)} = + 5·3$ and $\epsilon_{Al}^{(Si)} = + 7·0$. In each case the parameter $\epsilon_{Al}^{(i)}$ is for the infinitely dilute solution of i in Fe-Al alloys.

The relative effects of the three solutes, chromium, carbon and silicon, on the activity coefficient of aluminium at 1600°C, are shown in Fig. 26 from which it is clear that the effect of chromium is of the same order as that of carbon and silicon, and intermediate between them.

The positive parameters can be interpreted in terms of a competition between the various solute atoms, for iron atoms in the nearest neighbour shells. For example, the bonding of iron atoms to chromium will leave fewer iron atoms for the aluminium and so the activity coefficient of the latter will be increased. The positive parameters also imply that there are little or no intersolute attractive forces present in contrast to systems such as Fe-Al-O or Fe-Cr-O.

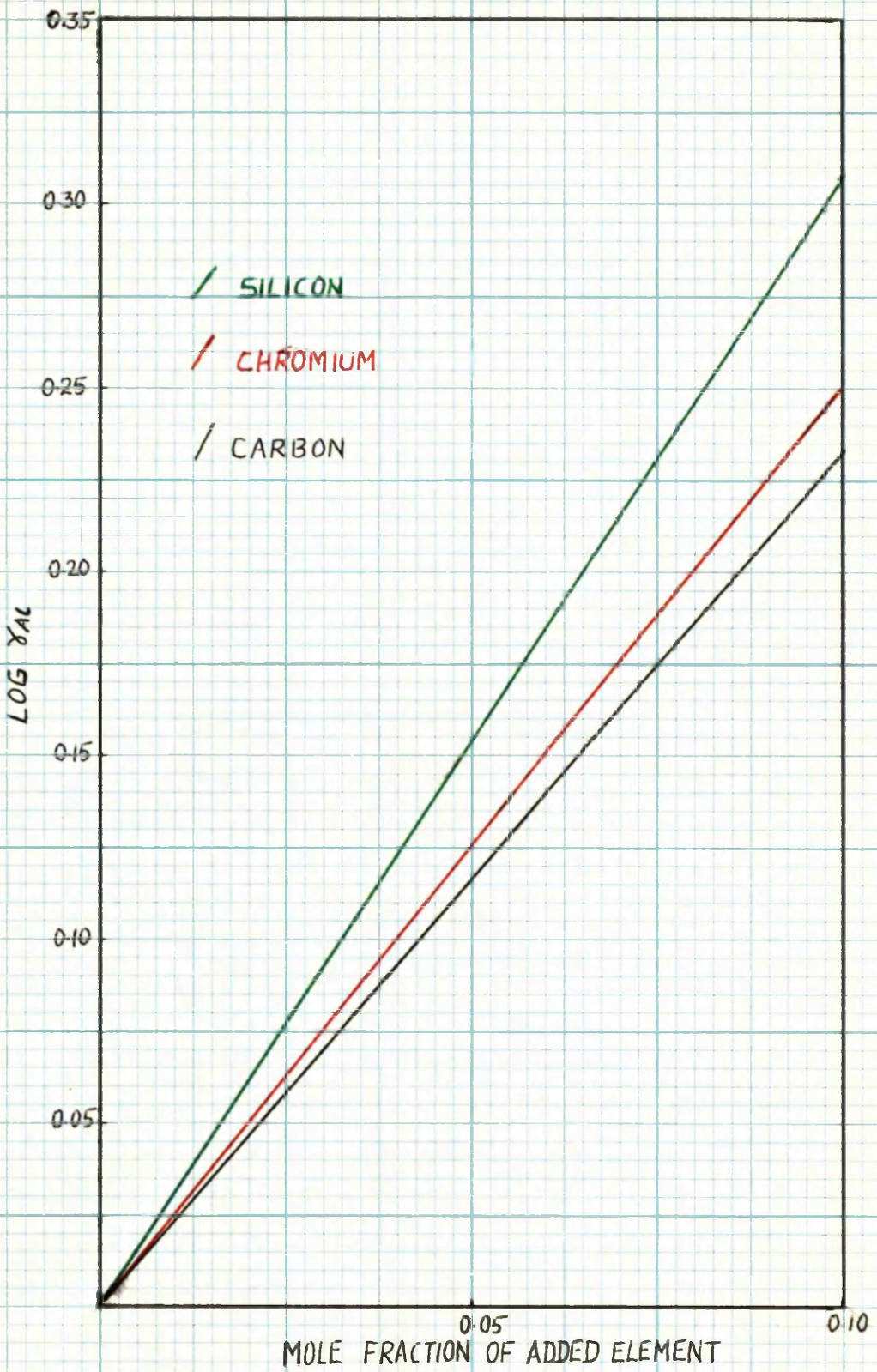

FIG 26 EFFECT OF SILICON, CHROMIUM AND CARBON ON THE ACTIVITY COEFFICIENTS OF ALUMINIUM IN LIQUID IRON AT 1600°C

5. Chromium-Aluminium-Oxygen Interaction in Liquid Iron

The effect of chromium on the deoxidation product $[\%Al]^2 \cdot [\%O]^3$ can be deduced from the values of $e_O^{(Cr)}$ and $e_{Al}^{(Cr)}$. A check on these values can be obtained from consideration of the data in Table 25 with reference to the following reaction. This reaction is to some extent independent of the two other reactions studied in that it does not involve water-vapour/hydrogen ratios.

$$Al_2O_{3(s)} = 2\,\underline{Al} + 3\,\underline{O}$$

The equilibrium constant K_1 may be written as:-

$$K_1 = f_{Al}^2 \cdot f_O^3 \cdot (\%Al)^2 (\%O)^3$$
$$= f_{Al}^2 \cdot f_O^3 \cdot K_1'$$

From the previous sections, $f_{Al} = f_{AL}^{(O)} \cdot f_{AL}^{(Cr)}$

and $$f_O = f_O^{(Al)} \cdot f_O^{(Cr)}$$

so that, $\log K_1 = \log K_1' + 2 \log f_{Al}^{(O)} + 3 \log f_O^{(Al)} + 2 \log f_{Al}^{(Cr)} + 3 \log f_O^{(Cr)}$

i.e. $\log K_1' + 2 \log f_{Al}^{(O)} + 3 \log f_O^{(Al)} = -2 e_{Al}^{(Cr)}[\%Cr] - 3 e_O^{(Cr)}[\%Cr] + \log K_1$

$$= -2\left\{ e_{Al}^{(Cr)} + 1.5 e_O^{(Cr)} \right\}[\%Cr] + \log K_1$$

A graph of $\left\{\log K_1' + 2 \log f_{Al}^{(O)} + 3 \log f_O^{(Al)}\right\}$ v $[\%Cr]$ is shown in Fig. 27. It is apparent that there is a scatter associated with the data similar to that observed in Fig 25, where it was attributed mainly to errors in the determination of very small quantities of aluminium. As the data of Fig 27 is also dependent on aluminium analysis, a similar type of scatter is to be expected. At zero per cent chromium, the intercept corresponds to the equilibrium constant K_1 calculated in Chapter VI. The gradient of the line is equal to + 0.123.

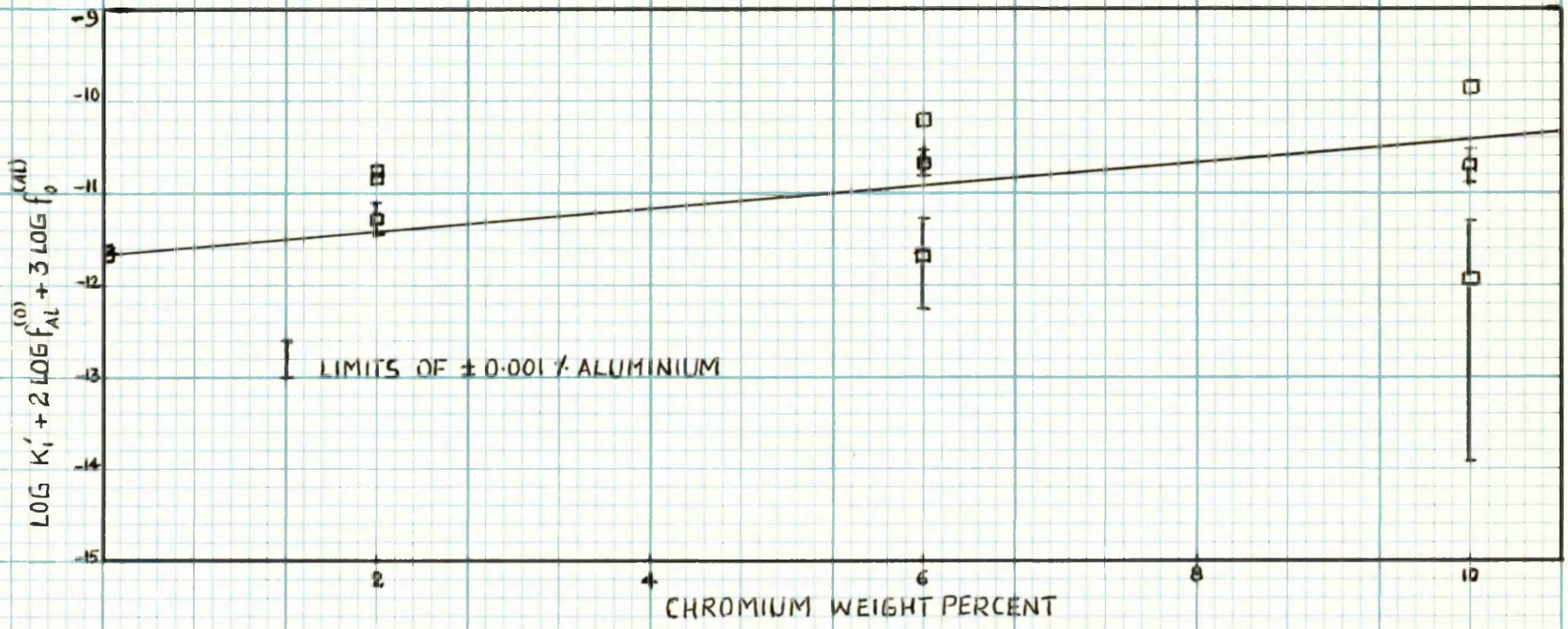

FIG 27 EFFECT OF CHROMIUM ON THE ALUMINIUM DEOXIDATION PRODUCT AT 1723°C

i.e. $-2\left\{e^{(Cr)}_{Al} + 1{\cdot}5\, e^{(Cr)}_{O}\right\} = +0{\cdot}123$

or, $e^{(Cr)}_{Al} + 1{\cdot}5\, e^{(Cr)}_{O} = -0{\cdot}0615$

From sections 2 and 3, $e^{(Cr)}_{Al} + 1{\cdot}5\, e^{(Cr)}_{O} = -0{\cdot}0605$

Thus consideration of the results pertaining to the deoxidation reaction, yields data which are in good agreement with the values calculated for the two parameters in the previous sections.

i.e. at 1723°C $e^{(Cr)}_{O} = -0{\cdot}057$

and $e^{(Cr)}_{Al} = +0{\cdot}025$

On the basis of these parameters a graph is constructed as shown in Fig 28. This illustrates the effect of chromium on the activity coefficients of aluminium and oxygen in liquid iron at 1723°C.

The effect of chromium on the aluminium-oxygen content of liquid iron is shown in Fig 29 where the broken line represents aluminium and oxygen activities, and the full lines represent actual concentrations. The full lines were deduced from consideration of the equation:-

$$\log K_1 = \log K_1' + 2 \log f^{(o)}_{Al} + 3 \log f^{(Al)}_{O} + 2\left\{e^{(Cr)}_{Al} + 1{\cdot}5\, e^{(Cr)}_{O}\right\}[\%Cr]$$

Taking the values for K_1, $e^{(Al)}_{o}$ and $e^{(o)}_{Al}$ calculated in Chapter VI together with the values for $e^{(Cr)}_{O}$ and $e^{(Cr)}_{Al}$ deduced in the present chapter, this equation can be expressed in the following form:-

$$-11{\cdot}63 = 2 \log[\%Al] + 3 \log[\%O] - 9{\cdot}9[\%Al] - 11{\cdot}15[\%O] - 0{\cdot}121[\%Cr]$$

From this equation oxygen concentrations corresponding to a series of aluminium and chromium concentrations were calculated and are shown in Fig 29.

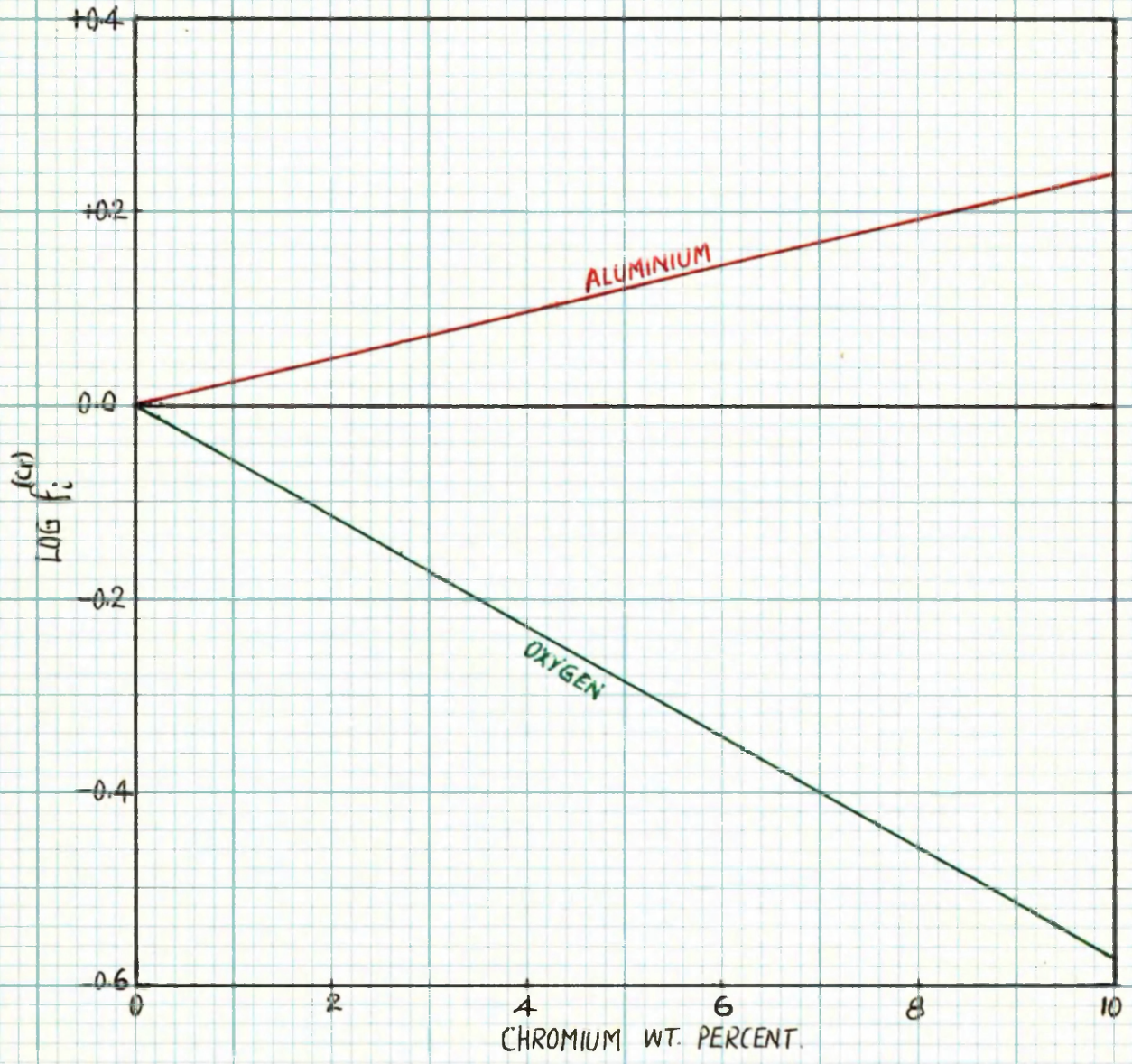

FIG 28. EFFECT OF CHROMIUM ON THE ACTIVITY COEFFICIENTS OF ALUMINIUM AND OXYGEN IN LIQUID IRON AT 1723°C

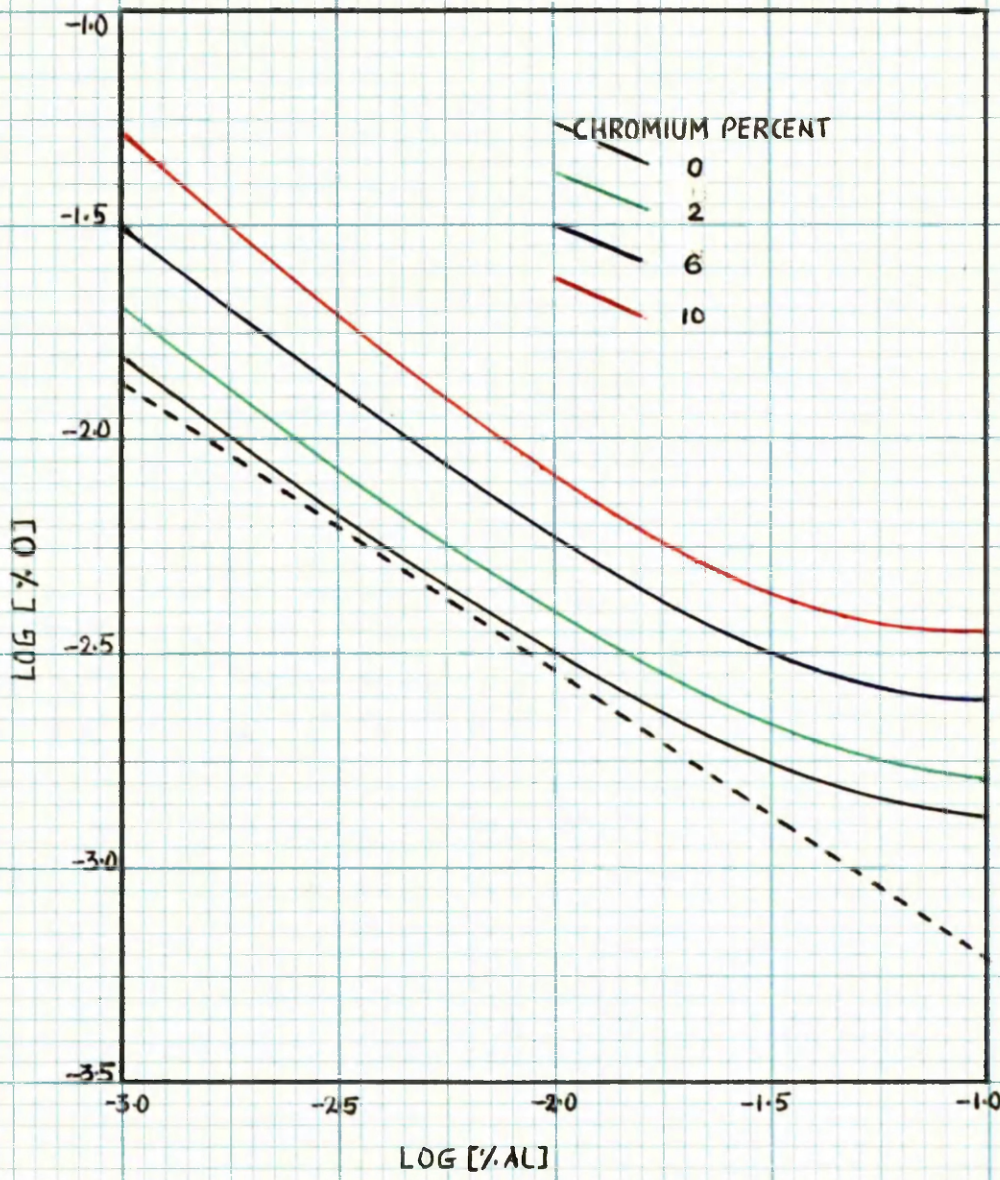

FIG 29 EFFECT OF CHROMIUM ON THE CONCENTRATIONS OF ALUMINIUM AND OXYGEN IN LIQUID IRON AT 1723°C. BROKEN LINE SHOWS ACTIVITIES. SOLID LINES ARE CORRESPONDING PERCENTAGES.

Summary

A study has been made of the equilibria existing between pure alumina, Fe-Cr-Al-O melts and controlled water-vapour/hydrogen gas atmospheres at 1723°C. When combined with the values for the parameters $e_o^{(Al)}$ and $e_{Al}^{(O)}$ from Chapter VI, the data from this investigation yield values for the parameters $e_o^{(Cr)}$ and $e_{Al}^{(Cr)}$. On the assumption that the parameters are inversely proportional to the absolute temperature values are deduced for $\epsilon_o^{(Cr)}$ and $\epsilon_{Al}^{(Cr)}$ at 1600°C.

Reasonable agreement with published data is indicated by a direct comparison in the case of $\epsilon_o^{(Cr)}$ and an indirect comparison in the case of $\epsilon_{Al}^{(Cr)}$. For $\epsilon_{Al}^{(Cr)}$, the comparison depends on the validity of Wagner's relationship[2], $\epsilon_2^{(1)} \cong \pm \left[\epsilon_2^{(2)} \cdot \epsilon_3^{(3)}\right]^{1/2}$.

C H A P T E R VIII

SILICON-ALUMINIUM-OXYGEN EQUILIBRIA IN LIQUID IRON

1. Introduction

2. Presentation of the Basic Data

3. Implications of the Experimental Data

4. Reassessment of the Data on the Basis of Silicon Monoxide Formation

5. Consideration of Some Published Data on the Activity of Silicon in Liquid Iron.

SILICON-ALUMINIUM-OXYGEN EQUILIBRIA IN LIQUID IRON

1. Introduction

The effect of silicon on the activity coefficient of aluminium in liquid iron has been the subject of a number of investigations[27,32,36] based on partition experiments. Experiments of this type have shown that the activity coefficient of aluminium is increased by the presence of silicon. Thus at 1600°C, $\epsilon_{Al}^{(Si)} = +7{\cdot}0$. From the data of the previous chapter this effect is slightly greater than that of chromium.

Gas-metal equilibrium studies of the Fe-Si-O system[22,57,58] have shown that the activity coefficient of oxygen is decreased by the presence of silicon and the activity coefficient of silicon is decreased by the presence of oxygen. Since the oxygen concentration is usually low, this latter effect is often negligible and the activity coefficient of silicon may be taken as equal to that in the Fe-Si binary[30,58]. Using this assumption together with data derived from studies of gas-metal equilibria Chipman and Pillay[50] have calculated an average value of + 36 for the parameter $\epsilon_{Si}^{(Si)}$ at 1600°C. This value, however, is in marked disagreement with that obtained from experiments involving the partition of silicon between liquid iron and liquid silver. Such experiments[51,52] yield a value of about 13 for $\epsilon_{Si}^{(Si)}$ at 1600°C.

Thus there is a discrepancy in the data for the activity of silicon in liquid iron.

This chapter is devoted to a discussion of the data

derived from a study of the effect of silicon on the activity coefficients of aluminium and oxygen in Fe-Si-Al-O melts. In the light of the results obtained, some of the published data on Fe-Si-O gas-metal equilibria are re-examined and a hypothesis is put forward to explain the discrepancy mentioned above.

The experimental technique was similar to that described in the previous chapters.

2. Presentation of the Basic Data

Data obtained from a number of heats involving Fe, Si, Al and O, are used to calculate values for the products K_1', K_2', and K_3' as shown in Table 27.

In the following three sections expressions are deduced, which when combined with the data of Table 28, yield information on the effect of silicon on the activity coefficients of oxygen and aluminium.

(a) The Effect of Silicon on the Activity Coefficient of Oxygen

For the reaction:-

$$H_2(g) + \underline{O} = H_2O_{(g)}$$

$$K_3 = \frac{p_{H_2O}}{p_{H_2}} \cdot \frac{1}{[f_o \cdot \%O]} = \frac{K_3'}{f_o}$$

where the activity coefficient of oxygen f_o is given by:-

$$f_o = f_o^{(Al)} \cdot f_o^{(Si)}$$

TABLE 27 Computation of K_1', K_2' and K_3' at 1723°C.

Heat No.	Si, Wt Pct Charged	Si, Wt Pct Analysed	$p_{H_2O}/p_{H_2} \times 10^3$	O, Wt Pct $\times 10$	Al, Wt Pct $\times 10^3$	$K_1' = [\%Al]^2[\%O]^3$	$K_2' = [\%Al]^2\left(\frac{p_{H_2O}}{p_{H_2}}\right)^3$	$K_3' = \frac{p_{H_2O}}{p_{H_2}}\frac{1}{[\%O]}$
7	0·0	0·0	3·54	2·7	21·7	$9·27 \times 10^{-12}$	$2·09 \times 10^{-11}$	1·31
12	0·0	0·0	4·92	3·5	10·5	$4·72 \times 10^{-12}$	$1·31 \times 10^{-11}$	1·41
31	0·0	0·0	6·56	4·1	6·0	$2·48 \times 10^{-12}$	$1·02 \times 10^{-11}$	1·60
35	0·25	0·17	3·59	3·1	29·5	$2·54 \times 10^{-11}$	$3·95 \times 10^{-11}$	1·16
30	0·25	0·19	4·96	3·7	17·5	$1·55 \times 10^{-11}$	$3·74 \times 10^{-11}$	1·34
36	0·25	0·14	6·53	4·9	9·2	$1·00 \times 10^{-11}$	$2·37 \times 10^{-11}$	1·33
24	0·50	0·39	3·67	3·7	46·2	$1·07 \times 10^{-10}$	$1·07 \times 10^{-10}$	0·99
23	0·50	0·42	4·97	4·5	36·2	$1·19 \times 10^{-10}$	$1·61 \times 10^{-10}$	1·11
25	0·50	0·34	6·73	3·8	21·1	$2·45 \times 10^{-11}$	$1·36 \times 10^{-10}$	1·77
21	1·0	0·67	3·62	4·4	66·6	$3·78 \times 10^{-10}$	$2·10 \times 10^{-10}$	0·82
22	1·0	0·64	5·07	4·8	48·7	$2·63 \times 10^{-10}$	$3·08 \times 10^{-10}$	1·06
20	1·0	0·50	6·72	3·0	34·1	$3·16 \times 10^{-11}$	$3·56 \times 10^{-10}$	2·24
32	2·0	1·81	3·56	2·8	78·0	$1·34 \times 10^{-10}$	$2·75 \times 10^{-10}$	1·27
33	2·0	1·73	4·87	3·1	60·0	$1·07 \times 10^{-10}$	$4·18 \times 10^{-10}$	1·57
34	2·0	1·70	6·50	2·4	41·0	$2·32 \times 10^{-11}$	$4·62 \times 10^{-10}$	2·71
39	4·0	3·44	3·51	2·0	123·6	$1·22 \times 10^{-10}$	$6·61 \times 10^{-10}$	1·76
37	4·0	3·35	4·82	2·8	73·6	$1·20 \times 10^{-10}$	$6·09 \times 10^{-10}$	1·72
40	4·0	3·25	6·68	2·1	63·0	$3·68 \times 10^{-11}$	$11·80 \times 10^{-10}$	3·18

TABLE 28 - Computation of Functions for Determination of Parameters $e_O^{(Si)}$ and $e_{Al}^{(Si)}$

Heat No	Si Wt Pct	Al Wt Pct x 10^3	O Wt Pct x 10^3	$-\log f_O^{(Al)}$	$-2\log f_{Al}^{(O)}$	$-\log K_1'$	$-\log K_2'$	$+\log K_3'$	$+\left[\log K_3' - \log f_O^{(Al)}\right]$	$-\left[\log K_2' + 2\log f_{Al}^{(O)}\right]$	$-\left[\log K_1' + 2\log f_{Al}^{(O)} + 3\log f_O^{(Al)}\right]$
7	0·00	21·7	2·7	0·07	0·03	11·03	10·68	0·12	0·19	10·71	11·27
12	0·00	10·5	3·5	0·03	0·04	11·33	10·88	0·15	0·18	10·92	11·46
31	0·00	6·0	4·1	0·02	0·05	11·61	10·99	0·20	0·22	11·04	11·72
						Average Values Taken from Chap. VI :-		0·21		10·99	11·63
35	0·17	29·5	3·1	0·10	0·03	10·60	10·40	0·06	0·16	10·43	10·93
30	0·19	17·5	3·7	0·06	0·04	10·81	10·43	0·13	0·19	10·47	11·03
36	0·14	9·2	4·9	0·03	0·05	11·0	10·63	0·12	0·15	10·68	11·14
						Average Values :-			0·17	10·53	11·03
24	0·39	46·2	3·7	0·15	0·04	9·97	9·97	0·00	0·15	10·01	10·46
23	0·42	36·2	4·5	0·12	0·05	9·92	9·79	0·05	0·17	9·84	10·33
25	0·34	21·1	3·8	0·07	0·04	10·61	9·87	0·25	0·32	9·91	10·86
						Average Values :-			0·21	9·92	10·58
21	0·67	66·6	4·4	0·22	0·05	9·42	9·68	0·09	0·13	9·73	10·13
22	0·64	48·7	4·8	0·16	0·05	9·58	9·51	0·03	0·19	9·56	10·11
28	0·50	34·1	3·0	0·11	0·03	10·50	9·45	0·35	0·46	9·48	10·86
						Average Values :-			0·26	9·59	10·37
32	1·81	78·0	2·8	0·26	0·03	9·87	9·56	0·10	0·36	9·59	10·68
33	1·73	60·0	3·1	0·20	0·03	9·97	9·38	0·20	0·40	9·41	10·67
34	1·70	41·0	2·4	0·14	0·03	10·63	9·34	0·43	0·57	9·37	11·08
						Average Values :-			0·44	9·46	10·75
39	3·44	123·6	2·0	0·41	0·02	9·91	9·18	0·25	0·66	9·20	11·16
37	3·35	73·6	2·8	0·24	0·03	9·92	9·22	0·24	0·48	9·25	10·67
40	3·25	63·0	2·1	0·21	0·02	10·43	8·93	0·50	0·71	8·95	11·08
						Average Values :-			0·62	9·13	10·9

The effect of aluminium on the activity coefficient of oxygen is represented as before by $f_o^{(Al)}$. Similarly the effect of silicon is represented by $f_o^{(Si)}$. As in previous chapters $f_o^{(O)}$ is taken as unity.

Thus:- $\log K_3 = \log K_3' - \log f_o$

$= \log K_3' - \log f_o^{(Al)} - \log f_o^{(Si)}$

i.e. $\log K_3' - \log f_o^{(Al)} = e_o^{(Si)}[\%Si] + \log K_3$

This expression is in the form of the equation for a straight line, the gradient of which represents the parameter $e_o^{(Si)}$ i.e. the effect of silicon on the activity coefficient of oxygen. The values for $\log K_3'$ from Table 27 together with values for $\log f_o^{(Al)}$ calculated in Table 28 are used to plot $\left\{\log K_3' - \log f_o^{(Al)}\right\}$ Y $[\%Si]$ in Fig 30. From the spread of the data it is obvious that the experimental results in this case cannot be represented adequately by a straight line. The implication of these results will be discussed more fully in a later section.

(b) The Effect of Silicon on the Activity Coefficient of Aluminium

For the Reaction:-

$$Al_2O_3(s) + 3H_2(g) = 2\,\underline{Al} + 3H_2O\,(g)$$

$$K_2 = [f_{Al}\,\%\,Al]^2\left(\frac{p_{H_2O}}{p_{H_2}}\right)^3$$

$$= K_2' \cdot f_{Al}^2$$

Where the activity coefficient of aluminium f_{Al} is given by:-

$$f_{Al} = f_{Al}^{(O)} \cdot f_{Al}^{(Si)}$$

$f_{Al}^{(O)}$ represents the effect of oxygen, and $f_{Al}^{(Si)}$ the effect of silicon on the activity coefficient of aluminium. As before $f_{Al}^{(Al)}$ is taken as unity.

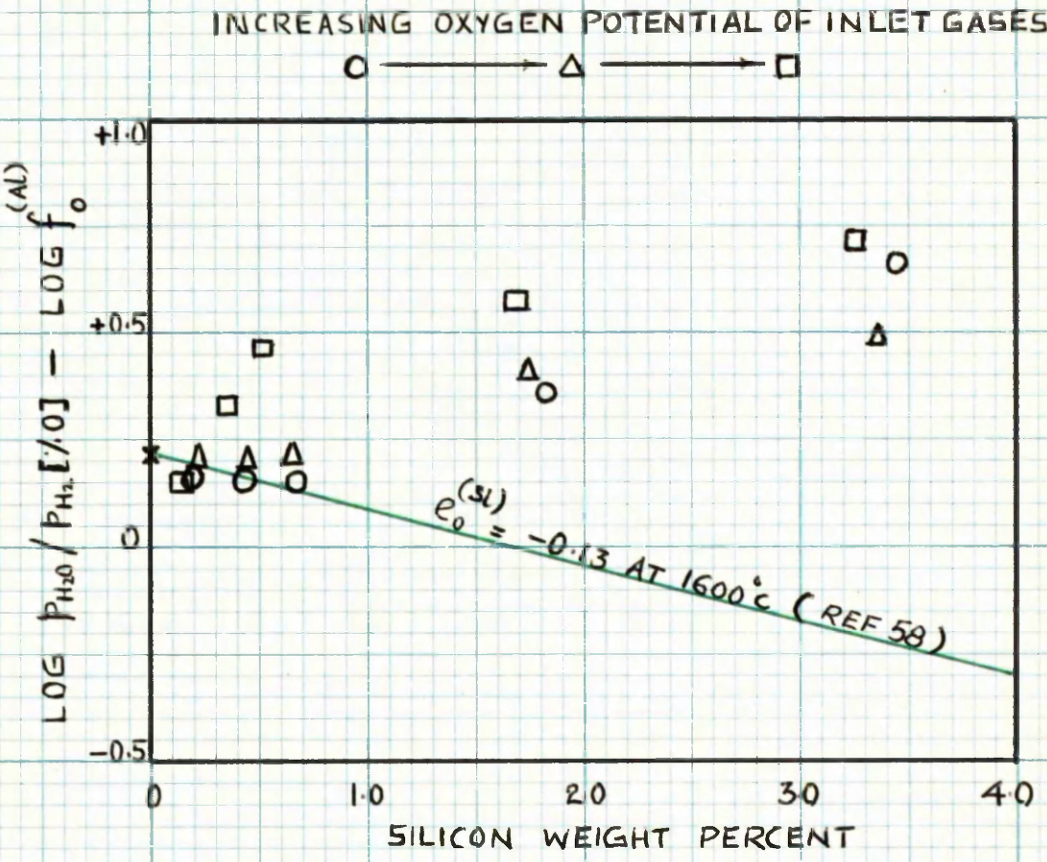

FIG 30 EFFECT OF SILICON ON LOG K_3'

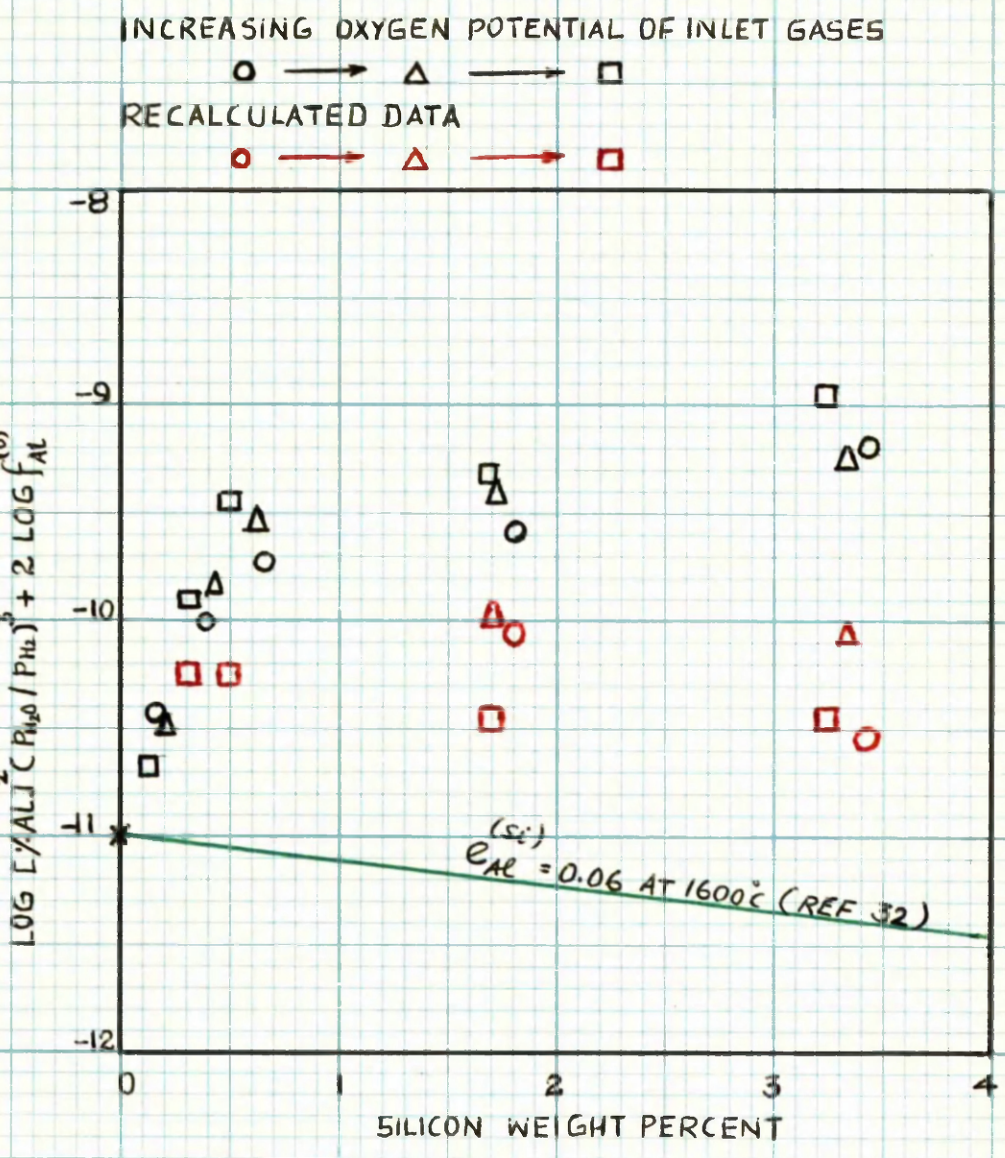

FIG 31 EFFECT OF SILICON ON LOG K_2'

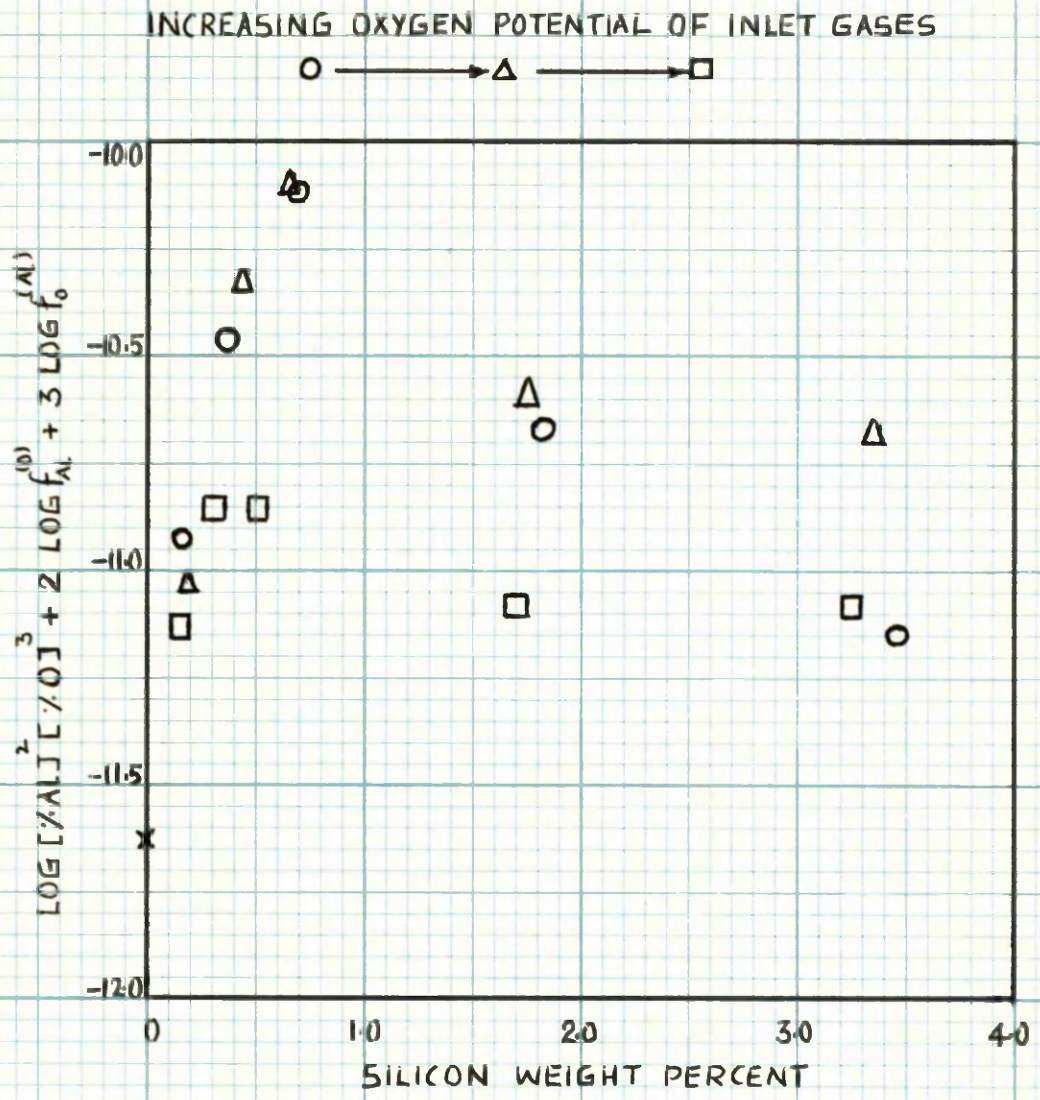

FIG 32 EFFECT OF SILICON ON THE ALUMINIUM DEOXIDATION PRODUCT AT 1723°C

Thus:- $\log K_2 = \log K_2' + 2 \log f_{Al}$

$= \log K_2' + 2 \log f_{Al}^{(O)} + 2 \log f_{Al}^{(Si)}$

i.e. $\log K_2' + 2 \log f_{Al}^{(O)} = -2 e_{Al}^{(Si)} [\%Si] + \log K_2$

Using the data of Table 28, a plot is given in Fig 31 of $\left\{\log K_2' + 2 \log f_{Al}^{(O)}\right\}$ v [%Si]. If this could be represented by a straight line, its gradient would be $-2e_{Al}^{(Si)}$. However, as in the previous section, the spread of the data is such that a straight line would be unjustified. Again, the implications of the data will be discussed in a later section.

(c) The Effect of Silicon on the Deoxidation Product

The equilibrium constant for the deoxidation reaction may be expressed in the following way:-

$$Al_2O_3(s) = 2\,\underline{Al} + 3\,\underline{O}$$

$$K_1 = [f_{Al} \times \%Al]^2 \cdot [f_O \times \%O]^3$$

$$= K_1' f_{Al}^2 f_O^3$$

i.e. $\log K_1 = \log K_1' + 2 \log f_{Al} + 3 \log f_O$

$= \log K_1' + 2\log f_{Al}^{(O)} + 3 \log f_O^{(Al)} + 2 \log f_{Al}^{(Si)} + 3 \log f_O^{(Si)}$

i.e, $\log K_1' + 2\log f_{Al}^{(O)} + 3 \log f_O^{(Al)} = -2 e_{Al}^{(Si)}[\%Si] - 3 e_O^{(Si)}[\%Si] + \log K_1$

$= 2\left\{e_{Al}^{(Si)} + 1.5 e_O^{(Si)}\right\}[\%Si] + \log K_1$

Values for the expression on the left hand side of the above equation are calculated in Table 28 and plotted against [% Si] in Fig 32. Again the data cannot be represented by a straight line.

3 Implications of the Experimental Data

The various data can be assessed in a qualitative way as follows:-

(a) Silicon-Oxygen Interaction. From the tabulated data and Fig 30 it can be seen that in general as the silicon content of the metal increases, the oxygen content for a given oxygen potential, after a small initial increase, progressively decreases. From this data, it would appear that the activity coefficient of oxygen is increased by the presence of silicon, i.e. $f_O^{(Si)}$ is greater than unity and $e_O^{(Si)}$ is positive. This is in fact the reverse of what is known to be the case. Independent studies[22,57,58] have shown that the behaviour of silicon in iron-oxygen alloys, is similar to that of aluminium in that the activity coefficient of oxygen is reduced by the presence of either element, although the effect is much more pronounced in the case of aluminium. In the presence of silicon, therefore, the equilibrium ratio K_3' would be expected to decrease with increasing silicon content. In the present study, the opposite effect has occurred. In view of these facts it would appear that the oxygen potential of the gas mixture at the metal-gas interface was much lower than had been anticipated from consideration of the inlet gas ratio.

(b) Silicon-Aluminium Interaction: From the tabulated data and Fig 31 it can be seen that for the same apparent oxygen potential in the gas phase, the aluminium concentration of the metal increases as the silicon content increases. This would imply that the activity coefficient of aluminium is decreased by the presence of silicon and that $e_{Al}^{(Si)}$ is negative. Previous studies of the effect of silicon on the activity coefficient of aluminium[27,32,33] are in agreement that

$e^{(Si)}_{Al}$ is positive. Thus for the same oxygen potential in the gas phase, the aluminium concentration of the melts would be expected to decrease with increasing silicon content. In the present work therefore the amount of alumina which has been reduced is greater than that expected. As in the previous section, this would suggest that for some reason, the oxygen potential of the gas phase at the metal-gas interface was much lower than that anticipated.

(c) The Deoxidation Product . Although the data presented in Fig 32 is independent of p_{H_2O}/p_{H_2} ratios, it is not entirely independent of the data given in Fig 30 and 31, since all three sets of data involve analyses for oxygen and/or aluminium. Thus the effects mentioned in sections (a) and (b) are also reflected in the data of Fig 32.

(d) Loss of Silicon. Analyses of the melts for silicon, by the standard sulphuric acid method[80] indicated that the silicon content at the end of a heat was lower than at the beginning (see Table 27). In general, the greater the oxidising potential of the inlet gases, the greater the decrease in silicon.

(e) General Trend of the Data . From Figs 30 and 31 it is apparent that the deviation of the present data from that of earlier studies[32,58] increases. (i) as the silicon content increases, and (ii) as the oxidising potential of the gas mixture increases.

The various factors discussed above can be summarised as follows:-

(1) The oxidising potential of the gas mixture at the

gas-metal interface appeared to be much lower than that anticipated from consideration of the composition of the inlet gases.

(2) The decrease observed in the silicon content of the melts was greatest when the oxidising potential of the inlet gases was greatest.

(3) The deviation of the data from that of previous studies increased with (a) the silicon content and (b) the oxidising potential of the inlet gases.

From these conclusions it would appear that a chemical reaction was taking place at the gas-metal interface between the silicon in the melt and the water vapour in the inlet gases, thus leading to a decrease in both of these components.

A reaction satisfying these conditions is:

$$\underline{Si} + H_2O_{(g)} = SiO_{(g)} + H_{2(g)}$$

4 Reassessment of the Data on the Basis of Silicon Monoxide Formation

In Table 29 the oxygen concentrations of the various melts are used to determine oxygen activities taking into account the effect of aluminium, but neglecting the smaller effect of silicon. Assuming $\log K_1 = 0{\cdot}21$ from the previous work on Fe-Al-O equilibrium (Chap VI) it is possible to calculate gas ratios, p_{H_2O}/p_{H_2}, which would be in equilibrium with the oxygen activities of the melts

$$H_{2\,(g)} + \underline{O} = H_2O_{(g)}$$

$$\log K_1 = \log\left(\frac{p_{H_2O}}{p_{H_2}}\right) - \log [a_O]$$

$$\text{i.e. } \log \frac{p_{H_2O}}{p_{H_2}} = 0{\cdot}21 + \log [a_O]$$

These calculated gas ratios, denoted by $\left(\frac{p_{H_2O}}{p_{H_2}}\right)_c$, are

TABLE 29 Computation of p_{SiO} Values

Heat No	O Wt Pct x 10^3	log %O	log $f_O^{(Al)}$	log a_O	log $\left(\frac{p_{H_2O}}{p_{H_2}}\right)_c$	$\left(\frac{p_{H_2O}}{p_{H_2}}\right)_c \times 10^3$	$\left(\frac{p_{H_2O}}{p_{H_2}}\right)$ x 10^3 Inlet	$\frac{\text{Argon}}{H_2}$	$p_{SiO} \times 10^4$
35	3·1	-2·51	-0·10	-2·61	-2·40	3·98	3·59		
30	3·7	-2·43	-0·06	-2·49	-2·28	5·25	4·96		
36	4·9	-2·31	-0·03	-2·34	-2·13	7·41	6·53		
24	3·7	-2·43	-0·15	-2·58	-2·37	4·27	3·67		
23	4·5	-2·35	-0·12	-2·47	-2·26	5·50	4·97		
25	3·8	-2·42	-0·07	-2·49	-2·28	5·25	6·73	6·8	2·18
21	4·4	-2·36	-0·22	-2·58	-2·37	4·27	3·62		
22	4·8	-2·32	-0·16	-2·48	-2·27	5·37	5·07		
20	3·0	-2·52	-0·11	-2·63	-2·42	3·80	6·72	6·8	4·30
32	2·8	-2·55	-0·26	-2·81	-2·60	2·51	3·56	6·1	1·72
33	3·1	-2·51	-0·20	-2·71	-2·50	3·16	4·87	6·1	2·80
34	2·4	-2·62	-0·14	-2·76	-2·55	2·82	6·50	6·1	6·04
39	2·0	-2·70	-0·41	-3·11	-2·90	1·26	3·51	6·1	3·69
37	2·8	-2·55	-0·24	-2·79	-2·58	2·63	4·82	6·1	3·60
40	2·1	-2·68	-0·21	-2·89	-2·68	2·09	6·68	6·1	7·52

TABLE 30 Computation of a_{Si} Values

Heat No	Si Wt Pct	$N_{Si} \times 10^3$	$\log \gamma_{Si}$	$\gamma_{Si} \times 10^3$	$a_{Si} \times 10^5$
25	0.34	6.5	-2.6523	2.23	1.45
20	0.50	10.0	-2.6320	2.33	2.33
32	1.81	35.0	-2.4870	3.26	11.4
33	1.73	33.3	-2.4970	3.18	10.6
34	1.70	32.5	-2.5015	3.15	10.2
39	3.44	66.0	-2.3075	4.93	32.5
37	3.35	64.2	-2.3180	4.81	30.9
40	3.25	62.2	-2.3290	4.69	29.2

TABLE 31 Computation of the Equilibrium Constant for the Reaction $Si + H_2O(g) = SiO(g) + H_2(g)$

Heat No.	$a_{Si} \times 10^5$	$\left(\frac{p_{H_2O}}{p_{H_2}}\right)_c \times 10^3$	$p_{SiO} \times 10^4$	$K = \frac{p_{SiO}\left(\frac{p_{H_2}}{p_{H_2O}}\right)_c}{a_{Si}} \times 10^{-3}$
25	1.45	5.25	2.18	2.86
20	2.33	3.80	4.30	4.86
32	11.4	2.51	1.72	0.60
33	10.6	3.16	2.80	0.84
34	10.2	2.82	6.04	2.10
39	32.5	1.26	3.69	0.90
37	30.9	2.63	3.60	0.44
40	29.2	2.09	7.52	1.24

Average value = 1.73

TABLE 32 Recalculation of K_2' Values

Heat No	Al Wt Pct x 10^3	$\left(\frac{p_{H_2O}}{p_{H_2}}\right)_c$ x 10^3	K_2' x 10^{11}	$-\log K_2'$	$-2\log f_{Al}^{(o)} - \left[\log K_2' + 2 \log f_{Al}^{(o)}\right]$	Si Wt Pct
25	21.1	5.25	6.44	10.19	0.04	10.23	0.34
20	34.1	3.80	6.38	10.20	0.03	10.23	0.50
32	78.0	2.51	9.65	10.02	0.03	10.05	1.81
33	60.0	3.16	11.40	9.94	0.03	9.97	1.73
34	41.0	2.82	3.76	10.42	0.03	10.45	1.70
39	123.6	1.26	3.05	10.52	0.02	10.54	3.44
37	73.6	2.63	9.86	10.01	0.03	10.04	3.35
40	63.0	2.09	3.62	10.44	0.02	10.46	3.25

TABLE 33 Formation of Silicon Monoxide

Heat No	Initial Sample Wt Grams	Si Wt Loss Pct	Si Wt Loss Grams x 10^2	Vol SiO V_1 cc(NTP)	p_{SiO} x 10^4 from T. 29	Total Gas Flow cc/min	Vol SiO V_2 cc(NTP)	$\frac{V_1}{V_2}$
25	19.1	0.16	3.05	24	2.18	1170	184	0.13
20	20.9	0.50	10.45	83	4.30	1170	362	0.23
32	20.4	0.19	3.87	31	1.72	1060	131	0.24
33	19.5	0.27	5.26	42	2.80	1060	214	0.20
34	19.9	0.30	5.97	48	6.04	1060	461	0.10
39	19.2	0.56	10.75	86	3.69	1060	282	0.31
37	19.5	0.65	12.70	101	3.60	1060	275	0.37
40	20.0	0.75	15.00	120	7.52	1060	573	0.21
						Average		0.22

compared with the inlet ratios, and after taking into account the argon/hydrogen ratios, yield values for p_{SiO}, since according to the reaction:-

$$\underline{Si} + H_2O_{(g)} = SiO_{(g)} + H_{2(g)}$$

any decrease in p_{H_2O}, will be accompanied by an increase in p_{SiO}.

At low silicon concentrations, particularly at the lower oxygen potentials this treatment of the data is subject to such large errors that the values of p_{SiO} in this range have been rejected.

In general, p_{SiO} increases with (a) the silicon content, and (b) the oxidising potential of the inlet gases. This trend corresponds exactly to that observed for the deviation of the present experimental results from those of previous investigations.

In Table 30 the activity of silicon relative to the pure liquid is calculated using the following data.

(a) the work of Smith[51] has recently shown that the activity coefficient of silicon in liquid iron, γ_{Si}, is related to the mole fraction of silicon by the equation:- $\partial \log \gamma_{Si} / \partial N_{Si} = 5{\cdot}8$, valid for the range 0·0 to 0·4 N_{Si}.

(b) From the data of Chipman and Baschwitz[52]

$$\log \gamma^{\circ}_{Si} = -2{\cdot}69 \text{ at } 1723^{\circ}C$$

Combining these two equations:- $\log \gamma_{Si} = 5{\cdot}8\ N_{Si} - 2{\cdot}69$

In Table 31 the silicon activities calculated in Table 30 are combined with the data for p_{SiO} and $\left(\frac{p_{H_2O}}{p_{H_2}}\right)_c$ from Table 29 to give values for the equilibrium constant of the reaction:-

$$\underline{Si} + H_2O_{(g)} = SiO_{(g)} + H_{2(g)}$$

$$K = \frac{p_{SiO}}{[a_{Si}]}\left(\frac{p_{H_2}}{p_{H_2O}}\right)_c$$

A value for the equilibrium constant of the silicon monoxide reaction can be calculated from available thermodynamic data in the following way.

The data of Elliott and Gleiser[74], corrected for the recently revised heat of formation of a -quartz[81,82] gives.

$$Si_{(\ell)} + \tfrac{1}{2}O_{2(g)} = SiO_{(g)}\ ; \quad \Delta G^\circ_{2000^\circ K} = -62{,}600 \text{ cal}$$

$$H_{2(g)} + \tfrac{1}{2}O_{2(g)} = H_2O_{(g)}\ ; \quad \Delta G^\circ_{2000^\circ K} = -32{,}310 \text{ cal}$$

$$\therefore \underline{Si} + H_2O_{(g)} = SiO_{(g)} + H_{2(g)}\ ; \Delta G^\circ_{2000^\circ K} = -30{,}290 \text{ cal}$$

$$\log K = \frac{30{,}290}{4{\cdot}575 \times 2000} = 3{\cdot}32$$

$$\text{i.e.} \quad K = 2{\cdot}1 \times 10^3$$

$$\text{And from Table 31} \quad K = 1{\cdot}7 \times 10^3$$

Thus the values derived for the equilibrium constant of the silicon monoxide reaction from (i) experimental data, and (ii.) thermodynamic data, are of the same order. In the light of this agreement it would appear that the oxidising potential of the gas phase at the gas-metal interface was lower than that expected from the inlet gas composition, due to the formation of silicon monoxide.

Recalculation of K_2' Values . In Table 32 the equilibrium ratio $K_2' = [\%Al]^2\left(\frac{p_{H_2O}}{p_{H_2}}\right)^3$ is recalculated using $\left(\frac{p_{H_2O}}{p_{H_2}}\right)_c$ values. The recalculated values for the expression $\log [\%Al]^2\left(\frac{p_{H_2O}}{p_{H_2}}\right)^3 + 2 \log f^{(0)}_{Al}$ are included in Fig 31. The scatter associated with the data may be due to the following factors.-

(i) Small errors in the oxygen analyses, which would affect the

values calculated for p_{SiO}.

(ii) In the thermodynamic data used for calculation of silicon activities, the limits placed on the values for log γ^{o}_{Si} are $\pm$ 0·1.

(iii) Failure of the melts to reach equilibrium with SiO, H_2 and H_2O.

With respect to the third factor, it is of interest to calculate and compare the amounts of silicon monoxide which would be expected to form during a 12-hour run, from consideration of (i) the decrease in silicon content of the melts and (ii) the partial pressure of silicon monoxide above the melt surface. The results of this calculation are shown in Table 33. In the last column of this table, the corresponding volumes of silicon monoxide are expressed in the form of a ratio of V_1/V_2 where V_1 and V_2 represent respectively the volumes of silicon monoxide formed from a consideration of (i) the decrease in silicon content of the melt and (ii) the partial pressure of silicon monoxide above the melt surface.

It is evident that the amount of silicon oxidised from the melts is on average only about 22 per cent of that expected from consideration of the partial pressure of silicon monoxide at the gas-metal interface and the overall gas flow-rate. Since the rate of silicon oxidation will be controlled by the rate of diffusion of water-vapour to the metal surface, the above data would suggest that this diffusion rate was less than the rate of flow of water vapour to the reaction chamber.

Although gas-metal equilibrium may not have been established, the close agreement between the values derived for the equilibrium

constant $K = p_{SiO} \cdot p_{H_2} / [a_{Si}] \cdot p_{H_2O}$ from (i) experimental data and (ii) thermodynamic data would imply that the partial pressure of silicon monoxide at the gas-metal interface was not far removed from the equilibrium value.

5. Consideration of Some Published Data on the Activity of Silicon in Liquid Iron

(a) Introduction

From the results obtained during the present study with Fe-Si-Al-O melts, it is evident that equilibrium measurements involving silicon, silica and water-vapour/hydrogen gas mixtures must be treated with some suspicion. In view of the fact that a discrepancy exists in the published data on the activity of silicon in iron as determined by (i) distribution between silver and iron, and (ii) gas-metal equilibria, it is worth while applying the above hypothesis of silicon monoxide formation in an attempt to resolve the discrepancy.

From experiments on the distribution of silicon between liquid iron and liquid silver, Chipman, Fulton, Gokcen and Caskey[49] have reported a value of about 4 for the parameter $\epsilon_{Si}^{(Si)} = \partial \ln \gamma_{Si} / \partial N_{Si}$ at 1600°C. However, a more probable value from their data would be about 11[50]. This higher value has been confirmed recently by the results from two independent investigations also based on partition experiments[51,52]. In both cases the value reported for $\epsilon_{Si}^{(Si)}$ at 1600°C was approximately 13. Chipman and Pillay[50] have deduced an average value of about 36 for $\epsilon_{Si}^{(Si)}$ at 1600°C. This value

was based mainly on the results of Matoba et alia[58] together with some of the earlier data of Gokcen and Chipman[22]. In each of the investigations, the data was derived from equilibrium studies of Fe-Si-O alloys in silica crucibles under controlled water-vapour/hydrogen atmospheres.

In the following section, the assumption is made that the correct value for the parameter $\epsilon_{Si}^{(Si)}$ at 1600°C is about 13 rather than 36, and on this basis the relevant data of Gokcen and Chipman and Matoba et alia are recalculated.

(b) Recalculation of Some Published Data

Although no experimental results were actually quoted in the paper by Chipman and Pillay[50], it was reported that data obtained from seven heats, which were thought to have reached equilibrium at 1600°C, were in good agreement with the data of Gokcen and Chipman[22] and Matoba et alia[58], for silicon concentrations up to 1 per cent. It was also stated that "Attempts to extend the study to higher silicon concentrations were unsuccessful on account of the transfer of silica from the metal bath to the upper portions of the crucible by means of a silicon-monoxide mechanism." In this respect, it is perhaps significant that while the data of Gokcen and Chipman and Matoba et alia are in reasonable agreement for low silicon concentrations, the two sets of data gradually diverge as the silicon concentration increases above 1 per cent.

In the following treatment attention is confined to results reported by Gokcen and Chipman and Matoba et alia at 1600°C

and 1625°C respectively.

The activity of silicon in the Fe-Si-O melts under consideration can be calculated with the aid of the following equations deduced from the combined data of Smith[51] and Chipman and Baschwitz[52] :-

At 1600°C, $\log \gamma_{Si} = 5.8\ N_{Si} - 2.90$

At 1625°C, $\log \gamma_{Si} = 5.8\ N_{Si} - 2.85$

In these calculations, it is assumed that (1) the influence of oxygen on the activity of silicon is negligible, and (2) for the temperature range involved, $\epsilon_{Si}^{(Si)}$ is constant.

Water vapour/hydrogen ratios denoted by $(p_{H_2O}/p_{H_2})c$ and corresponding to the various calculated silicon activities, can be deduced from the following equations based on published thermodynamic data:-

Ref.(74) corrected by the data of Ref (81),(82) gives:-

$$Si_{(\ell)} + O_2(g) = SiO_2(g); \quad \Delta G^\circ_{1873}\,^\circ K = -137,670 \text{ cal}; \quad \Delta G^\circ_{1900}\,^\circ K = -136,370 \text{ cal}$$

From Ref (74)

$$2H_2(g) + O_2(g) = 2H_2O(g); \quad \Delta G^\circ_{1873}\,^\circ K = -68,180 \text{ cal}; \quad \Delta G^\circ_{1900}\,^\circ K = -67,420 \text{ cal}$$

Combination of these equations gives:-

$$SiO_2(s) + 2H_2(g) = Si(\ell) + 2H_2O(g); \quad \Delta G^\circ_{1873}\,^\circ K = +69,490 \text{ cal}; \quad \Delta G^\circ_{1900}\,^\circ K = +68,950 \text{ cal}$$

$$K = [a_{Si}]\left(\frac{p_{H_2O}}{p_{H_2}}\right)^2 \qquad \text{assuming } a_{SiO_2} = 1 .$$

At the experimental temperatures the stable form of silica, to which the equations apply, is cristobalite.

$$\text{At } 1873^{\circ}K,\ \log K = \frac{-69,490}{4{\cdot}575 \times 1873} = -8{\cdot}11$$

$$\therefore K = 7{\cdot}76 \times 10^{-9}$$

$$\left(\frac{p_{H_2O}}{p_{H_2}}\right)_c = \frac{8{\cdot}81 \times 10^{-5}}{\sqrt{a_{Si}}}$$

$$\text{Similarly, at } 1900^{\circ}K \left(\frac{p_{H_2O}}{p_{H_2}}\right)_c = \frac{1{\cdot}07 \times 10^{-4}}{\sqrt{a_{Si}}}$$

The results of the calculations are shown in Table 34. Listed in the last column of this table are the apparent water-vapour/hydrogen ratios in contact with the melt, based on the composition of the inlet gas mixture.

From the data in Table 34, it is evident that on the assumption of $\epsilon_{Si}^{(Si)} = 13$, the oxygen potential of the gas phase is greater than that expected from consideration of the inlet gas composition. This is the reverse of what was found to be the case in the present study of Fe-Si-Al-O alloys, where the oxygen potential of the gas phase was lower than that expected from the inlet gas composition. Nevertheless, in the following section it will be shown that the data of Table 34 can also be explained in terms of silicon monoxide formation.

(C) A Possible Mechanism Based on the Reaction:- $SiO_{2(g)} + H_{2(g)} = SiO_{(g)} + H_2O_{(g)}$

The two sets of data shown in Table 34 indicate that the calculated water-vapour/hydrogen ratios are greater than the corresponding inlet ratios. This would imply that the oxidising potential of the gases at the melt surface was greater than that anticipated. Since both sets of data were derived from studies

of equilibria involving pure silica, a reaction which would account for the increase in oxidising potential of the gas mixture would be:-

$$SiO_2(s) + H_2(g) = SiO(g) + H_2O(g)$$

$$K = p_{SiO} \frac{p_{H_2O}}{p_{H_2}}, \text{ assuming } a_{SiO_2} = 1.$$

In Table 35, the equilibrium constant for the above reaction is calculated, assuming that p_{SiO} is equivalent to the difference between corresponding water-vapour/hydrogen ratios and taking into account a four-fold admixture of argon.

The equilibrium constant for this reaction can also be calculated from thermodynamic data in the following way:-

From Ref (74) corrected by the data of Ref (81)(82)

$Si(\ell) + O_2(g) = SiO_2(s)$; $\Delta G^\circ_{1873}\,^\circ K = -137,670$ cal; $\Delta G^\circ_{1900}\,^\circ K = -136,370$ cal

$Si(\ell) + \frac{1}{2}O_2(g) = SiO(g)$; $\Delta G^\circ_{1873}\,^\circ K = -61,200$ cal; $\Delta G^\circ_{1900}\,^\circ K = -61,500$ cal

From Ref (74):

$H_2(g) + \frac{1}{2}O_2(g) = H_2O(g)$; $\Delta G^\circ_{1873}\,^\circ K = -34,090$ cal; $\Delta G^\circ_{1900}\,^\circ K = -33,710$ cal

Combining these equations gives:

$SiO_2(s) + H_2(g) = SiO(g) + H_2O(g)$; $\Delta G^\circ_{1873} = +42,380$ cal, $\Delta G^\circ_{1900}\,^\circ = +41,160$ cal

At 1873°K, $\log K = \frac{-42,380}{4.575 \times 1873} = -4.95$

$\therefore K = 1.12 \times 10^{-5}$ From Table 35 $K = 1.78 \times 10^{-5}$

Similarly at 1900°K, $K = 1.82 \times 10^{-5}$ From Table 35 $K = 2.23 \times 10^{-5}$

Thus the values derived for the equilibrium constant from thermodynamic data are in reasonable agreement with the values in Table 35. The evidence would tend to suggest, therefore, that the oxidising potential of the gas mixture in contact with the melts

TABLE 34 Oxygen Potential of the Gas Phase

Si, Wt Pct Charged	Si, Wt Pct Analysed	N_{Si} x 10^3	γ_{Si} x 10^3	a_{Si} x 10^6	$\sqrt{a_{Si}}$ x 10^3	$(P_{H_2O}/P_{H_2})_c$ x 10^3	$(P_{H_2O}/P_{H_2})_{Inlet}$ x 10^3
Gokcen and Chipman - 1600°C							
0.20	0.227	4.5	1.34	6.03	2.46	35.8	32.3
0.35	0.378	7.0	1.36	9.65	3.10	28.4	23.05
0.73	0.613	12.0	1.48	17.8	4.22	20.9	17.03
1.10	1.01	19.0	1.62	30.8	5.55	15.9	13.10
1.77	1.61	31.0	1.91	59.1	7.68	11.5	9.69
4.60	4.39	84.0	3.86	324.0	18.00	4.9	4.56
Matoba et alia - 1625°C							
0.101	0.033	0.7	1.43	1.00	1.00	107	104.5
0.162	0.070	1.4	1.44	2.02	1.42	75.4	70.0
0.340	0.198	4.0	1.49	5.95	2.44	43.8	43.7
0.430	0.337	7.0	1.55	10.9	3.30	32.5	32.3
0.680	0.580	11	1.64	18.0	4.24	25.2	21.8
0.800	0.830	16	1.75	28.0	5.29	20.2	17.5
1.24	1.120	22	1.90	41.8	6.46	16.6	13.4
1.62	1.60	31	2.14	66.2	8.13	13.2	10.3
1.91	1.88	36	2.29	82.5	9.07	11.8	8.1
2.51	2.33	45	2.58	116.0	10.8	9.9	6.1
2.29	2.31	45	2.58	116.0	10.8	9.9	6.1
2.88	2.84	55	2.94	162.0	12.7	8.4	4.7

TABLE 35 Computation of the Equilibrium Constant for the Reaction: $SiO_2 + H_2 = SiO + H_2O$

$P_{SiO} \times 10^3$	$(P_{H_2O}/P_{H_2})_c \times 10^3$	$K = P_{SiO}(P_{H_2O}/P_{H_2})_c \times 10^5$
Gokcen and Chipman - 1600°C		
0·88	35·8	3·15
1·33	28·4	3·78
0·98	20·9	2·05
0·70	15·9	1·11
0·45	11·5	0·52
0·08	4·9	0·04
		Average Value = 1·78
Matoba et alia - 1625°C		
0·63	107	6·74
1·35	75·4	10·15
0·03	43·8	0·13
0·05	32·5	0·16
0·85	25·2	2·14
0·68	20·2	1·37
0·80	16·6	1·33
0·73	13·2	0·96
0·93	11·8	1·10
0·95	9·9	0·94
0·95	9·9	0·94
0·93	8·4	0·78
		Average Value = 2·23

TABLE 36 Computation of the Equilibrium Ratio for the Reaction

$$H_{2(g)} + \underline{O} = H_2O_{(g)}$$

Si Wt Pct	O, Wt Pct x 10^3	$(p_{H_2O}/p_{H_2})_e$ x 10^3	K_3'	log K_3'
Gokcen and Chipman - 1600°C				
0.227	11.7	35.8	3.06	0.49
0.378	9.0	28.4	3.16	0.50
0.613	6.8	20.9	3.32	0.52
1.01	5.0	15.9	3.18	0.50
1.61	4.6	11.5	2.50	0.40
4.39	2.3	4.7	2.13	0.33
Matoba et alia - 1625°C				
0.033	31.1	107	3.44	0.54
0.070	20.6	75.4	3.63	0.56
0.196	14.0	43.6	3.14	0.50
0.337	11.1	32.5	2.93	0.47
0.500	7.7	25.2	3.27	0.51
0.830	6.2	20.2	3.26	0.51
1.120	5.6	16.6	2.96	0.47
1.60	4.7	13.2	2.81	0.45
1.88	4.2	11.8	2.81	0.45
2.33	4.4	9.9	2.25	0.35
2.31	4.5	9.9	2.20	0.34
2.64	3.5	8.4	2.40	0.38

was much closer to that indicated by the calculated, rather than the inlet, water-vapour/hydrogen ratios, due to the reduction of silica by hydrogen with the consequent formation of silicon and water vapour.

(d) The Activity Coefficient of Oxygen in Fe-Si-O Melts

The effect of silicon on the activity coefficient of oxygen can be deduced from a consideration of the following reaction:-

$$H_2(g) + \underline{O} = H_2O(g)$$

$$K_3 = \frac{p_{H_2O}}{p_{H_2}} \cdot \frac{1}{[f_O \times \%O]}$$

$$= K_3'/f_O$$

On the assumption that $f_O = f_O^{(Si)}$

$$\log K_3' = \log f_O^{(Si)} + \log K_3$$

$$= e_O^{(Si)}[\%Si] + \log K_3$$

The results obtained by Gokcen and Chipman and Matoba et alia for this reaction are given in Fig 33. The slope of the line drawn through the data of Matoba yields a value for the parameter $e_O^{(Si)}$ of -0·13. A broken line has been drawn through the data of Gokcen and Chipman for the following reason. In the original paper, an attempt was made to fit both their own data on the Fe-Si-O system and that of Dastur and Chipman[10] on the Fe-O binary system, by a single curved line. This curvilinear relationship was later retracted[57] since it was at variance with the theoretical requirement of a finite slope at infinite dilution.

The values obtained by Gokcen and Chipman and Matoba et alia

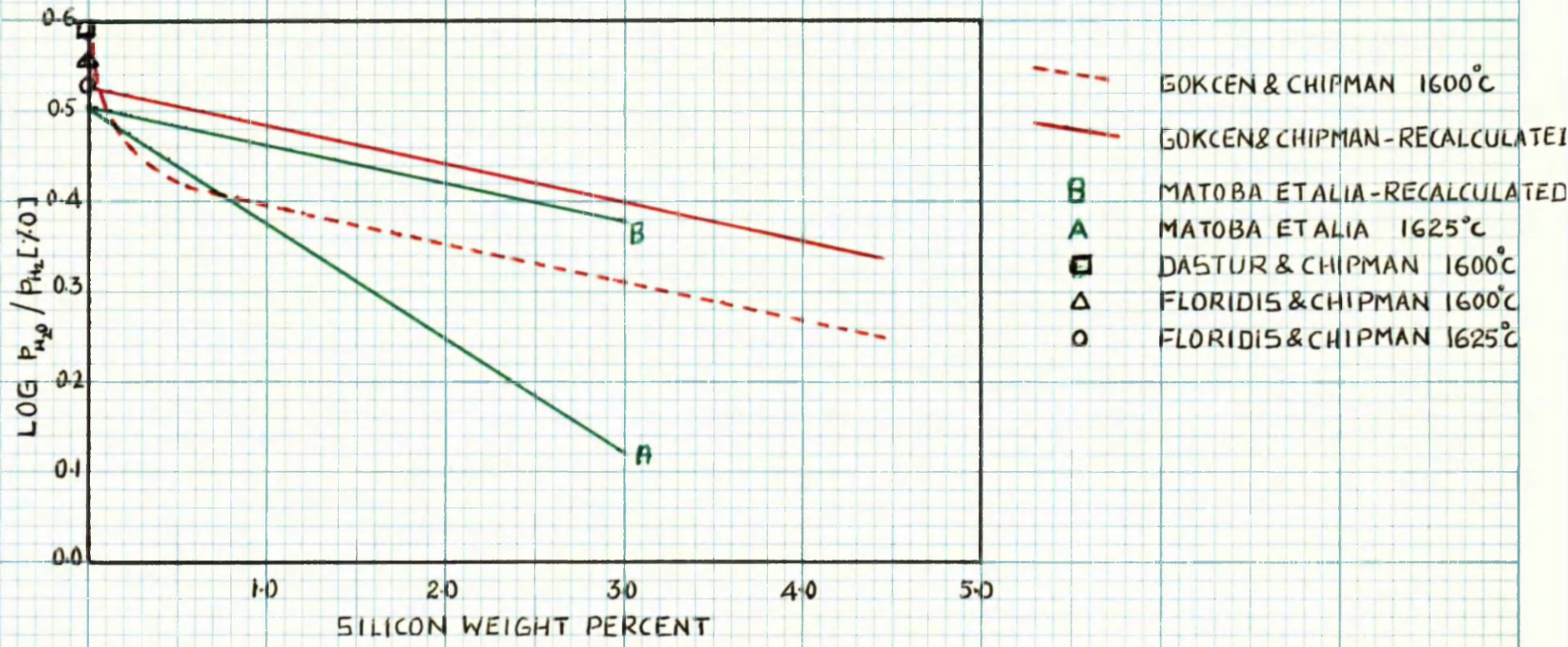

FIG 33 EFFECT OF SILICON ON THE EQUILIBRIUM PRODUCT P_{H_2O} / P_{H_2} [%O]

for the equilibrium ratio K_3' are recalculated in Table 36 using the $(p_{H_2O}/p_{H_2})_c$ ratios given in Table 34. The new values for K_3' are included in Fig 33. Consideration of this graph leads to the following conclusions.

(1) There is reasonable agreement between the two sets of data[22,58] over the full range of silicon concentrations involved.

(2) At zero per cent silicon, there is good agreement between each set of data and that of Floridis and Chipman for the Fe-O binary system.

(3) Although the two sets of data are at slightly different temperatures, the data are not sufficiently precise to indicate any variation in the parameter $e_o^{(Si)}$ with temperature. The gradient of the lines yield a value for this parameter of -0.045. Using this value a graph has been constructed of $\log f_o^{(Si)}$ v [%Si], and this is shown in Fig 34.

(e) The Deoxidation Constant $[a_{Si}][a_O]^2$

The deoxidation constant for silicon is obtained from the reaction.

$$SiO_2(s) = \underline{Si} + 2\,\underline{O}$$

$$K_4 = [a_{Si}][a_O]^2$$

$$= K_4' \cdot f_{Si} \cdot f_O^2$$

On the assumption that $f_{Si} = f_{Si}^{(Si)}$ and $f_O = f_O^{(Si)}$, i.e. neglecting the effect of oxygen in each case.-

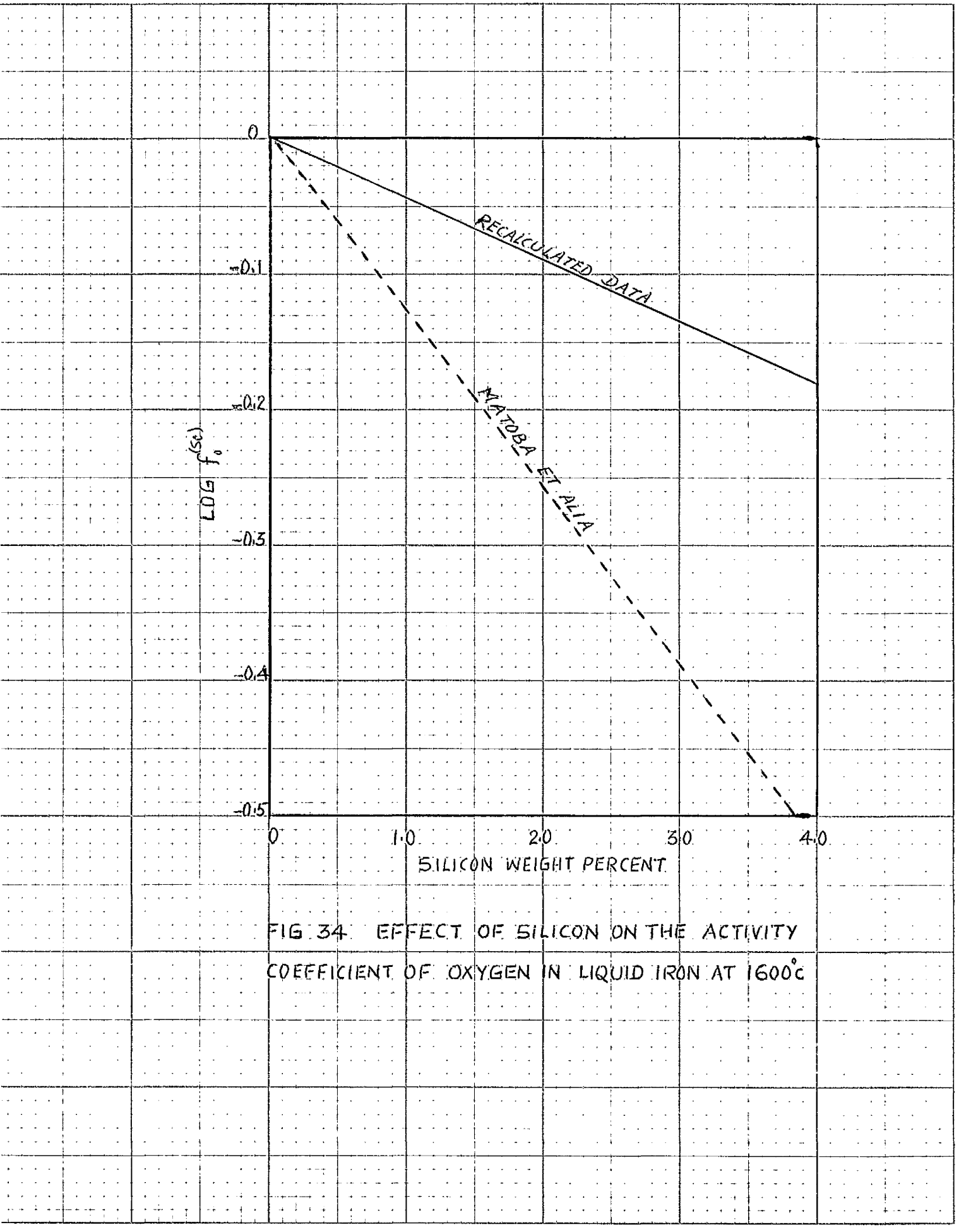

FIG 34 EFFECT OF SILICON ON THE ACTIVITY COEFFICIENT OF OXYGEN IN LIQUID IRON AT 1600°C

$$\log K_1 = \log K_1' + \log f_{Si}^{(Si)} = 2 \log f_O^{(Si)}$$
$$= \log K_1' + e_{Si}^{(Si)}[\%Si] + 2e_O^{(Si)}[\%Si]$$
$$= \log K_1' + [\%Si]\left\{e_{Si}^{(Si)} + 2e_O^{(Si)}\right\}$$

At temperatures about 1600°C

$$\epsilon_{Si}^{(Si)} = +13 \text{ and therefore } e_{Si}^{(Si)} = +0.112$$

From Fig 34 $e_O^{Si} = -0.045$

Thus $\left\{e_{Si}^{(Si)} + 2e_O^{(Si)}\right\} = 0.112 - 0.090 = +0.022$

This would imply that at temperatures of approximately 1600°C, the deoxidation product K_1' and the deoxidation constant K_1 should be almost identical since the parameters $e_{Si}^{(Si)}$ and $e_O^{(Si)}$ tend to compensate each other. This is confirmed by the fact that in each of the investigations the product $[\%Si][\%O]^2$ was approximately constant, and equal to the product $[a_{Si}]\cdot[a_O]^2$. At 1600°C the average value suggested for either product by Chipman and Pillay is 2.3×10^{-5}.

SUMMARY

A study has been made of Fe-Si-Al-O alloys in pure alumina crucibles maintained at a constant temperature of 1723°C, under controlled water-vapour/hydrogen atmospheres. After a period of about 12 hours, the melts were quenched in hydrogen and analysed.

From the results obtained it is apparent that the oxygen potential of the gas phase at the gas-metal interface was

lower than that expected from consideration of the inlet gas composition. This was particularly evident from the aluminium content of the melts. A decrease in the silicon content was also observed and this was most obvious at the highest oxygen potentials.

In an attempt to explain these effects a hypothesis has been put forward based on the formation of silicon monoxide by the reaction.

$$\underline{Si} + H_2O_{(g)} = SiO_{(g)} + H_{2(g)}$$

Values for the equilibrium constant of this reaction calculated from both experimental and thermodynamic data are in reasonable agreement.

In view of the above results and the discrepancy which exists in the published data for the activity of silicon in liquid iron, some gas-metal equilibrium data have been re-examined. On the assumption that silicon activities derived from partition experiments are reliable, calculations have been made the results of which indicate that the oxygen potential of the gas phase at the gas-metal interface was greater than that expected from consideration of the inlet gas composition. This fact has been shown to fit into the hypothesis of silicon monoxide formation. In this instance the reaction involved is:-

$$SiO_{2(s)} + H_{2(g)} = SiO_{(g)} + H_2O_{(g)}$$

Again there is good agreement between the experimental and thermodynamic data for the equilibrium constant of this

reaction.

Using calculated values for the oxygen potential of the gas phase, the activity coefficient of oxygen in Fe-Si-O melts has been redetermined and a new value estimated for the parameter $e_O^{(Si)}$.

The effect of the new data on the silicon deoxidation constant is extremely small due to the fact that in dilute solutions the parameters $e_{Si}^{(Si)}$ and $e_O^{(Si)}$ approximately compensate each other.

In conclusion, this work has shown that studies of equilibria involving silicon, silica and water-vapour/hydrogen gas mixtures are subject to large errors due to the formation of silicon monoxide. It is therefore, essential that this type of effect should be taken into account in all gas-metal investigations where there is a possibility of the formation of a volatile oxide.

A C K N O W L E D G E M E N T S

The author acknowledges with gratitude the guidance and help unstintingly given throughout this work by Dr. H.B. Bell.

He also wishes to express his thanks to Professor E. C. Ellwood for his encouragement at all times.

The research was carried out in the Metallurgy Department of the Royal College of Science and Technology, Glasgow.

REFERENCES

REFERENCES

1. C. Wagner — Thermodynamics of Alloys, Addison Wesley Press, (1952), 51 - 53.

2. C. Wagner — J. Chem. Phys. (1951), 19, 626.

3. J. Chipman — Trans. A.I.M.E. (1950), 188, 334

4. J. Chipman and J.F. Elliott-Trans. A.S.M., (1950), 42A, 102.

5. L.S. Darken and R.W. Gurry - Physical Chemistry of Metals, McGraw-Hill Book Co. (1953) Ed. p. 351.

6. J. Chipman — J. Am. Chem. Soc., (1933), 55, 3131.

7. "Basic Open Hearth Steelmaking" Physical Chemistry of Steelmaking Comm. A.I.M.E., New York, (1951), 2nd Ed., p. 627.

8. M.G. Fontana and J. Chipman - Trans. A.S.M., (1936), 24, 313.

9. J. Chipman and A.M. Samarin- Trans.A.I.M.E., (1937) 125, 331

10. M.N. Dastur and J. Chipman - Ibid, (1949), 185, 441.

11. T.P. Floridis and J. Chipman - Trans.Met. Soc.A.I.M.E., (1958),212, 549.

12. N.A. Gokcen — Trans.A.I.M.E., (1956), 206, 1558.

13. S. Matoba — Anniversary Volume, Tohuku Imp.Univ. Sendai, J Japan (1936), 548.

14. V.V. Averin, A.Y. Polyakov and A.M. Samarin - Izvest. Akad. Nauk S.S.S.R., Otdel, Tekn. Nauk (3), (1955). 90.

15. F.S. Tritton and D. Hanson - J. I.S.I., (1924),110, 90

16. G.H. Herty and M. Gaines -Mining and Met. Investigations Bulletin (1927), No. 34.

17. F. Körber and W. Oelsen Mitt K.W.I., (1932), 14, 181

18. J. Chipman and K.L. Fetters - Trans. A.S.M., (1941), 29, 953

19. C.R. Taylor and J. Chipman-Trans.A.I.M.E.(1943), 154, 228.

20. H.A. Sloman — 3rd Report Oxygen Sub-Committee, Iron and Steel Inst.,(1941), 311.

21. W.A. Fischer and H. vom Ende-Arch.Eisenhuttenw (1952), 23, 21,

22. N.A. Gokcen and J. Chipman-Trans. A.I.M.E., (1952), 194, 171.

23. L.S. Darken and R.W. Gurry-J. Am. Chem. Soc., (1946), 68, 798

24. J. Chipman — Trans. A.S.M., (1934), 22, 385.

25. Y.H. Chou — Doctorate Thesis, Carnegie Institute of Technology, 1947.

26. J.F. Elliott — Unpublished

27. J. Chipman and T.P. Floridis-Acta Met., (1955), 3, 456.

28. M. Hillert, B.L. Averbach and M. Cohen -Ibid, (1956),4, 31.

29. M. Kawakami — Sci.Rep.Tohoku Imp.Univ.,(1930),16, 521.

30. M. Hansen — Der Aufbau der Zweistofflegierungen, J. Springer, Berlin, (1936), 1-4.

31. H. Phillips — Annotated Equilibrium Diagrams, No.21, The Institute of Metals (1956)

32. T.C. Wilder and J.F. Elliott-J. Electrochem.Soc.,(1960), 107, 628.

33, H. Wentrup and G. Hieber Arch.Eisenhuttenew (1939-40), 13, 15.

34. W. Geller and K. Dicke — Ibid, (1943), 16, 431.

35. D.C. Hilty and W. Crafts Trans.A.I.M.E., (1950), 188, 414.

36. N.A. Gokcen and J. Chipman- Ibid, (1953), 197, 173.

37. J. Chipman - Reference 7. Page 672

38. J. Chipman and F.C. Langenberg -The Physical Chemistry of Steelmaking, Technology Press, M.I.T.,(1958), p. 46.

39. F. Adcock — J.I.S.I. (1931), 124, 99

40. A. Hellawell — Annotated Equilibrium Diagrams, No. 25, The Institute of Metals.

41. H.M. Chen and J. Chipman Trans.A.S.M. (1947), 38, 70.

42. A.P. Lyubimov and A.A. Granovskaya-Moskov. Inst. Stali im I.V. Stalina, Sbornik (1955), No. 34, 95.

43. H. Wada, Y. Kawai and T. Saito-Sci. Rep. RITU, (1961), A-B, 96.

44. K. Charlton — Private communication

45. J. Chipman — J.I.S.I. (1955), 180, 97.

46. B.V. Lincainskii and A.M. Samarin -Izvest. Akad., Nauk.S.S.S.R. Otdel, Tekn. Nauk 5, (1953), 691.

47. E.T. Turkdogan — J.I.S.I., (1954), 178, 278.

48. J. Chipman, J.C. Fulton, N.A. Gokcen - Acta Met., (1954), 2, 439. and G.R. Caskey

49. (i) G.L. Humphrey and E.G. King - J. Am. Chem. Soc.(1952),74,2041
(ii) K.K. Kelley — U.S. Bur. Mines Bull.(1949), 476,(1950),477

50. J. Chipman and T.C.M. Pillay-Trans. Met. Soc.A.I.M.E.,(1961), 221,1277.

51. G. Smith — Private communication

52. J. Chipman and R. Baschwitzy - Private communication

53. F. Körber and W. Oelsen- Mitt. K.W.I., (1933), 15, 271.

54. C.A. Zapffe and C.E. Sims-Trans. A.I.M.E., (1943), 154, 191.

55. D.C. Hilty and W. Crafts Ibid, (1950), 188, 425.

56. L.S. Darken — Ibid, p. 1346.

57. N.A. Gokcen and J. Chipman - Ibid, (1953), 197, 1017.

58. S. Matoba, K. Gunjii and T. Kuwana-Tetsu to Hagane,(1959),45, 229.

59. L. Enskog — Physik Z, (1911), 12, 56 and 533.

60. S. Chapman — Phil. Trans. Roy. Soc.A.,(1916),216, 279; (1917), 217, 115.

61. S. Chapman and F. Dootson - Phil. Mag., (1917), 33, 248

62. P.H. Emmett and J.F. Schultz-J.Am.Chem.Soc., (1933),55, 1376.

63.L.S. Darken and R.W. Gurry J.Am. Chem.Soc.,(1945), 67, 1398.

64.M.N. Dastur and J. Chipman Disc. Faraday Soc., (1948), No. 4, p.100.

65.L.J. Gillespie J. Chem.Physics,(1939), 7, 530.

66.N.A. Gokcen A.J.Am.Chem. Soc.,(1951),73, No.3 , 3789.

67.F.H. Huttig and F. Reuscher-Z.anorg.Chem.,(1924), 137, 155.

68.A. Lannung J. physik.Chem., (1934), A170, 134

69.M.P. Applebey and R.P. Cook J. Chem.Soc., (1938), 547.

70.F.H. Schofield and A. Grace -Eighth Report on Heterogeneity of Steel Ingots,Iron and Steel.Inst. Spec. Report, (1939) No. 25.

71.M.N. Dastur and N.A. Gokcen-Trans.A.I.M.E.(1949), 185, 665

72.U.T. Hill Analytical Chemistry,(1959), 31 No.3 ,429.

73.A.A. Murad Ph.D. Thesis, Glasgow University, 1951

74. J.E.Elliott and M. Gleiser"Thermochemistry for Steelmaking"(1960)Vol.1

75.Ref. 7, page 40

76. S. Marshall and J. Chipman-Trans.A.S.M.(1942), 30, 695.

77. J.F. Elliott -The Physical Chemistry of Steelmaking" Technology Press, M.I.T. (1958)

78. H.B. Bell Metallurgical Progress - 2, (1954), p. 47.

79. J. Chipman Trans.A.I.M.E. (1950), 188, 1342

80. Standard Methods of Analysis-The United steel Companies,Ltd.(1951) 4th Ed., p.69.

81. W.D. Good J. Phys.Chem.,(1962) 66, 380.

82. S.S. Wise, J.L. Margrave, H.M. Feder and W.N. Hubbard & Ibid, p.381.

APPENDIX

EXPERIMENTAL HEATS

All heats reported in the following tables were made with gas flow rates of approximately 150 cc/min hydrogen and 900 cc/min argon. The preheater was maintained at 1550°C unless otherwise stated.

Table (i) Iron-Aluminium-Oxygen Melts

Heat No	Temp °C	Hours at Temp	Temp of Saturated Li Cl Soln.	Atm. Press. mm Hg	Internal Press. mm Hg
1	1823	6·0	30·5	745·5	5
2	1823	10·0	30·5	759·7	5
3	1823	1·0	24·8	759·0	5
4	1823	4·5	24·8	766·7	5
5	1823	12·0	24·8	764·1	4
6	1723	6·0	25·0	765·5	4
7	1723	12·0	25·0	761·0	5
8	1823	11·5	35·4	768·0	5
9	1823	10·5	40·5	756·7	5
10	1823	11·5	45·5	751·0	5
12	1723	12·0	30·4	767·6	5
15	1723	12·0	40·4	763·3	4
31	1723	12·0	35·4	762·2	5

Table (ii) Iron-Silicon-Aluminium-Oxygen Melts

The following heats were maintained at 1723°C for 12 hours under a 6 : 1 argon/hydrogen ratio.

Heat No	Silicon charged wt pct	Temp of Saturated Li Cl Soln. °C	Atmospheric Pressure mm Hg	Internal Pressure mm Hg
17	1	30·2	743·2	4 No preheat
18	1	35·4	748·3	4 No preheat
19	1	25·0	752·5	4 No preheat
20	1	35·5	750·1	3
21	1	25·0	751·3	3
22	1	30·1	780·5	4
23	0·5	30·1	744·8	4
24	0·5	25·1	749·0	4
25	0·5	35·6	752·9	4
30	0·25	30·3	755·0	5
32	2	25·0	758·5	7
33	2	30·2	757·4	6
34	2	35·4	768·8	6
35	0·25	25·2	760·8	7
36	0·25	35·5	767·5	3
37	4	30·1	764·1	7
39	4	24·7	755·7	7
40	4	35·5	752·4	6

Table (ii) Iron Chromium-Aluminium Oxygen Melts

The following heats were maintained at 1723°C for 12 hours under a 6 : 1 argon-hydrogen ratio.

Heat No	Chromium Charged Wt Pct	Temp of Saturated Li Cl Soln. °C	Atmospheric Pressure mm Hg	Internal Pressure mm Hg
43	2	35·4	750·6	6
44	2	29·9	755·7	6
45	10	30·1	765·5	6
46	10	35·5	763·1	5
47	6	30·2	766·6	6
48	6	35·7	753·2	6
49	2	24·9	758·5	6
50	10	24·9	752·1	6
51	6	24·9	757·3	6

On occasions during the investigation heats had to be abandoned for several reasons, for example, (i) blockages in the bubbling tubes due to crystallisation of lithium chloride, (ii) failure of the preheater winding and(iii) failure of the power supply. Such heats are not reported in the above tables.